ARL-TR-79-4

LEVEL 12

Copy No. 39

PARRAY TECHNOLOGY PAPERS PRESENTED AT SCIENTIFIC AND TECHNICAL MEETINGS

Tommy G. Goldsberry et al.

APPLIED RESEARCH LABORATORIES
THE UNIVERSITY OF TEXAS AT AUSTIN
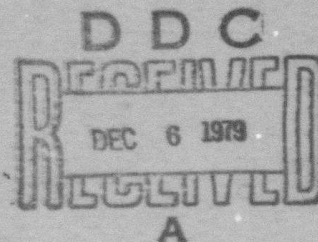POST OFFICE BOX 8029, AUSTIN, TEXAS 78712

2 August 1979

Technical Report

APPROVED FOR PUBLIC RELEASE;
DISTRIBUTION UNLIMITED.

Prepared for:
DEFENSE ADVANCED RESEARCH PROJECTS AGENCY
1400 WILSON BLVD
WASHINGTON, DC 22209

Monitored by:
NAVAL ELECTRONIC SYSTEMS COMMAND
DEPARTMENT OF THE NAVY
WASHINGTON, DC 20360

79 12 6 127

REPORT DOCUMENTATION PAGE		READ INSTRUCTIONS BEFORE COMPLETING FORM
1. REPORT NUMBER	2. GOVT ACCESSION NO.	3. RECIPIENT'S CATALOG NUMBER
4. TITLE (and Subtitle) PARRAY TECHNOLOGY PAPERS PRESENTED AT SCIENTIFIC AND TECHNICAL MEETINGS		5. TYPE OF REPORT & PERIOD COVERED Technical Report.
		6. PERFORMING ORG. REPORT NUMBER ARL-TR-79-4
7. AUTHOR(s) Tommy G. Goldsberry C. Richard Reeves Voldi E. Maki, Jr. David F. Rohde Wiley S. Olsen M. Ward Widener		8. CONTRACT OR GRANT NUMBER(s) N00039-76-C-0231
9. PERFORMING ORGANIZATION NAME AND ADDRESS Applied Research Laboratories The University of Texas at Austin Austin, Texas 78712		10. PROGRAM ELEMENT, PROJECT, TASK AREA & WORK UNIT NUMBERS ARPA ORDER-2910 Program Code 5G10
11. CONTROLLING OFFICE NAME AND ADDRESS Defense Advanced Research Projects Agency 1400 Wilson Blvd. Arlington, VA 22209		12. REPORT DATE 2 August 79
		13. NUMBER OF PAGES 167
14. MONITORING AGENCY NAME & ADDRESS(If different from Controlling Office) Naval Electronic Systems Command Department of the Navy Washington, D. C. 20360		15. SECURITY CLASS. (of this report) UNCLASSIFIED
		15a. DECLASSIFICATION/DOWNGRADING SCHEDULE

16. DISTRIBUTION STATEMENT (of this Report)

Approved for public release; distribution unlimited.

17. DISTRIBUTION STATEMENT (of the abstract entered in Block 20, If different from Report)

18. SUPPLEMENTARY NOTES

19. KEY WORDS (Continue on reverse side if necessary and identify by block number)

PARRAY	Transducers
Nonlinear acoustics	Crystal oscillators
Parametric reception	Sideband detectors

20. ABSTRACT (Continue on reverse side if necessary and identify by block number)

The parametric acoustic receiving array (PARRAY) exploits the inherent nonlinearity in the pressure-density relationship of water to achieve directional reception of low frequency acoustic waves using only two small high frequency transducers and some associated electronics. This report describes the PARRAY and summarizes several papers on the subject that have been presented at scientific and technical meetings. Copies of the papers are included as appendices. Procedures for selection of optimal parameter

DD FORM 1473   EDITION OF 1 NOV 65 IS OBSOLETE

values are developed.   State of the art advances in stable oscillators,
reception of sideband signals with very small modulation indices, and simple
high efficiency transducer elements are described.   Results of experiments
with a 340 m aperture PARRAY are presented which demonstrate that the experi-
mental PARRAY is ambient noise limited in Lake Travis (Texas).

TABLE OF CONTENTS

LIST OF FIGURES

v

I. INTRODUCTION

The parametric acoustic receiving array (PARRAY) exploits the inherent nonlinearity in the pressure density relationship of water to achieve directional reception of low frequency acoustic waves using only two small high frequency transducers and some associated electronics. Characterized as a volumetric, virtual array synthesized in the water column between the two high frequency transducers, denoted pump and hydrophone, the directional response function of the PARRAY is similar to that of a continuous end-fire array of length equal to the distance between the pump and hydrophone. The maximum response axis of the synthesized array lies along the directed line segment from the hydrophone to the pump. A more complete description of the PARRAY and a summary of its major characteristics are given in Section II. References to earlier analyses and investigations are provided for those who desire more detailed information.

A brief summary of the appendices, which constitute the major portion of the report, is given in Section III. The appendices are several papers on various phases of the PARRAY that were presented at scientific and technical meetings by scientists and engineers of ARL:UT. These papers were produced in the course of research and development on a large aperture PARRAY for detection of low frequency signals; additional information is provided in a companion technical report, ARL-TR-79-5.[1] A.072 307

Some of the papers contained in this report have been expanded in scope and submitted for publication in the archival journals. Others of these papers will be similarly expanded and submitted for publication as time permits; however, it seems appropriate to collect these papers in one document and distribute it at this time to make the results available without further delay.

1

II. DESCRIPTION OF THE PARRAY

The parametric reception concept was first proposed by Westervelt and shortly thereafter it was demonstrated experimentally by Berktay.[2,3] A number of theoretical and experimental investigations followed, most of which emphasized demonstrating the existence of the phenomenon and developing and validating mathematical models to describe the basic physics of the process.[4-13]

The operation of the PARRAY is illustrated schematically in Fig. 1. A continuous, high frequency acoustic wave, symbolized by the closely spaced, concentric arcs, is projected from one of the transducers (pump) to the second transducer (hydrophone), which is located a distance L from the pump. A low frequency acoustic wave, represented by the widely spaced diagonal lines, propagates through the area and interacts nonlinearly with the pump wave to generate modulation sidebands of the pump signal. The phasing of this interaction process is such that a continuous, end-fire array of length L is synthesized in the interaction volume between the pump and hydrophone. The maximum response of the synthesized end-fire array is in the direction of a line extending from the hydrophone through the pump. It is this end-fire array effect that provides the directivity of the PARRAY and hence its ability to discriminate against low frequency ambient noise that otherwise masks the signal wave.

Ideally, the pump signal is a pure sinusoid of frequency f_p; however, in practice, the characteristic spectrum of the pump signal is similar to that shown in the box at the upper left. The level of the sideband noise is dependent on the quality of the signal generation equipment, i.e., on the spectral purity of the pump electronics. As a result of the nonlinear mixing in the water, the pump signal spectrum is modulated by the signal frequency spectrum and contains the signal frequency information in the upper and lower sidebands $(f_p \pm f_s)$, illustrated in the box at the lower right of Fig. 1.
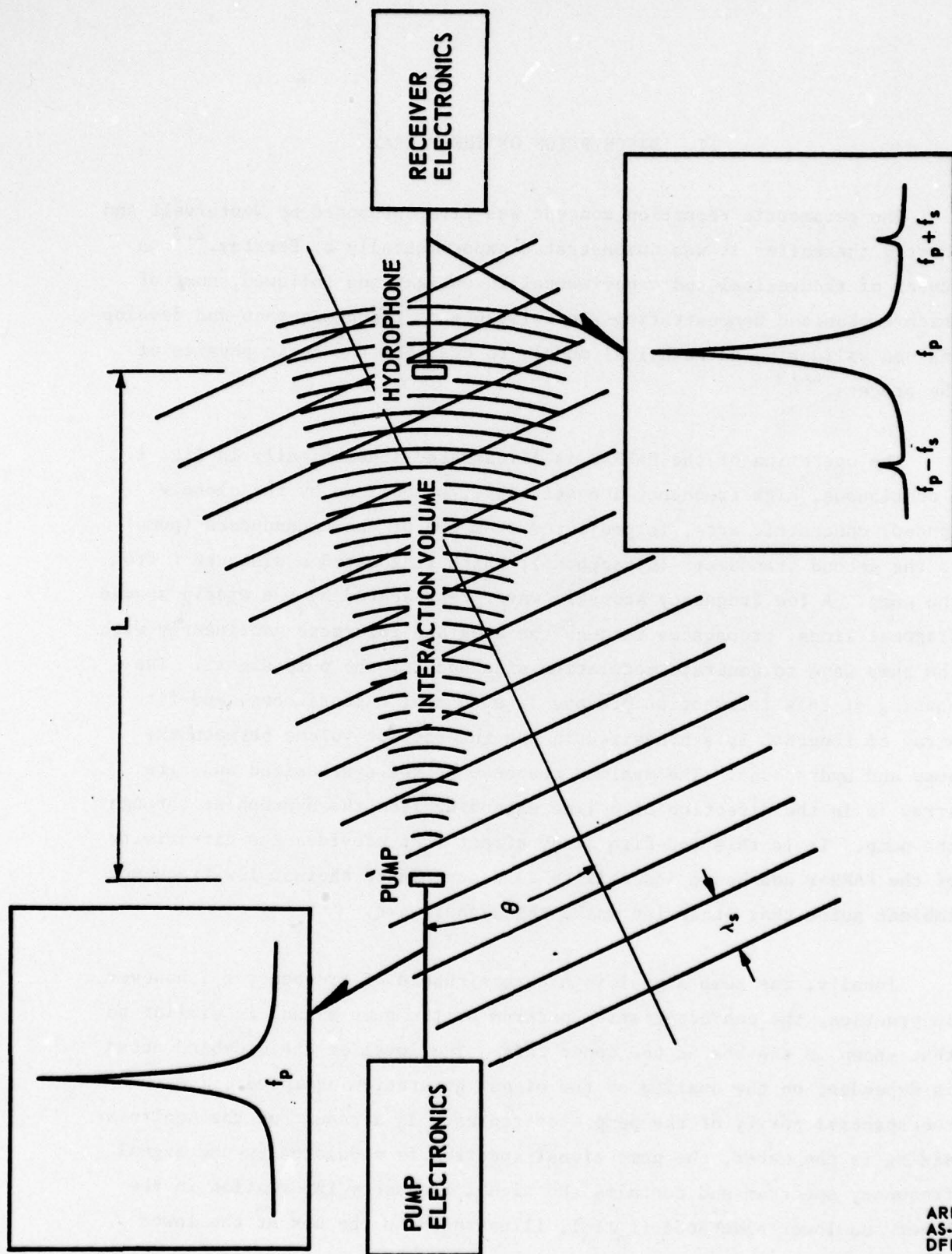
FIGURE 1
PARRAY FUNCTIONAL DIAGRAM

The directional response of the PARRAY, which is similar to that of a continuous, end-fire array of length L, is given by[6]

$$D(\theta) = \frac{\beta - (1-\cos\theta)}{\beta} \frac{\sin[(kL/2)(1-\cos\theta)]}{(kL/2)(1-\cos\theta)} \quad , \tag{1}$$

where

   θ is the plane angle measured from the line joining the pump and hydrophone,

   k is the acoustic wave number of the signal to be detected,

   L is the pump-hydrophone separation, and

   β is the coefficient of nonlinearity of the medium, approximately equal to 3.5 in sea water.

The value of β is approximately 8% less in fresh water than in sea water.[14,15]

The directional response of the PARRAY is symmetric about the line joining the pump and hydrophone, i.e., the PARRAY has a conical beam pattern. The half-power beamwidth of the PARRAY, in degrees, is given approximately by

$$\theta = 105\sqrt{\lambda/L} \quad , \tag{2}$$

where λ is the acoustic wavelength of the signal to be detected. These characteristics are illustrated in Fig. 2, which shows the directional response of the PARRAY for a kL of 33π. Since the directional response of the PARRAY is symmetric about the line joining the pump and hydro-phone, the beam pattern is the same in both the vertical and horizontal planes.

The detection of low frequency signals from a distant source is closely related to the ability of the acoustic sensor to discriminate against low frequency ambient noise and thus to improve the signal-to-noise ratio (S/N) compared to a simple, omnidirectional sensor. One
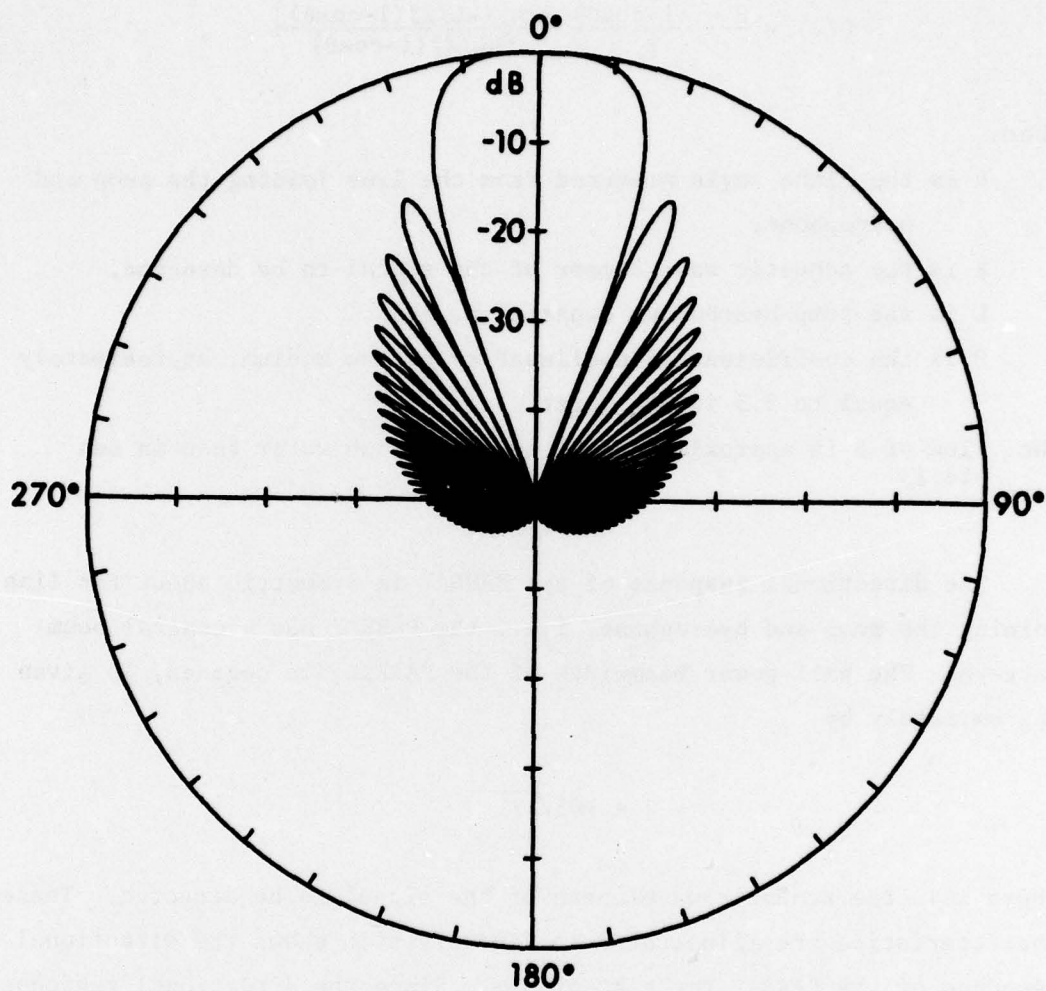
5

FIGURE 2
DIRECTIONAL RESPONSE FUNCTION OF PARRAY
$kL = 33\pi$

6

measure of the S/N improvement of an acoustic sensor is spatial
processing gain (SPG). The SPG of an acoustic sensor is given by

$$SPG = \frac{\int_{4\pi} N(\theta,\phi)d\Omega}{\int_{4\pi} b(\theta,\phi) \, N(\theta,\phi)d\Omega} \quad , \tag{3}$$

where $b(\theta,\phi)$ is the directional response function of the acoustic sensor,
$N(\theta,\phi)$ is the noise power per unit solid angle, and the integral is over
4π steradians. If $N(\theta,\phi)$ is a constant, i.e., if the noise is isotropic,
Eq. (3) reduces to the familiar expression for the DI of the acoustic
sensor,

$$DI = 10 \, \log \frac{4\pi}{\int_{4\pi} b(\theta,\phi)d\Omega} \quad . \tag{4}$$

Although the ambient noise field is rarely isotropic, the DI is a
convenient and useful measure for the first order comparisons of
different acoustic sensors. The DI of the PARRAY is given by

$$DI = 10 \, \log[1.86+4L/\lambda] \quad .$$

The lower curve in Fig. 3 shows the DI of the PARRAY as a function of
the pump-hydrophone separation in wavelengths.

The front-to-back ratio (F/B) of the PARRAY is also a function of
the acoustic aperture. For $kL>1$, the ratio of the maximum response of
the PARRAY to the envelope of the back lobes is given by (in decibels)

$$F/B_{dB} = 20 \, \log(7kL/3) \quad .$$
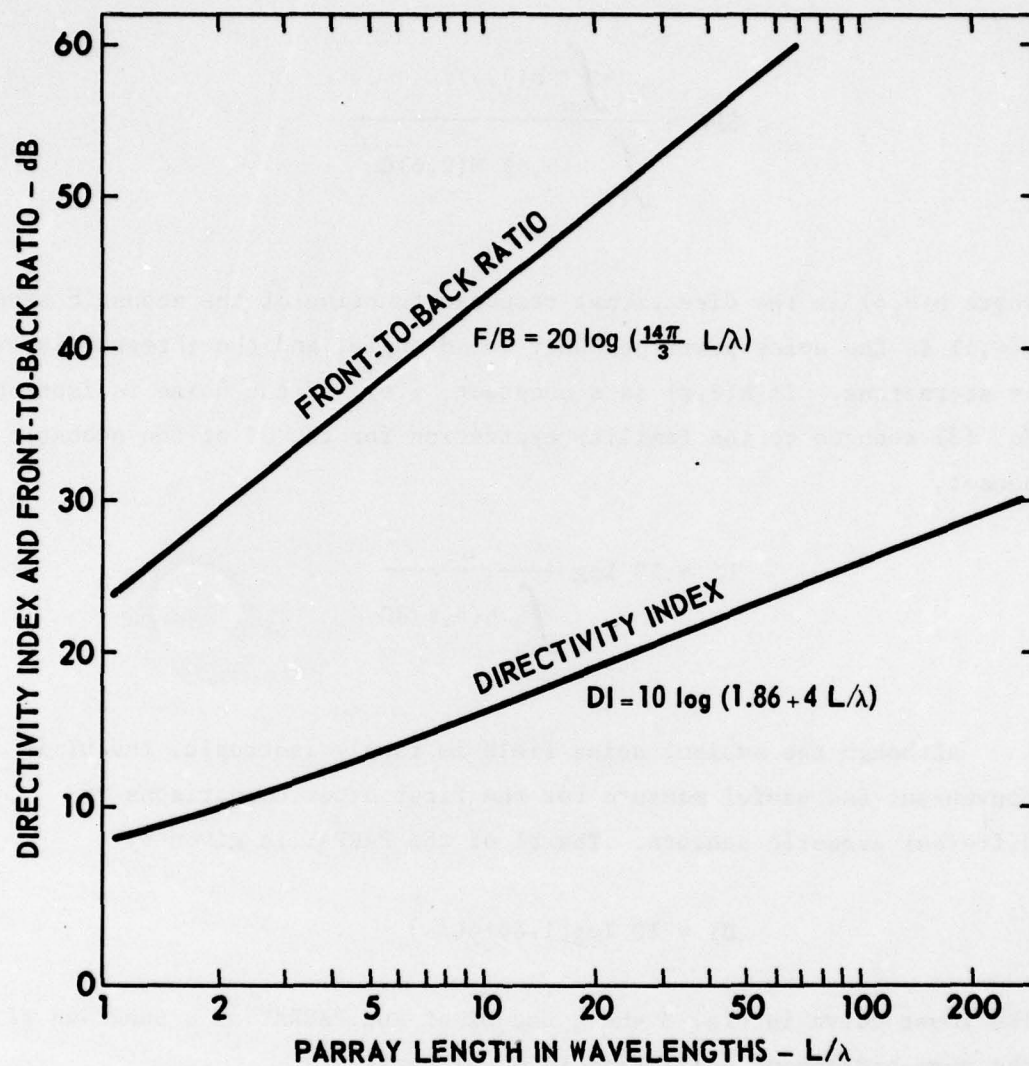
7

FIGURE 3
DIRECTIVITY INDEX AND FRONT-TO-BACK RATIO OF THE PARRAY
AS A FUNCTION OF ACOUSTIC APERTURE IN WAVELENGTHS (L/λ)

8

The F/B of the PARRAY is shown in the upper curve in Fig. 3. It should
be noted that both the DI and the F/B of the PARRAY are functions of the
acoustic aperture and hence do not depend upon the pump frequency.

Several desirable characteristics derive from the fact that the
PARRAY is essentially a continuous, end-fire array synthesized in the
water.

- Vertical Directivity - Since the directional response is
  symmetric about the line joining the pump and hydrophone, the
  PARRAY provides vertical as well as horizontal discrimination
  against noise.

- No Grating Lobes - Grating lobes are not generated as the signal
  frequency increases because the PARRAY is a continuous end-fire
  array.

- Good Sidelobe Behavior - The sidelobes are well behaved and
  decrease monotonically to a minimum on the back side of the
  PARRAY.

- High Front-to-Back Ratio - The PARRAY is relatively insensitive
  to signals arriving from the back side.

- Wide Bandwidth - The PARRAY is inherently wideband because the
  heterodyne process translates the absolute bandwidth of the high
  frequency transducers to the low frequency signal region.

- Minimum Number of Transducers - Two relatively small high
  frequency transducers are required to form the PARRAY because
  the nonlinearity of the water is exploited to synthesize the
  array in the region between the transducers.

9

III. SUMMARY OF APPENDICES

Although a number of researchers investigated the parametric
reception process in the decade following Westervelt's proposal, by the
end of that period parametric reception was considered by most researchers
to be an academic novelty. It was recognized, however, that if the PARRAY
were to become more than an academic novelty, systematic methods would
have to be developed to select optimal parameter values within the con-
straints of existing engineering technology. Studies conducted at Applied
Research Laboratories, The University of Texas at Austin (ARL:UT), by one
of the authors addressed this problem. Techniques and analytical models
were developed to permit selection of optimal parameter values within the
existing engineering state of the art for electronics and transducers. A
paper describing these techniques was presented at The 88th Meeting of
The Acoustical Society of America in St. Louis, Missouri, on 4-8 November
1974. The text of this paper is included as Appendix A of this report.

As a result of the investigation of optimal parameter selection
techniques, four major technology areas were identified in which signifi-
cant development of the state of the art was required. To test the
hypotheses involved in the parameter selection process, an experimental
PARRAY was assembled at Lake Travis Test Station (LTTS) of ARL:UT. Some
new electronic equipment was constructed and some existing equipment was
modified for the purpose. Experiments were performed that confirmed the
importance of one of the parameters, namely, spectral purity of the pump
signal. Results of these experiments were reported at The 89th Meeting
of The Acoustical Society of America in Austin, Texas, on 8-11 April 1975.
The text of this paper is included as Appendix B.

As a result of the above studies, a program to develop an experimental
large aperture PARRAY was begun at ARL:UT. The effort was structured as

11

an integrated program of analysis, experiments, hardware design, fabrication, lake testing, and sea testing. Four major hardware development areas were addressed: high spectral purity pump signal generation; commensurate power amplification; high efficiency, high power transducer element and array design; and detection of sideband signals with very small modulation indices.

A band elimination processor was developed to suppress the high level pump (carrier), amplify the low level sideband signals, and detect the information in the sidebands. The processor is capable of detecting signals with carrier to sideband ratios approaching 180 dB. This receiver was described in a paper presented at The 92nd Meeting of The Acoustical Society of America in San Diego, California, on 16-19 November 1976. The text of this paper is included as Appendix C.

In the PARRAY, the equivalent input noise (and hence the minimum signal that can be detected) is dependent upon the spectral purity of the pump signal source. Since commercial oscillators with adequate spectral purity were not available, a high spectral purity, crystal controlled oscillator was developed for the experimental PARRAY. Spectral purity of this oscillator is approximately four orders of magnitude better than commercially available oscillators in the 65 kHz frequency region. A paper describing this oscillator was presented at The 92nd Meeting of The Acoustical Society of America in San Diego, California, on 16-19 November 1976 and is included as Appendix D.

The PARRAY places a premium on high efficiency transducers capable of continuous operation at high power levels. In addition, the transducers must not generate spurious noise that will degrade the spectral purity of the pump signal and mask the low level sideband signals. A simple, efficient transducer element design was developed and several transducers consisting of up to 432 elements were constructed for use in the experimental PARRAY. A paper describing this development was presented at The 92nd Meeting of The Acoustical Society of America in

San Diego, California, on 16-19 November 1976. A somewhat revised
version of this paper was presented at a specialists meeting of the
Underwater Acoustics Group, The Institute of Acoustics, at The
University of Birmingham, Birmingham, England, on 15 December 1976 and
was published in the Proceedings of that meeting. Copies of these
papers are included as Appendices E and F, respectively.

To develop an optimum design for a PARRAY receiver preprocessor, it
is important to have an analytical model of the parametric reception
process expressed in familiar signal processing terms. Since there was
some diversity in the modulation processes expressed in the different
published forms of the parametric reception models, experiments were
performed to directly measure the modulation processes involved. The
results of these measurements were presented at The 92nd Meeting of The
Acoustical Society of America in San Diego, California, on 16-19 November
1976. A copy of this paper is included as Appendix G.

The PARRAY exhibits sensitivity to motion of its transducers in a
manner significantly different from that of conventional linear arrays.
This sensitivity must be understood to evaluate those applications of
the PARRAY where the transducers may be subjected to vibration. A theory
was developed that relates motion of the PARRAY transducers to signal out
of the PARRAY and experiments were performed to verify the analytical
model. The results of this investigation were reported at the 1978 IEEE
International Conference on Acoustics, Speech, and Signal Processing at
Tulsa, Oklahoma, on 10-12 April 1978. A copy of the paper was published
in the Record of that conference and is included as Appendix H.

An experimental PARRAY with a 340 m pump-hydrophone separation was
installed in 45 m of water in Lake Travis (Texas). The PARRAY operated
over the 35 to 800 Hz frequency range and demonstrated that the self-
noise level of the experimental PARRAY is below the ambient noise level
in this environment. Some of the results of measurements with the

experimental PARRAY were reported at The 96th Meeting of The Acoustical
Society of America in Honolulu, Hawaii, on 27 November - 1 December 1978.
These same basic results were presented at the 1979 IEEE International
Conference on Acoustics, Speech, and Signal Processing in Washington, DC,
on 2-4 April 1979. A copy of that paper was published in the Record of
that conference and is included as Appendix I.

REFERENCES

1. Tommy G. Goldsberry et al., "Development and Evaluation of an Experimental Parametric Acoustic Receiving Array (PARRAY)", Applied Research Laboratories Technical Report No. 79-5 (ARL-TR-79-5), Applied Research Laboratories, The University of Texas at Austin, 16 February 1979.

2. P. J. Westervelt, "Parametric acoustic array", J. Acoust. Soc. Am. $\underline{35}$, 535-537 (1963).

3. H. O. Berktay, "Parametric amplification by the use of acoustic non-linearities and some possible applications", J. Sound Vib. $\underline{2}$, 462-470 (1965).

4. H. Date and Y. Tozuka, "Parametric Directional Microphones", Proceedings of The 6th International Congress on Acoustics, Tokyo, Japan, 21-28 August 1968.

5. H. O. Berktay and C. A. Al-Temimi, "Virtual arrays for underwater reception", J. Sound Vib. $\underline{9}$, 295-307 (1969).

6. V. A. Zverev and Z. I. Kalachev, "Modulation of sound by sound in the intersection of sound waves", Soviet Phys.-Acoust. $\underline{16}$, 204-208 (1970).

7. W. L. Konrad, R. H. Mellen, and M. B. Moffett, "Parametric Sonar Receiving Experiments", NUSC TM No. PA4-304-71, Naval Underwater Systems Center, New London, Connecticut, 9 December 1971.

8. G. R. Barnard, J. G. Willette, J. J. Truchard, and J. A. Shooter, "Parametric acoustic receiving array", J. Acoust. Soc. Am. $\underline{52}$, 1437-1441 (1972).

9. H. O. Berktay and T. G. Muir, "Arrays of parametric receiving arrays", J. Acoust. Soc. Am. $\underline{53}$, 1377-1383 (1973).

10. H. O. Berktay and J. A. Shooter, "Parametric receivers with spherically spreading pump waves", J. Acoust. Soc. Am. $\underline{54}$, 1056-1061 (1973).

11. P. H. Rogers, A. L. Van Buren, A. O. Williams, Jr., and J. M. Barber "Parametric detection of low frequency acoustic waves in the near-field of an arbitrary directional pump transducer", J. Acoust. Soc. Am. $\underline{55}$, 528-534 (1974).

12. J. J. Truchard, "Parametric acoustic receiving array. I. Theory", J. Acoust. Soc. Am. 58, 1141-1145 (1975).

13. J. J. Truchard, "Parametric acoustic receiving array. II. Experiment", J. Acoust. Soc. Am. 58, 1146-1150 (1975).

14. R. T. Beyer, "Parameter of nonlinearity in fluids", J. Acoust. Soc. Am. 32, 719-721 (1960).

15. A. B. Coppens, Robert T. Beyer, M. B. Seiden, James Donohue, Frans Guepin, Richard H. Hodson, and Charles Townsend, "Parameter of nonlinearity in fluids, II", J. Acoust. Soc. Am. 38, 797-804 (1965).

APPENDIX A

PARAMETER SELECTION CRITERIA FOR PARAMETRIC RECEIVERS

Paper T3, Presented at The 88th Meeting of The Acoustical Society of America

4-8 November 1974, St. Louis, Missouri

PARAMETER SELECTION CRITERIA FOR PARAMETRIC RECEIVERS

Tommy G. Goldsberry
Applied Research Laboratories
The University of Texas at Austin
Austin, Texas 78712

ABSTRACT

Selection of parameters for a parametric acoustic receiver is complicated by the fact that the basic parameters are not independent. The parametric receiver is an active device; hence, there is a self-noise contribution to the output which is a function of the selected parameter values. A systematic procedure has been developed for selecting optimum values of these parameters by minimizing the total self-noise output of the parametric receiver. Equations were derived that define the impact on self-noise of the basic parameters that are not independent. These equations were evaluated to obtain optimum parameter values for specified sets of boundary conditions. The results of this analysis and examples of the parameter selection procedures are presented and discussed.

Paper T3, Presented at The 88th Meeting of The Acoustical Society of America
4-8 November 1974, St. Louis, Missouri

PARAMETER SELECTION CRITERIA FOR PARAMETRIC RECEIVERS

Tommy G. Goldsberry
Applied Research Laboratories
The University of Texas at Austin
Austin, Texas 78712

Just a little over a decade ago, Westervelt proposed nonlinear
interaction of a high frequency pump wave with an incoming low frequency
acoustic wave as a method of obtaining highly directional reception of
the low frequency wave, i.e., a parametric receiver.[1] Since that time a
number of theoretical and experimental investigations of the parametric
receiver have been conducted.[2-9] The emphasis in these studies was on
demonstrating existence of the phenomenon and on developing and validat-
ing mathematical models to describe the basic physics. Beam patterns
were obtained and the acoustic pressures of the interaction components
were measured. As is typical with basic measurements using available
laboratory equipment, the incoming low frequency signals were relatively
high amplitude signals to assure adequate signal-to-noise ratios for
reliable measurement.

Parameters for the earlier experiments were selected for compatibility
with existing equipment rather than to optimize the parametric receiver
design. However, if the parametric receiver is to progress from the status
of an academic novelty to that of a useful tool in underwater acoustics,
methods must be developed to select optimum parameter values within the
constraints of present engineering technology. This is the problem that I
wish to consider.

In many respects the parametric receiver is analogous to a heterodyne
communications receiver--a radio. In each case the incoming signal is fre-
quency translated and amplitude shifted to a more hospitable frequency region
for further processing. In each case we wish to obtain a more sensitive

21

receiver in exchange for the added complexity of the heterodyne receiver. The parametric receiver is illustrated schematically in Slide 1. The low frequency signal to be detected, symbolized by the widely spaced vertical lines, is assumed incident from the left of the figure. The high frequency pump wave, symbolized by the closely spaced concentric arcs, radiates from the pump transducer and mixes nonlinearly with the signal wave in the region between the pump and hydrophone, labeled the interaction volume. The phasing of the interaction process is such that a virtual end-fire array is formed in the region between the pump and hydrophone. It is this end-fire array effect that provides the directivity of the parametric receiver and hence its ability to discriminate against the low frequency ambient noise that otherwise might mask the signal wave.

The parametric receiver pump is analogous to the mixer oscillator in our radio. Ideally, the pump, or mixer oscillator, signal is a pure sinusoid of frequency f_p (or perhaps a perfect square wave of fundamental frequency f_p). However, in practice the characteristic spectrum of the pump signal is similar to that shown in the box at the left of the figure. The level of the sideband noise is dependent upon the quality of the signal generation equipment. The water column between the pump and hydrophone is the nonlinear element in the parametric receiver. It is analogous to the mixer diode in the radio. Unfortunately--or fortunately, depending upon one's viewpoint--the water is weakly nonlinear. Thus, where conversion efficiencies of near 100% are common in radio mixers, conversion efficiencies of 1% or less are the norm for the parametric receiver.

As a result of the nonlinear mixing in the water, at the hydrophone the pump signal spectrum has been modulated by the signal frequency spectrum, and contains that information as the upper and lower sidebands ($f_p \pm f_s$), as illustrated in the box at the upper right. To complete the analogy, the hydrophone and receiver electronics serve the purpose of the IF amplifier, detectors, etc., in processing the signal frequency information for display.

In light of the poor conversion efficiency of the parametric receiver, many researchers have dismissed it as an interesting academic novelty without
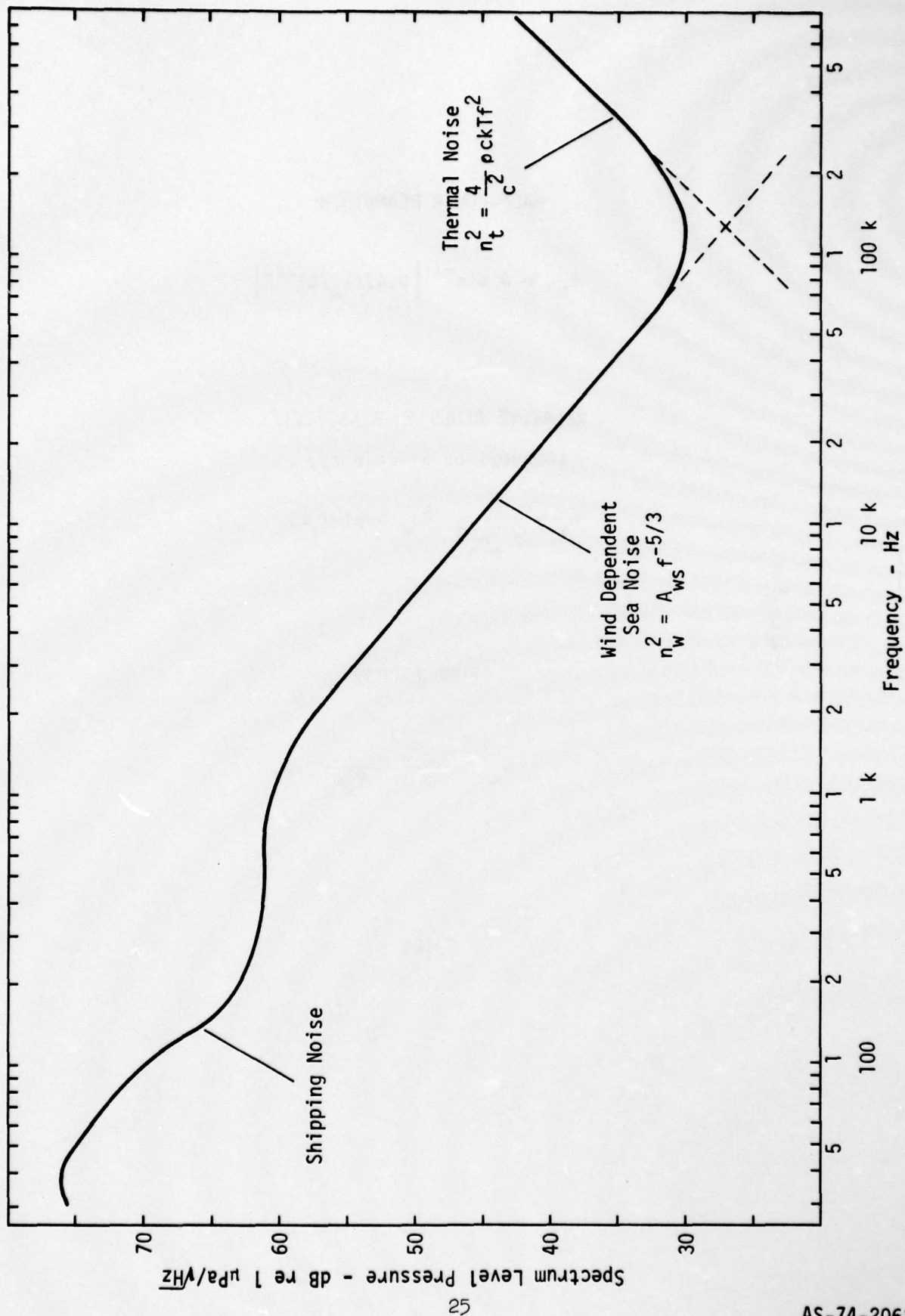
22
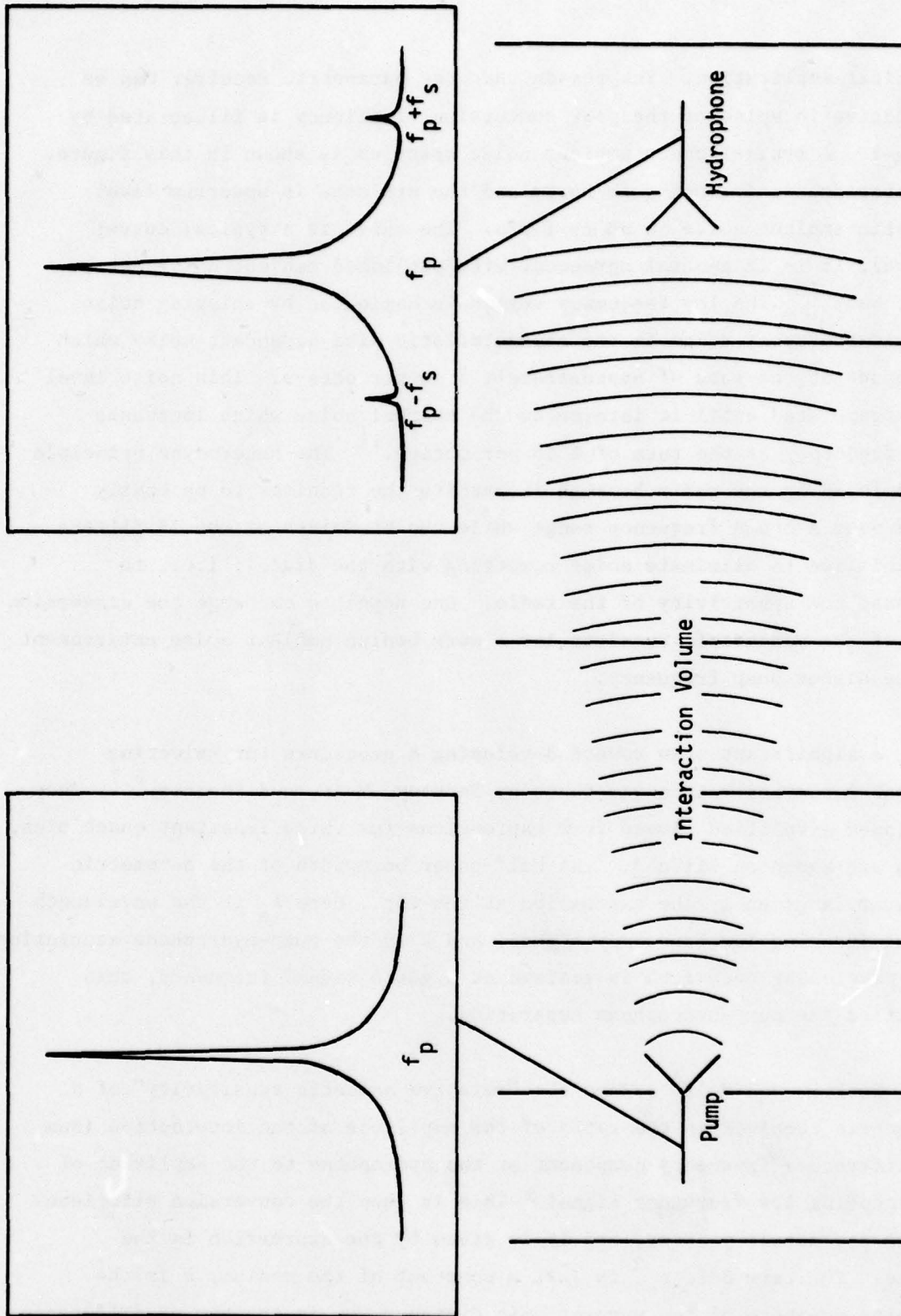
PARAMETRIC RECEIVER FUNCTIONAL DIAGRAM

AS-74-2076
TGG-0166-7

SLIDE 1

practical application. The reason that the parametric receiver can be
attractive in spite of the poor conversion efficiency is illustrated by
Slide 2. A typical ocean ambient noise spectrum is shown in this figure.
The abscissa is frequency in hertz and the ordinate is spectrum level
acoustic ambient noise in dB re 1 μPa. The curve is a typical curve;
however, it is in general agreement with published ambient noise data,
e.g., Wenz.[10] The low frequency region is dominated by shipping noise.
The mid-frequency range is the characteristic wind dependent noise which
decreases at the rate of approximately 5 dB per octave. This noise level
is extrapolated until it intersects the thermal noise which increases
with frequency at the rate of 6 dB per octave.[11] The heterodyne principle
is employed in the radio because it permits the receiver to be easily
tuned over a broad frequency range while the bandwidth of the IF filters
is minimized to eliminate noise competing with the signal; i.e., to
increase the sensitivity of the radio. One hopes to exchange the conversion
loss of the parametric receiver for a more benign ambient noise environment
at the higher pump frequency.

A significant step toward developing a procedure for selecting
optimal parameter values was taken by Berktay, Muir, and Shooter.[6,7] They
developed simplified closed form expressions for three important quantities,
which are shown on Slide 3. The half-power beamwidth of the parametric
receiver is given by the expression at the top. Here λ_s is the wavelength
of the incoming low frequency signal, and L is the pump-hydrophone separation.
If a particular beamwidth is desired at a given signal frequency, this
specifies the pump-hydrophone separation.

Berktay and Muir[6] define the "relative acoustic sensitivity" of a
parametric receiver as the ratio of the amplitude of the interaction (sum
or difference) frequency component at the hydrophone to the amplitude of
the incoming low frequency signal. This is then the conversion efficiency
of the parametric process, and it is given by the expression in the
middle. The term $\beta/2\rho_o c_o^3$ is just a constant of the medium, P is the
acoustic pressure of the pump at unit distance, $\omega_{\pm}$ is the sum or difference

24

Thermal Noise
$n_t^2 = \frac{4}{c^2} \pi \rho c k T f^2$

Wind Dependent
Sea Noise
$n_w^2 = A_{ws} f^{-5/3}$

Shipping Noise

Spectrum Level Pressure – dB re 1 μPa/$\sqrt{Hz}$

Frequency – Hz

TYPICAL OCEAN AMBIENT NOISE SPECTRUM

25

HALF-POWER BEAMWIDTH

$$\theta_{HP} = 4 \sin^{-1}\left[0.47(\lambda_s/L)^{1/2}\right]$$

RELATIVE ACOUSTIC SENSITIVITY

(Conversion Efficiency)

$$s_r = \frac{\beta}{2\rho_o c_o^3}\ P\omega_{\pm}\ \exp(-\alpha_{\pm}L)$$

PUMP EXCESS

$$e_x = \frac{2\rho_o c_o^3}{\beta}\ \frac{1}{LP_s\omega_{\pm}}$$

SLIDE 3

26

frequency, $\alpha_{\pm}$ is the absorption coefficient of the water at the sum or difference frequency, and L is the pump-hydrophone separation. Pump excess is defined as the ratio of the amplitude of the pump frequency signal to the amplitude of the sum or difference frequency signal, both measured at the hydrophone. Pump excess is given by the bottom expression where the first term, L, and $\omega_{\pm}$ are as defined above. The acoustic pressure of the incoming signal is denoted P_s. Pump excess is a measure of the pump rejection requirements of the receiver electronics and of the spectral purity requirements for the pump signal.

An examination of the equations for θ_{HP}, s_r, and e_x illustrates the conflicting design requirements of the parametric receiver. The conversion efficiency increases with pump frequency (for a specified signal frequency) until absorption dominates. Conversion efficiency also increases as the pump-hydrophone separation is decreased, but so does pump excess and the half-power beamwidth. Pump excess is inversely proportional to the acoustic pressure of the signal wave.

To provide a method of evaluating tradeoffs in the parameter values, we will develop an expression for the plane wave equivalent noise of the parametric receiver referenced to the input to the parametric receiver, i.e., the equivalent low frequency plane wave noise at the pump. As a first step, consider the equivalent plane wave noise at the face of the hydrophone from four sources as shown in Slide 4. The first expression represents the wind dependent ambient noise pressure squared divided by the directivity factor of the hydrophone d_H. The implicit assumption is that the wind dependent noise is isotropic, which is not generally true. However, this is an acceptable approximation for the present development. The second expression is the square of the thermal noise pressure as formulated by Mellen,[11] again divided by the directivity factor of the hydrophone.

27

EQUIVALENT NOISE AT HYDROPHONE

Wind Dependent Noise

$$\frac{n_w^2}{d_H} = \frac{A_{ws} \, f_p^{-5/3}}{d_H}$$

Thermal Noise

$$\frac{n_t^2}{d_H} = \frac{1}{d_H} \frac{4\pi}{c_o^2} \rho_o c_o kT \, f_p^2$$

Receiver Electronic Noise

$$n_e^2 = \frac{4v_e^2}{m_H^2}$$

Pump Sideband Noise

$$n_{q\pm}^2 = \left[\frac{q_\pm \, P}{L} \exp(-\alpha_\pm L) \right]^2$$

SLIDE 4

28

The third expression gives the equivalent plane wave noise pressure squared corresponding to the electronic noise of the receiver electronics. The equivalent input noise, in volts, of the receiver electronics, with the impedance matched to the hydrophone, is designated v_e. The open circuit voltage sensitivity of the hydrophone is represented by m_H. The factor 4 results from the fact that the hydrophone is impedance matched to the receiver.

The last expression shows the sum or difference frequency noise at the hydrophone due to the sideband noise of the pump signal. As before, P is the pump frequency acoustic pressure at unit distance from the pump, L is the pump-hydrophone separation, and $\alpha_\pm$ is the absorption coefficient at the sum or difference frequency. The symbol $q_\pm$ represents the ratio of the sideband noise in a 1 Hz bandwidth about the sum or difference frequency to the amplitude of the pump frequency signal.

Summing these uncorrelated noises yields the expression at the top of Slide 5 for the equivalent noise pressure squared at the hydrophone in a 1 Hz bandwidth about the sum or difference frequency. This equivalent noise at the hydrophone can then be referenced to the input of the parametric receiver by dividing by the conversion efficiency of the parametric receiver, s_r. Performing the indicated operations yields the last expression. This is then the noise pressure at the signal frequency which is equivalent to the self-noise of the parametric receiver from the specified sources. The expression does not contain the low frequency ambient noise. The spatial distribution of the low frequency noise and the directivity function of the parametric receiver define the plane wave equivalent low frequency ambient noise.

The expression for equivalent input noise provides a connection between the various parameters in the parametric receiver. Thus, the gain to be achieved or the loss to be sustained from changing a parameter value can be evaluated. The last three slides very briefly illustrate this process.

29

SUM OF EQUIVALENT NOISE AT HYDROPHONE

$$n_{\Sigma H}^2 = \frac{A_{ws}f_{\pm}^{-5/3}}{d_H} + \frac{1}{d_H}\frac{4\pi}{c_o^2}\rho_o c_o kTf_{\pm}^2 + \frac{4v_e^2}{m_H^2} + \left[\frac{q_{\pm}P}{L}\exp(-\alpha_{\pm}L)\right]^2$$

EQUIVALENT INPUT NOISE OF THE PARAMETRIC RECEIVER

$$EIN = \left(\frac{n_{\Sigma H}^2}{s_r^2}\right)^{1/2}$$

$$EIN = \left\{\left[\frac{\rho_o c_o^3}{\pi\beta}\frac{\exp(\alpha_{\pm}L)}{Pf_{\pm}}\right]^2\right.$$

$$\left.\times\left[\frac{1}{d_H}\left(A_{ws}f_{\pm}^{-5/3} + \left(\frac{4\pi}{c_o^2}\rho_o c_o kT\right)f_{\pm}^2\right) + \frac{4v_e^2}{m_H^2}\right] + \left(\frac{\rho_o c_o^3}{\pi\beta}\frac{q_{\pm}}{Lf_{\pm}}\right)^2\right\}^{1/2}$$

SLIDE 5

The equivalent input noise of the parametric receiver as a function of pump frequency for three different pump-hydrophone separations is shown in Slide 6. The abscissa is the pump frequency in kilohertz and the ordinate is the equivalent input noise of the parametric receiver obtained by evaluating the expression on the previous slide. The values of all parameters except the pump-hydrophone separation (array length, L) are the same for each of the curves. It may be seen that there is an optimum pump frequency for each array length. We also note that the equivalent input noise increases and the optimum pump frequency decreases as the pump-hydrophone separation increases.

The effect of pump source level on the equivalent input noise is illustrated in Slide 7. The format is the same as in the previous slide except that the pump-hydrophone separation remains constant and the pump source level is allowed to vary. We note here that the equivalent input noise decreases as the pump source level increases, as expected. The optimum pump frequency also shifts upward slightly with increasing pump source level.

The effect of pump spectral purity is illustrated in Slide 8. Again, the format is the same as for the previous two slides except that the pump sideband noise level is the parameter that is varied. As one would expect, the equivalent input noise decreases as the pump sideband noise level is reduced. The optimum pump frequency also shifts downward slightly as the spectral purity of the pump signal is improved.

31
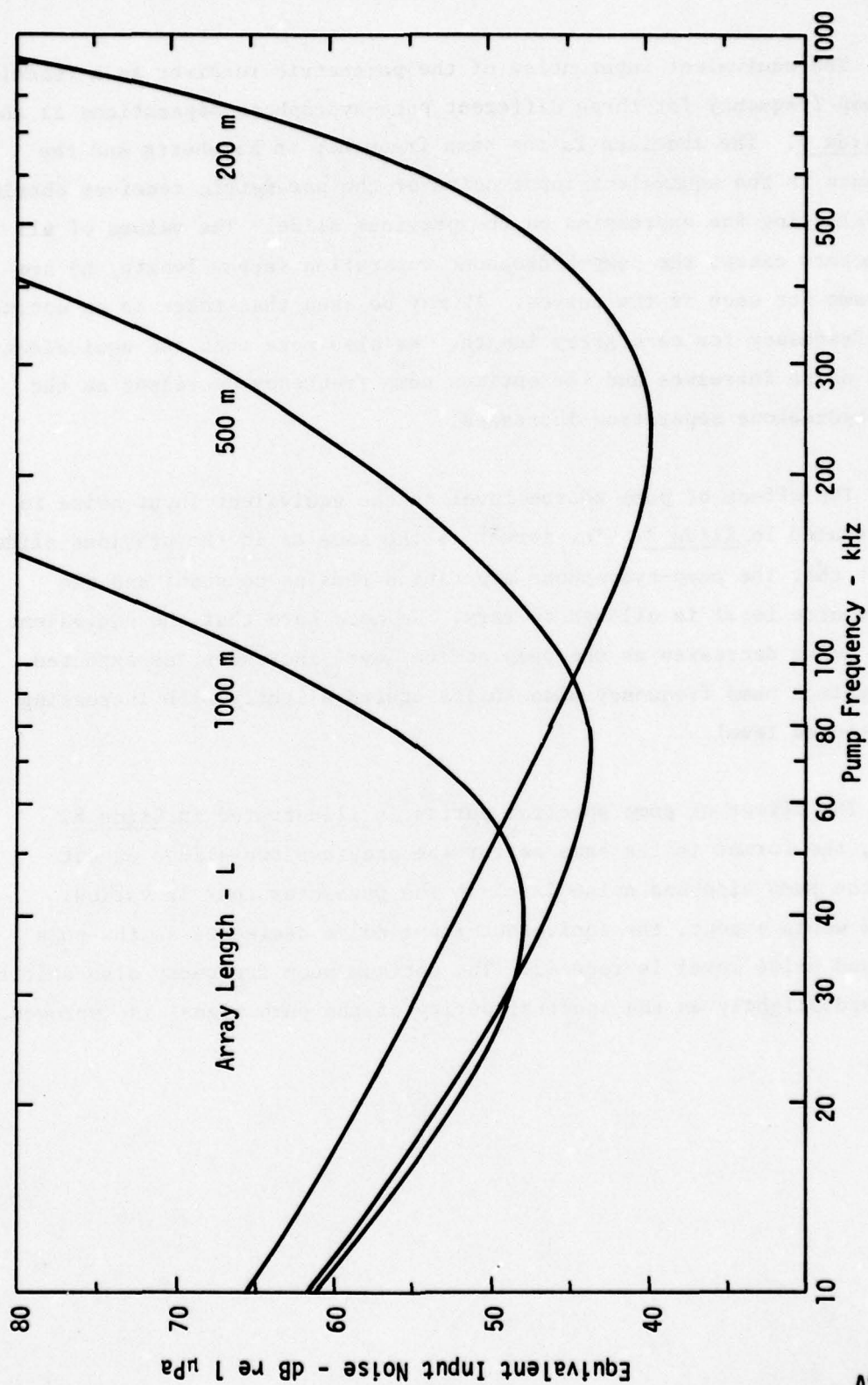
EQUIVALENT INPUT NOISE OF THE PARAMETRIC RECEIVER FOR DIFFERENT ARRAY LENGTHS
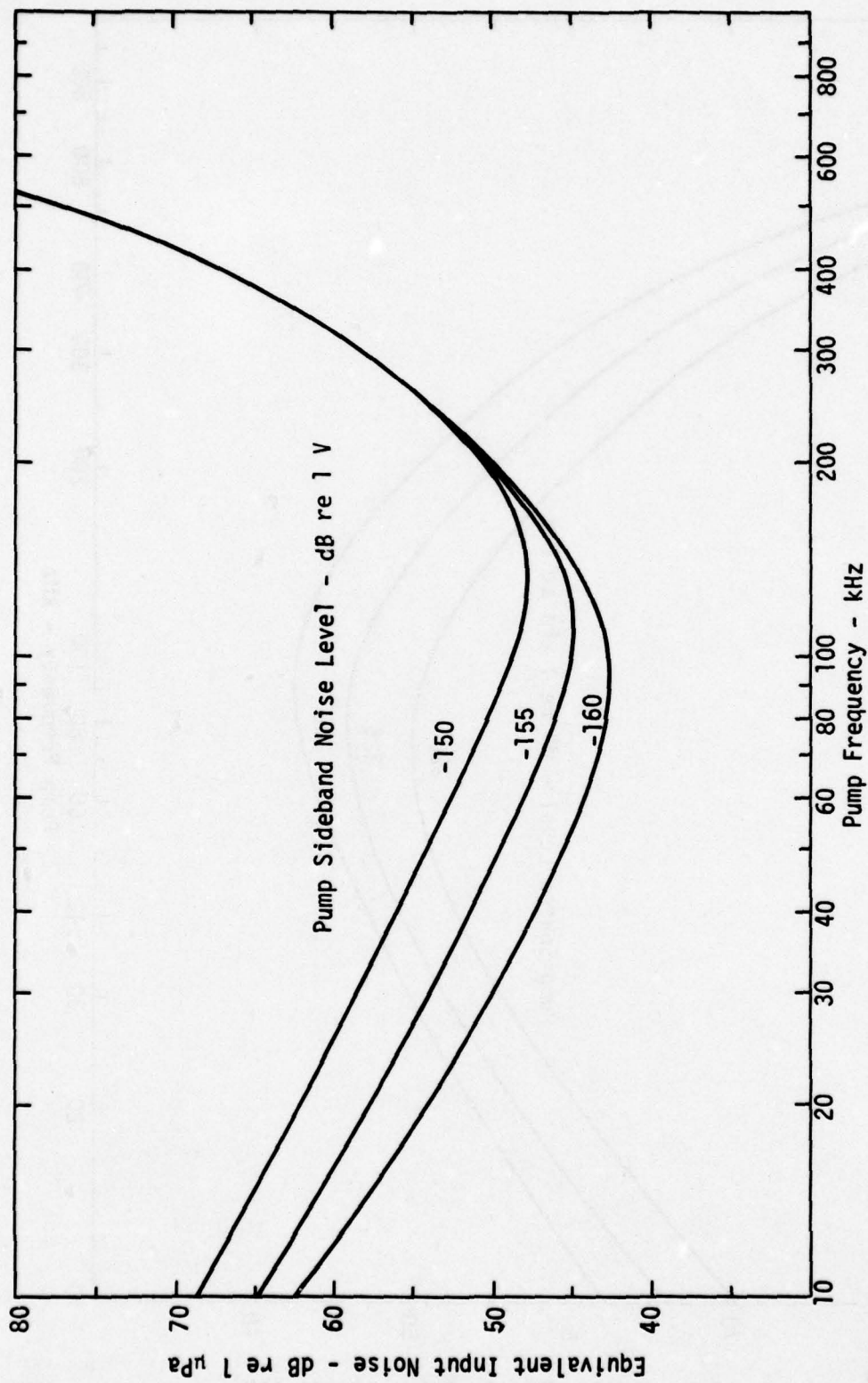
AS-74-2077
TGG-0166-7

SLIDE 6
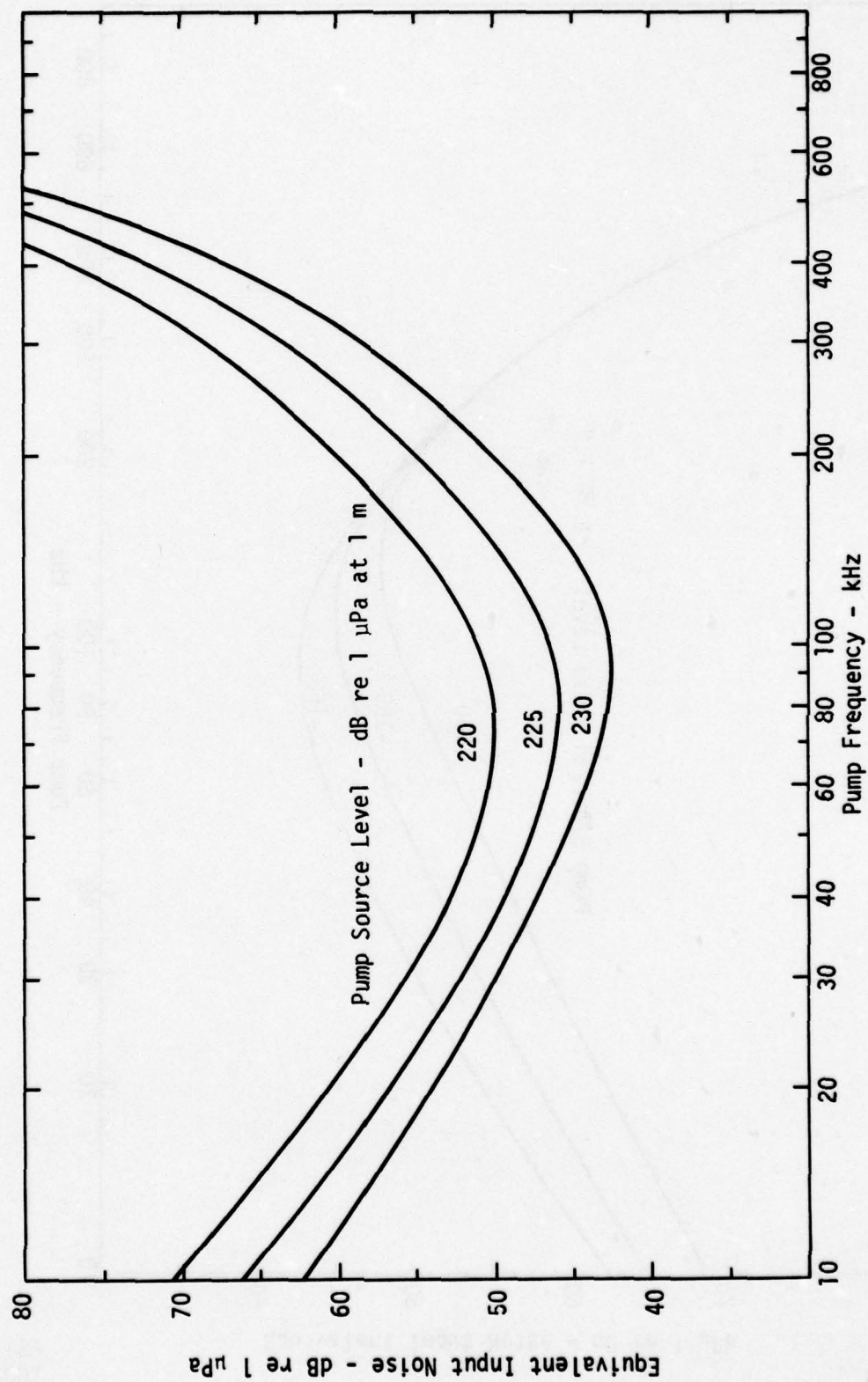
EQUIVALENT INPUT NOISE OF THE PARAMETRIC RECEIVER FOR VARIOUS PUMP SOURCE LEVELS

AS-74-2078
TGG-0166-7

33

SLIDE 7

EQUIVALENT INPUT NOISE OF THE PARAMETRIC RECEIVER FOR VARIOUS PUMP SIDEBAND NOISE LEVELS

AS-74-2079
TGG-0166-7

34

SLIDE 8

SUMMARY AND CONCLUSIONS

A systematic procedure has been presented that permits selection of optimum parameter values for the parametric receiver in the context of a specified set of boundary conditions. Not all noise sources have been explicitly considered in the analysis. For example, noise due to pump reflections from boundary surfaces or scattering by inhomogeneities in the medium are ignored in the present analysis. The procedure can be extended in a straightforward manner to account for these noise sources when models for these effects are developed. The expression for equivalent input noise as developed applies to spherically spreading pump waves. Again the extension to collimated pumps is straightforward.

35

REFERENCES

1. P. J. Westervelt, "Parametric Acoustic Array", J. Acoust. Soc. Am. 35, 535-537 (1963).

2. H. O. Berktay, "Parametric Amplification by the Use of Acoustic Non-Linearities and Some Possible Applications", J. Sound Vib. 2, 462-470 (1965).

3. H. O. Berktay and C. A. Al-Temimi, "Virtual Arrays for Underwater Reception", J. Sound Vib. 9, 295-307 (1969).

4. W. L. Konrad, R. H. Mellen, and M. B. Moffett, "Parametric Sonar Receiving Experiments", NUSC Tech. Memo. PA4-304-71, Naval Underwater Systems Center, 9 December 1971.

5. G. R. Barnard, J. G. Willette, J. J. Truchard, and J. A. Shooter, "Parametric Acoustic Receiving Array", J. Acoust. Soc. Am. 52, 1437-1441 (1972).

6. H. O. Berktay and T. G. Muir, "Arrays of Parametric Receiving Arrays", J. Acoust. Soc. Am. 53, 1377-1383 (1973).

7. H. O. Berktay and J. A. Shooter, "Parametric Receivers with Spherically Spreading Pump Waves", J. Acoust. Soc. Am. 54, 1056-1061 (1973).

8. P. H. Rogers, A. L. Van Buren, A. O. Williams, Jr., and J. M. Barber, "Parametric Detection of Low Frequency Acoustic Waves in the Nearfield of an Arbitrary Directional Pump Transducer", J. Acoust. Soc. Am. 55, 528-534 (1974).

9. J. J. Truchard, "A Theoretical and Experimental Investigation of the Parametric Acoustic Receiving Array", Applied Research Laboratories Technical Report No. 74-17 (ARL-TR-74-17), Applied Research Laboratories, The University of Texas at Austin, May 1974 (also PhD dissertation, The University of Texas at Austin, May 1974).

10. G. M. Wenz, "Acoustic Ambient Noise in the Ocean: Spectra and Sources", J. Acoust. Soc. Am. 34, 1936-1956 (1962).

11. R. H. Mellen, "The Thermal Noise Limit in the Detection of Underwater Acoustic Signals", J. Acoust. Soc. Am. 24, 478-480 (1952).

APPENDIX   B

NOISE IN PARAMETRIC RECEIVERS

Paper II 6, Presented at The 89th Meeting of The Acoustical Society of America

8-11 April 1975, Austin, Texas

NOISE IN PARAMETRIC RECEIVERS

Tommy G. Goldsberry
Applied Research Laboratories
The University of Texas at Austin
Austin, Texas   78712

ABSTRACT

Interfering noise sources that limit the sensitivity of a
parametric receiver were discussed at the last meeting of this
Society [T. G. Goldsberry, J. Acoust. Soc. Am. 56, S41 (Fall,
1974)]. The individual noise sources in an experimental
parametric receiver have been measured to test the hypotheses
presented in that paper. The predicted effect of these noise
sources on sensitivity is compared to the measured performance
of the parametric receiver. Factors that limited the sensi-
tivity of the experimental parametric receiver are discussed.

41

NOISE IN PARAMETRIC RECEIVERS

Tommy G. Goldsberry
Applied Research Laboratories
The University of Texas at Austin
Austin, Texas 78712

At the last meeting of this Society, equations were presented that permit the self-noise of a parametric receiver to be predicted from measurements of the noise characteristics of the component parts of the parametric receiver.[1] At that time an analogy was drawn between the parametric receiver and a heterodyne radio receiver; i.e., pump-mixer oscillator, water-mixer diode, pump rejection filters-IF filters, demodulator-detector, etc. The sensitivity of a radio is characterized in terms of an equivalent noise level at the input that produces a noise level at the output equal to the sum of the noise sources within the radio. In a similar fashion, the equivalent noise pressure at the face of a conventional hydrophone is that plane wave noise pressure that produces a noise voltage at the output terminals equivalent to the internal noise generated within the hydrophone. Combining these ideas, since the parametric receiver is an active device, leads to the concept of an equivalent input noise for a parametric receiver. Thus the equivalent input noise of a parametric receiver is defined as the plane wave noise pressure at the input of the parametric receiver (i.e., at the pump) that produces an output noise equal to the sum of the noise sources within the parametric receiver.

The development of any equation to describe a physical phenomenon has behind it the intention of performing an experiment to test the validity of the equation. Such an experiment was performed to test the validity of the equations developed in the earlier paper. To discuss

43

the results of that experiment an intermediate result from that paper is required. The first four expressions in Fig. 1 describe the plane wave equivalent noise pressure at the face of the hydrophone due to the labeled noise source. The numerator of Eq. (1) is just the usual wind dependent noise which decreases with frequency at approximately 5 dB per octave. In this equation, $f_{\pm}$ represents the pump frequency, d_H represents the hydrophone directivity, and A_{ws} is the constant primarily dependent upon the wind speed. The equivalent plane wave noise pressure at the hydrophone due to thermal noise is given by Eq. (2), which is just the thermal noise expression derived by Mellen[2] divided by the directivity of the hydrophone. The equivalent plane wave noise pressure at the face of the hydrophone due to the electronic noise of the receiver electronics is given by Eq. (3). The open circuit voltage sensitivity of the hydrophone including any impedance matching network is represented by M_h, and V_e represents the equivalent electronic noise at the input to the receiver electronics. The factor 4 results from the fact that the hydrophone is impedance matched to the receiver electronics.

The effect of spectral purity of the pump signal is shown in Eq. (4), which is an expression for the plane wave equivalent noise pressure at the face of the hydrophone due to the sideband noise of the pump. The ratio of the amplitude of the sideband noise at the sum or difference frequency to the amplitude of the pump signal is denoted by $q_{\pm}$, the pump amplitude at unit distance is represented by P, the pump-hydrophone separation is represented by L, and $\alpha_{\pm}$ is the absorption coefficient at the sum or difference frequency. In the specification of $q_{\pm}$, a bandwidth is implicit and that bandwidth is taken as 1 Hz.

The noise sources above are uncorrelated; therefore, the plane wave equivalent noise pressure at the face of the hydrophone due to all of these sources is given by the expression in Eq. (5). This expression can be used to select parameter values to minimize the self-noise of the parametric receiver. Conversely, if the parameter values are fixed and subsystem characteristics are known, the self-noise of the parametric receiver can be calculated from the expression in Eq. (5).

44

EQUIVALENT NOISE AT HYDROPHONE

Wind Dependent Noise

$$\frac{n_w^2}{d_H} = \frac{A_{ws}f_\pm^{-5/3}}{d_H} \tag{1}$$

Thermal Noise

$$\frac{n_t^2}{d_H} = \frac{1}{d_H} \frac{4\pi}{c_o^2} \rho_o c_o kTf_\pm^2 \tag{2}$$

Receiver Electronic Noise

$$n_e^2 = \frac{4v_e^2}{m_H^2} \tag{3}$$

Pump Sideband Noise

$$n_{q\pm}^2 = \left[\frac{q_\pm P}{L} \exp(-\alpha_\pm L) \right]^2 \tag{4}$$

SUM OF EQUIVALENT NOISE AT HYDROPHONE

$$n^2{}_H = \frac{A_{ws}f_\pm^{-5/3}}{d_H} + \frac{1}{d_H} \frac{4\pi}{c_o^2} \rho_o c_o kTf_\pm^2 + \frac{4v_e^2}{m_H^2} + \left[\frac{q_\pm P}{L} \exp(-\alpha_\pm L) \right]^2 \tag{5}$$

FIGURE 1

45

The latter situation existed for our experiment. A block diagram of the experimental system is shown in Fig. 2. The crystal oscillator, power amplifier, transducers, and the crystal filters used in the receiver were from earlier Doppler signature studies. The availability of these pieces of equipment dictated the pump frequency, maximum source level, and spectral purity of the pump signal. The signal source was a 60 kHz single frequency crystal oscillator. The power amplifier was a solid state class AB amplifier with an output of approximately 100 W. Three lead-acid storage batteries served as the power supply for the amplifier. The vertical and horizontal beamwidths of the transducers were 3.0° and 4.7°, respectively. The crystal filters were bandpass filters with a nominal 3 dB bandwidth of 250 Hz. A balanced modulator and low-pass filter were used to translate the sideband signals to base-band for spectral analysis. Narrowband analysis was performed by a spectrum analyzer with a nominal bandwidth of 1 Hz over the analysis range of 1 Hz to 500 Hz. The output of the analyzer was displayed on an oscilloscope and recorded on an X-Y recorder.

The experiment was performed at Applied Research Laboratories Lake Travis Test Station (LTTS). The test station and the geometry of the experiment are shown in Fig. 3. The small railroad car and the railroad that runs down into the water near the center of the picture are used to transport large transducer arrays to the test barge in the center of the picture. The pump was mounted on the side of this rail car which was lowered to approximately the position marked by the arrow "T1". The hydrophone was mounted on a column on the side of the barges at the right of the picture at the point marked by the arrow "T2". Off the picture to the right about 600 m away is a large dam and hydroelectric plant. Off the picture to the left, the shore line runs approximately parallel to a line through the pump and hydrophone for about 2000 m and then curves back to the left. The pump-hydrophone separation was 66.3 m and the pump and hydrophone were each 4.5 m below the surface. The pump was attached to the side of the rail car and was about half a meter to a meter off the bottom of the lake. The lake bottom slopes down toward the hydrophone location and the water depth beneath the hydrophone was approximately 15 m.
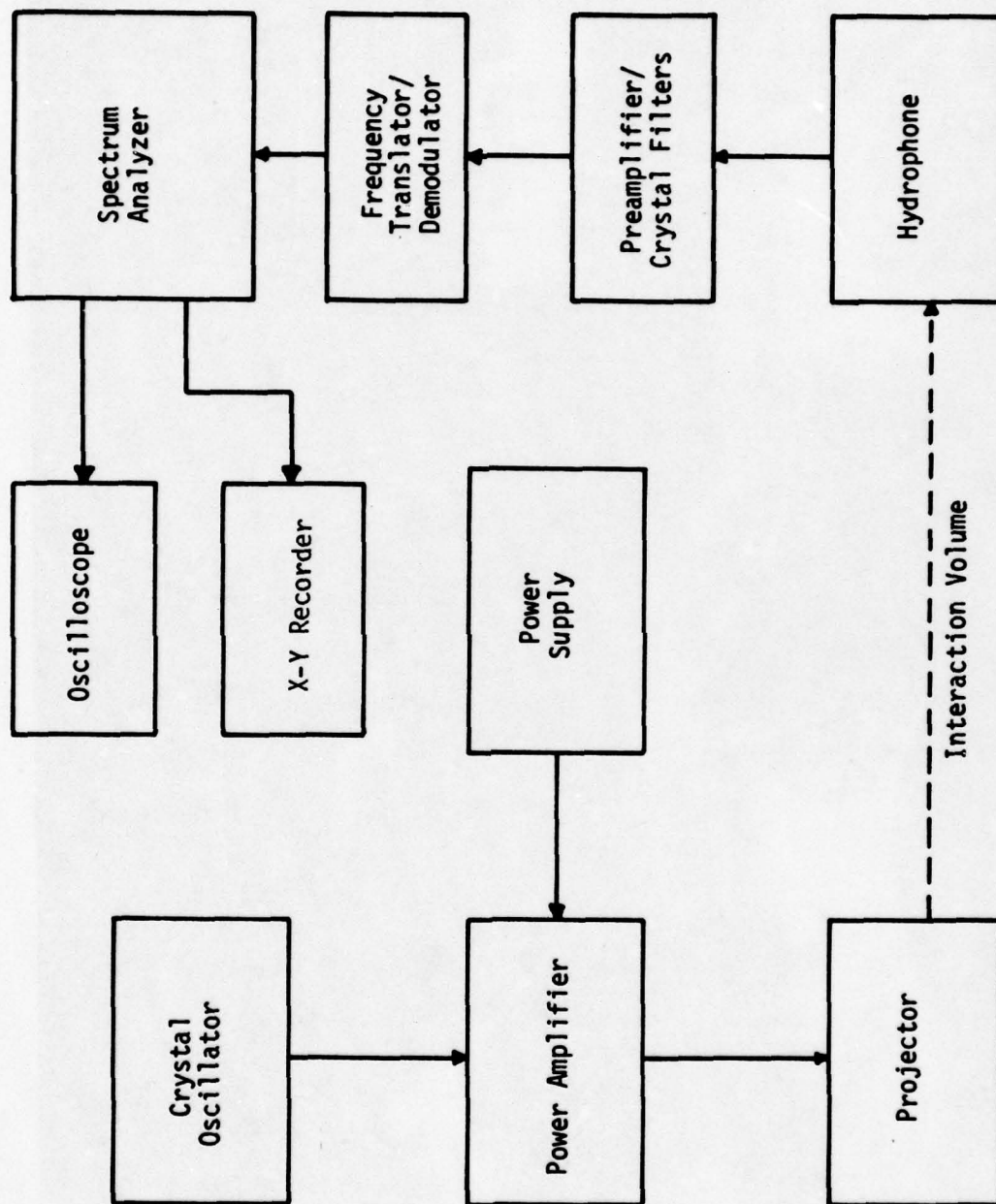
46

FIGURE 2
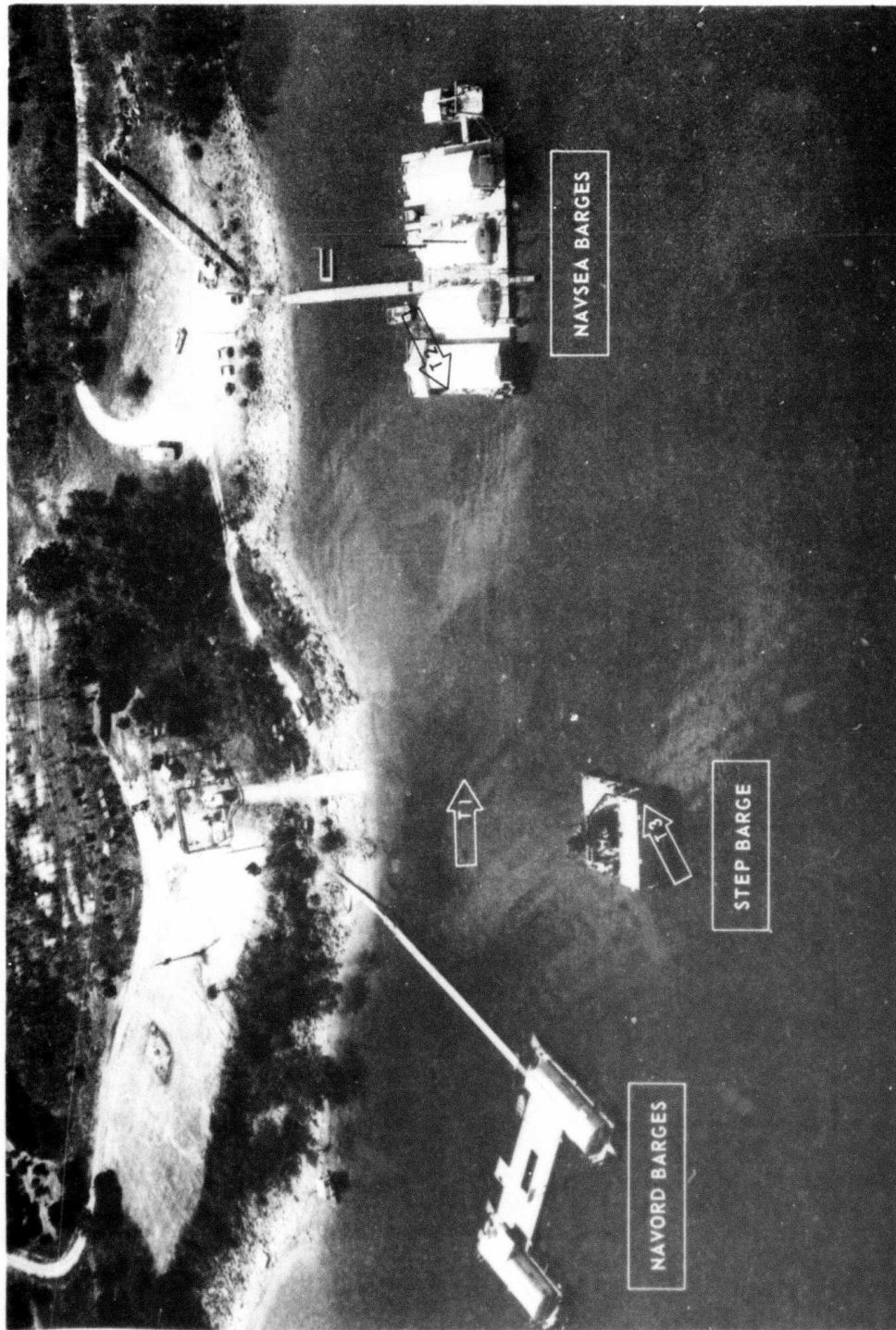
BLOCK DIAGRAM OF EXPERIMENTAL PARAMETRIC RECEIVER

47

FIGURE 3
AERIAL VIEW OF LAKE TRAVIS TEST STATION ILLUSTRATING EXPERIMENT GEOMETRY

The sound pressure level of the pump signal was measured at the hydrophone with a type H-23 standard hydrophone. The sensitivity of the hydrophone was measured in place at the pump frequency of 60.004 kHz and at 59.800 kHz by comparison with the H-23. The usual open circuit voltage sensitivity of the hydrophone was measured and, in addition, the voltage sensitivity of the hydrophone was measured with the hydrophone connected to the receiver electronics.

In an experiment of this type, we would like to isolate, identify, and independently measure as many noise sources as possible. This is easily accomplished for the receiver electronic noise. Simply disconnecting the hydrophone and shunting the receiver input with an appropriate resistor provides a measure of the electronic noise of the receiver. The next step would be to connect the hydrophone to the receiver electronics, but leave the pump turned off. Assuming the electronic noise level is low enough, this provides a measure of the plane wave equivalent of the ambient noise at the pump frequency sideband. Finally, with the pump on, the noise level of the parametric receiver can be measured. The results of the above sequence of measurements are shown in Fig. 4. The abscissa is the frequency in hertz relative to the pump frequency. The ordinate is sound pressure level at the face of the hydrophone, in dB re 1 μPa/$\sqrt{Hz}$. The lower trace in this figure represents the receiver electronic noise, with input shunted by a resistor, referenced to an equivalent noise pressure level at the face of the hydrophone. The receiver noise is equivalent to a noise pressure level of approximately 10 dB re 1 μPa/$\sqrt{Hz}$ over the receiver bandwidth. The curve just above this represents the plane wave equivalent noise pressure at the hydrophone due to the ambient noise at the pump frequency sideband. Over the bandwidth of the receiver, this level is approximately 14 dB re 1 μPa/$\sqrt{Hz}$. The top trace represents the noise pressure level of the parametric receiver at the face of the hydrophone. The pump source level is 221.5 dB re 1 μPa at 1 m, and the pump-hydrophone separation is 66.3 m. Since the noise level of the parametric receiver is some 50 dB above the equivalent plane wave noise pressure level due to the pump frequency ambient noise and the receiver electronic noise, it is clear that the sensitivity of this parametric
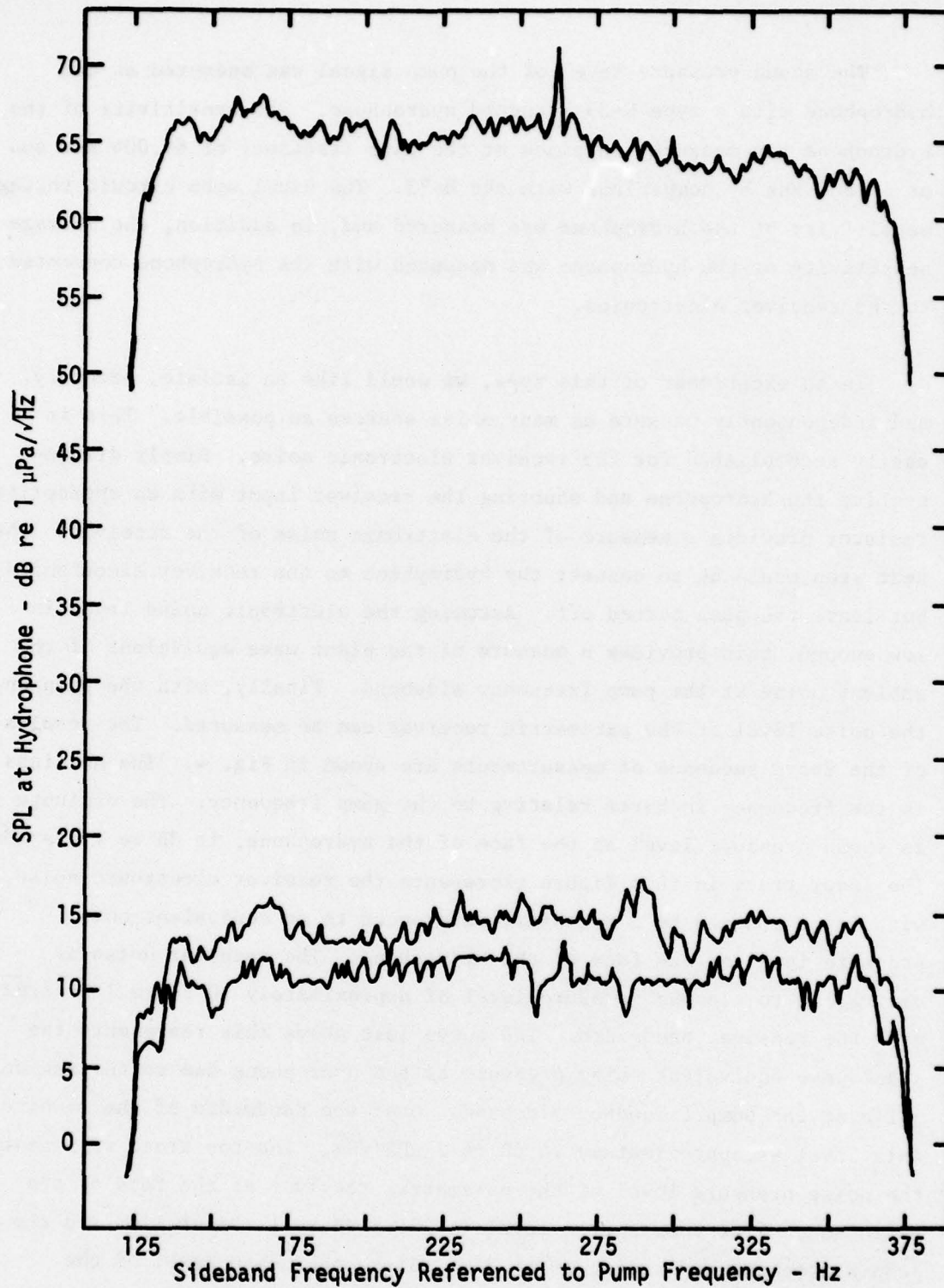
49

FIGURE 4

COMPARISON OF PARAMETRIC RECEIVER NOISE WITH
PUMP FREQUENCY AMBIENT AND ELECTRONIC NOISE EQUIVALENT

AS-75-1628
TGG-0166-7

receiver is not limited by receiver noise nor is it limited by pump frequency ambient noise.

The above conclusion was not unexpected since laboratory measurements on the crystal oscillator, power amplifier, and receiver electronics had identified pump spectral purity as the factor that would limit the sensitivity of the experimental parametric receiver. In this case the expression for the plane wave equivalent noise pressure at the face of the hydrophone reduces to the form shown on Fig. 5. The equation has been converted to a sound pressure level format for computational convenience in handling measured quantities. The curve at the top of the figure represents the noise pressure level at the face of the hydrophone predicted from this equation. The curve was obtained by measuring the sideband noise current into the pump transducer. The ordinate at the right is the level of the sideband noise referenced to the current at the pump frequency. Since the pump source level and the pump-hydrophone separation were also measured, the reference sound pressure level for the curve could be determined from the equation.

The predicted noise of this parametric receiver is compared to the measured noise of the experimental parametric receiver in Fig. 6. The format of the figure is the same as for the previous figure. The upper curve represents the noise pressure level at the hydrophone predicted from measurement of the spectral purity of the pump source. The lower curve represents the measured noise pressure level referenced to the face of the hydrophone. The hydrophone sensitivity at 59.800 kHz (200 Hz from the pump frequency) was used to determine the reference sound pressure level for this curve. The similarity of the curves is obvious. The difference in level is 1 to 4 dB over the bandwidth of the receiver. This is well within the expected experimental error.

Summary and Conclusions

An experimental parametric receiver with a pump-hydrophone separation of 66.3 m, and a pump source level of 221.5 dB re 1 μPa at 1 m at a pump

51

Spectrum Level Sideband Noise -
dB re Pump Signal Level
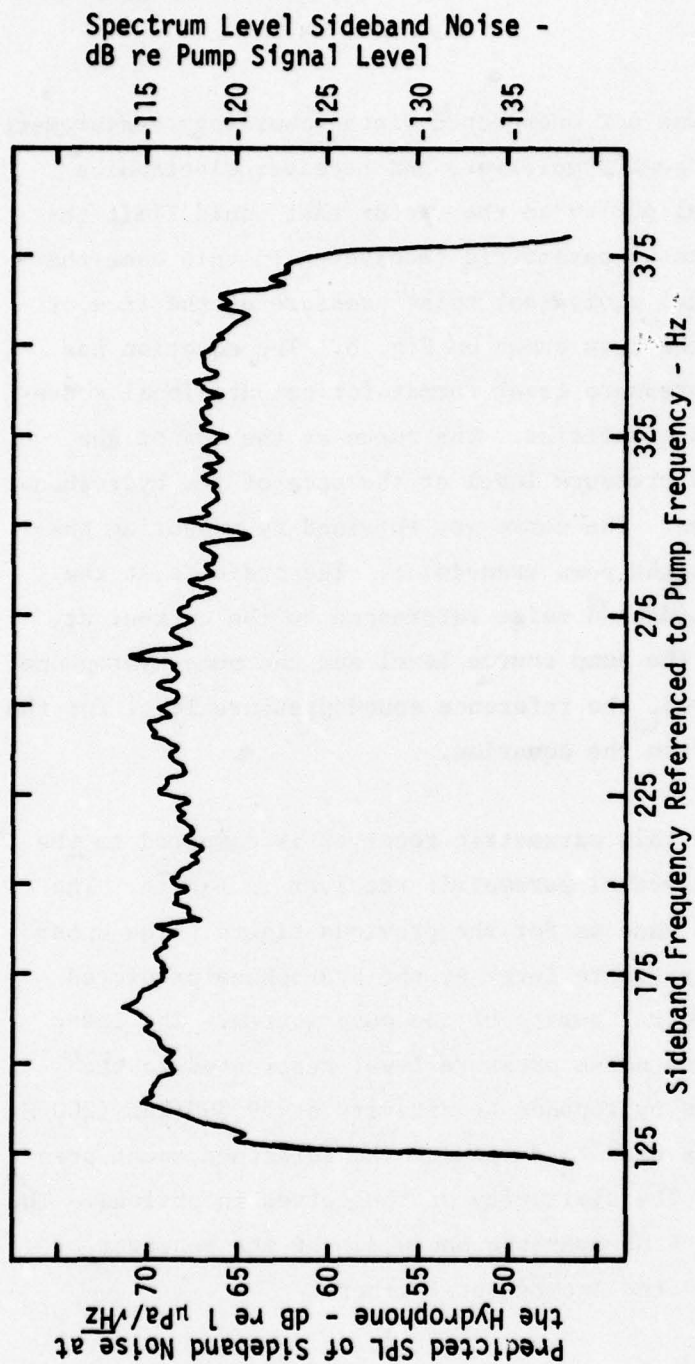
$N_{SB} = SL_p + LNSB - 20 \log L - \alpha_p L$

SL_p = Pump Source Level, dB re 1 μP at 1 m
LNSB = Spectrum Level Sideband Noise, dB re Pump Level
L = Pump-Hydrophone Separation, m
α_p = Absorption Coefficient, dB/m

FIGURE 5

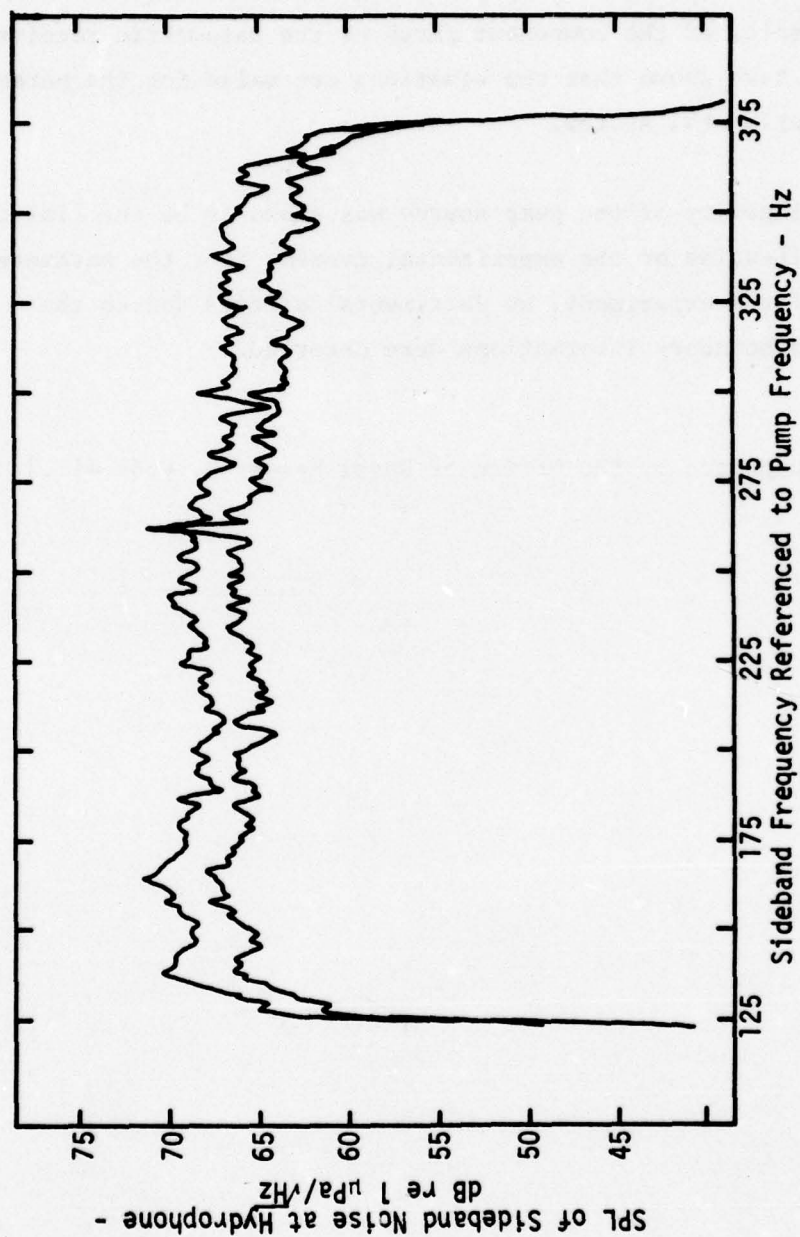PREDICTED SIDEBAND NOISE AT HYDROPHONE DUE TO PUMP SPECTRAL PURITY LIMITATIONS

AS-75-1629
TGG-0166-7

FIGURE 6

COMPARISON OF PREDICTED AND MEASURED SIDEBAND NOISE OF THE EXPERIMENTAL PARAMETRIC RECEIVER

53

frequency of 60 kHz was set up at Lake Travis Test Station, Applied
Research Laboratories. Measurements were made with this system to test
the validity of equations, developed previously, that permit the self-
noise of a parametric receiver to be predicted from measurements of the
noise characteristics of the component parts of the parametric receiver.
The measurements have shown that the equations are valid for the param-
eters of the experimental system.

The spectral purity of the pump source was shown to be the limiting
factor in the self-noise of the experimental system. For the parameters
and conditions of the experiment, no detrimental effects due to the
medium or to pump-boundary interactions were observed.

REFERENCES

1. T. G. Goldsberry, "Parameter Selection Criteria for Parametric Receivers", Paper T3, presented at The 88th Meeting of The Acoustical Society of America, St. Louis, Missouri, 4-8 November 1974.

2. R. H. Mellen, "The Thermal Noise Limit in the Detection of Underwater Acoustic Signals", J. Acoust. Soc. Am. 24, 478-480 (1952).

APPENDIX C

A BAND ELIMINATION PROCESSOR FOR AN EXPERIMENTAL

PARAMETRIC ACOUSTIC RECEIVING ARRAY

57

A BAND ELIMINATION PROCESSOR FOR AN EXPERIMENTAL
PARAMETRIC ACOUSTIC RECEIVING ARRAY

D. F. Rohde, T. G. Goldsberry, W. S. Olsen, C. R. Reeves

Applied Research Laboratories
The University of Texas at Austin
Austin, Texas 78712

ABSTRACT

In the Parametric Acoustic Receiving Array (PARRAY), a low
frequency acoustic wave modulates a locally generated high
frequency carrier wave. The information in the low frequency
signal wave then appears as low level, modulation sidebands of
the carrier. The function of the receiver electronics is to
suppress the high level carrier while simultaneously amplifying
the low level, near-sideband signals. A band elimination
processor has been developed that is capable of detecting
signals with carrier to sideband ratios approaching 180 dB.
Cascaded crystal filters and low noise amplifiers provide the
high order of carrier suppression. Additional circuitry is
incorporated to permit independent observation of the upper
and lower sidebands. The band elimination processor is
described in detail and test data for sideband signals 40 Hz
to 4 kHz from a 65 kHz carrier are presented.

Since Westervelt proposed the parametric acoustic receiving array as a method of obtaining highly directional reception of low frequency signals, the existence of the phenomenon has been demonstrated and mathematical models have been validated. Most of these basic measurements were obtained using available laboratory equipment with relatively high amplitude signals.[1-9] In order for the parametric receiver to progress from the status of an academic novelty to that of a useful tool in underwater acoustics, methods were developed at Applied Research Laboratories, The University of Texas at Austin (ARL:UT), for selecting optimum parameter values within the constraints of present engineering technology.[10] Using these parameter values, special purpose electronic hardware has recently been developed at ARL:UT. This paper describes one electronic subsystem of the parametric receiving array, the band elimination receiver, so that design documentation will be available for future underwater experimenters.

In the Parametric Acoustic Receiving Array (PARRAY), a low frequency acoustic wave modulates a locally generated high frequency carrier wave. As shown in Slide 1, the high frequency pump wave radiates from the pump transducer to the receive hydrophone. Low frequency signals, represented by the widely spaced diagonal lines, interact nonlinearly with the pump signal to form intermodulation products in the interaction volume. The phasing of the interaction process forms a virtual end-fire array that provides the directivity of the parametric receiver.[6]

The signal spectrum at the hydrophone is illustrated in Slide 2. As a result of the nonlinear mixing in the water, the pump signal spectrum has been modulated by the signal frequency spectrum, and contains the signal frequency information as the upper and lower sideband $f_p \pm f_s$. Since the in-water mixing process is weakly nonlinear, the intermodulation products are very small in relation to the pump signal (carrier). In many practical experimental systems the sidebands may approach 160 dB below the level of the carrier. The ratio of the amplitude of the pump signal to that of the sum or difference signal is the pump excess.[7] In addition to the intermodulation products of the signal frequency spectrum,

PARRAY FUNCTIONAL DIAGRAM

62
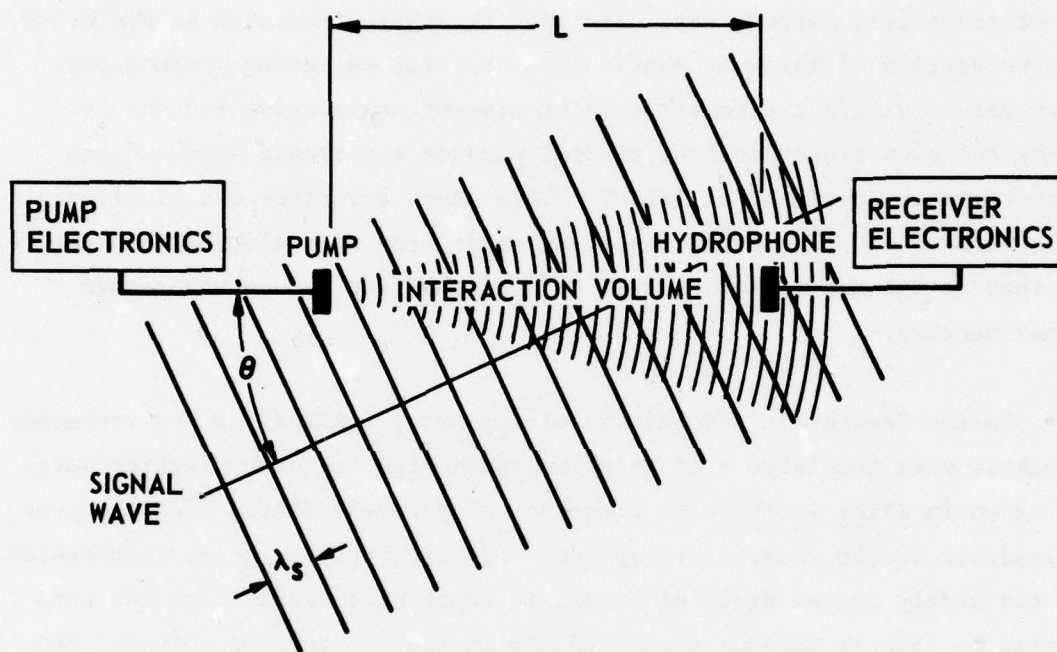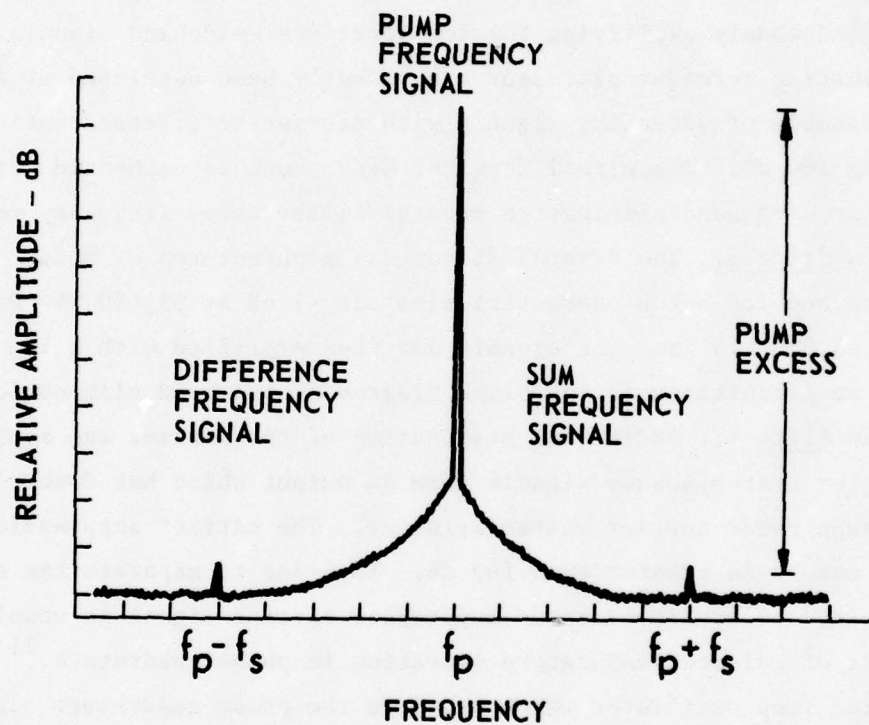
ILLUSTRATIVE PARAMETRIC RECEIVER SIGNAL SPECTRUM

SLIDE 2

the sideband noise of the imperfect pump generator is also present. The relative level of this near-sideband noise of the carrier determines the level of the signal necessary for detection for a given conversion efficiency of the parametric process.

In a parametric acoustic receiving array the function of the receiver electronics is to suppress the high level pump signal carrier while simultaneously amplifying the low level near-sideband signals. A band elimination receiver processor has recently been developed at ARL:UT which is capable of detecting signals with carrier to sideband ratios approaching 180 dB. The signal from the hydrophone is connected directly to the input of a band elimination crystal filter whose frequency response is shown in Slide 3. The crystal filter was manufactured by McCoy Electronics and its notch characteristics are -1 dB at 65,000 ±40 Hz and -40 dB at 65,000 ±10 Hz. The signals are then amplified with a low noise amplifier as illustrated in the block diagram of the band elimination receiver in Slide 4. Additional elimination of the carrier and amplification of the near-sideband signals form an output which has double sideband suppressed carrier characteristics. The carrier suppression with this method is greater than 140 dB. In order to separate the sideband signals, the double sideband suppressed carrier signal is coupled into a pair of balanced modulators operating in phase quadrature.[11] The phase locked loop oscillator which provides the phase quadrature signals to the balanced modulators may use one of several reference signals for operation: (1) the pump oscillator, (2) an external frequency synthesizer, or (3) pump carrier signal from the hydrophone. The frequency translated signals out of each balanced modulator are then low pass filtered to extract the difference frequency components. Each signal is then phase shifted by a quadrature phase shift network. These phase shift networks utilize an all-pass design with resistors and capacitors in an operational amplifier circuit. This network has less than a 1° error over a range of frequencies from 40 Hz to 4 kHz.[12,13] The phase error of the signal is directly related to the amount of spurious sideband suppression. The output from the phase shift circuits are then summed with appropriate

64
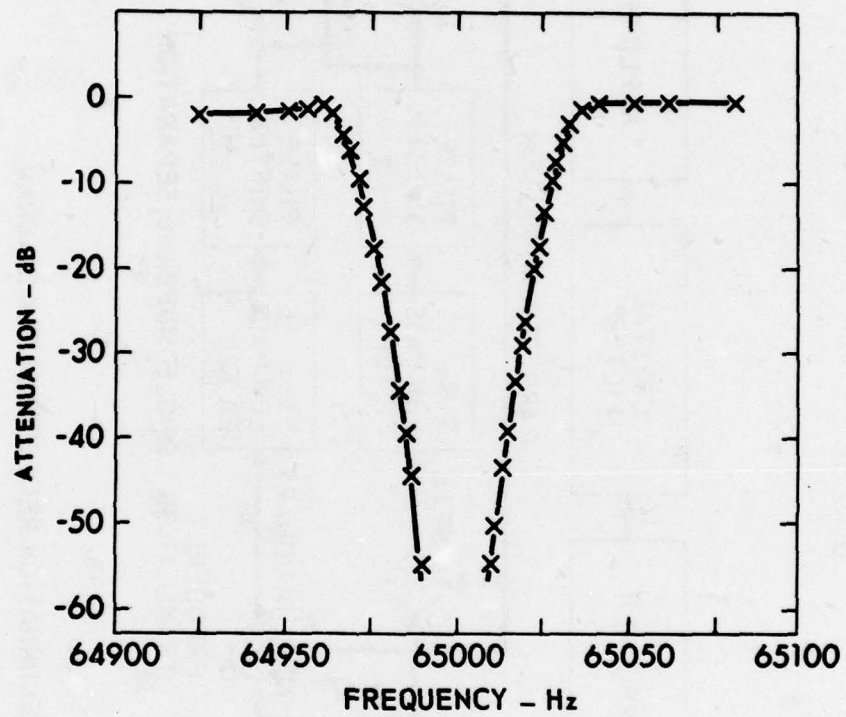
BAND ELIMINATION FILTER RESPONSE
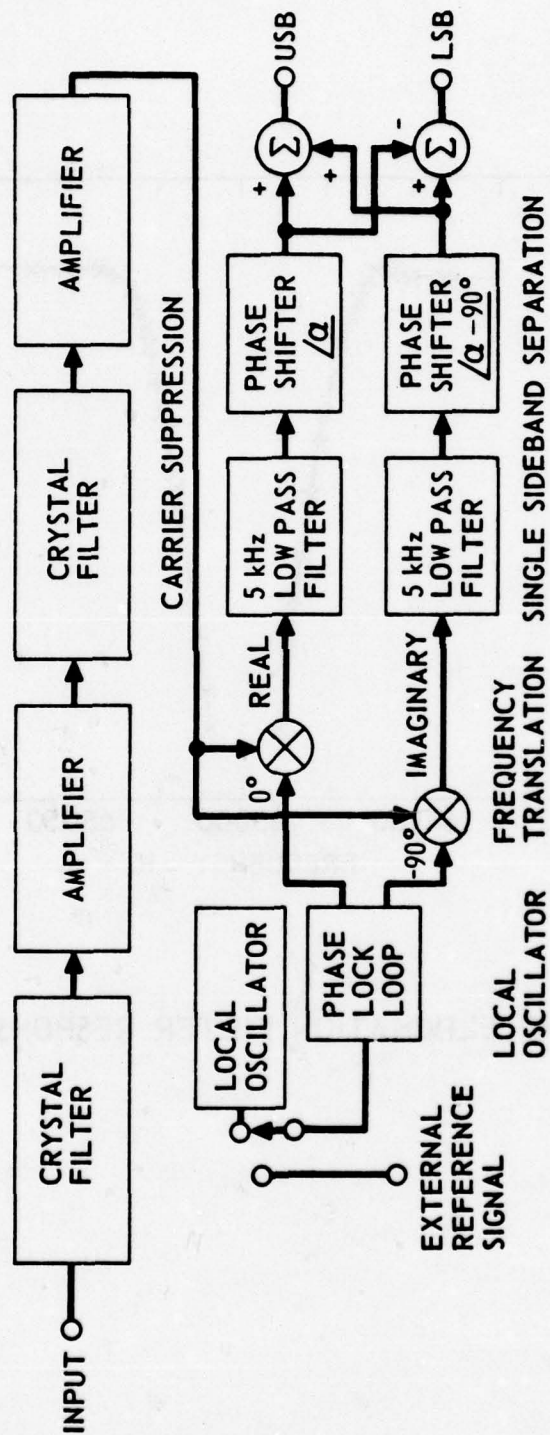
BAND ELIMINATION RECEIVER BLOCK DIAGRAM

66

SLIDE 4

polarities to yield both the upper and lower sideband signals simultaneously. This receiver processor allows the independent analysis of the upper or lower sideband signals.

The single sideband signals observed at the output of the receiver processor contain the intermodulation products as well as noise from the pump oscillator and the receiver electronics. The receiver electronics should contaminate the signals as little as possible since the noise will only mask the signal energy in the sidebands. The self-noise of the band elimination receiver was measured and is illustrated in Slide 5. The output noise of the upper sideband is given referenced to the input for a receiver sideband gain of 100 dB. The noise was measured using a spectrum analyzer with 1 Hz BW resolution for 256 ensemble averages. The self-noise of the receiver is approximately -150 dB re 1 V over the frequencies shown. Since the maximum power dissipation for the input crystal filter is 1 mW, which corresponds to a maximum voltage level of +29 dB re 1 V, the receiver should be able to display signals 180 dB below the maximum carrier level.

Using the noise measurement system illustrated in Slide 6, the signal from a 65 kHz low noise oscillator is impedance matched to the input of the band elimination processor. The 65 kHz carrier signal is removed and the near-sideband noise is frequency translated to baseband by the receiver and monitored by a narrowband spectrum analyzer. With this measurement scheme the sideband noise levels from a low noise pump signal generator were measured in the laboratory. In Slide 7, the sideband noise level relative to the carrier level is presented. The noise level is more than 165 dB below the carrier for frequencies greater than 200 Hz from the 65 kHz carrier. The noise level for frequencies to 800 Hz and greater is very near the receiver self-noise. Higher input signal levels would allow observation of larger carrier to sideband ratios. The 60 Hz harmonic line components are present in the oscillator noise and should be reduced with better shielding and isolation. The low noise oscillator was developed at ARL:UT and is discussed in detail in the next paper of the session.[14]
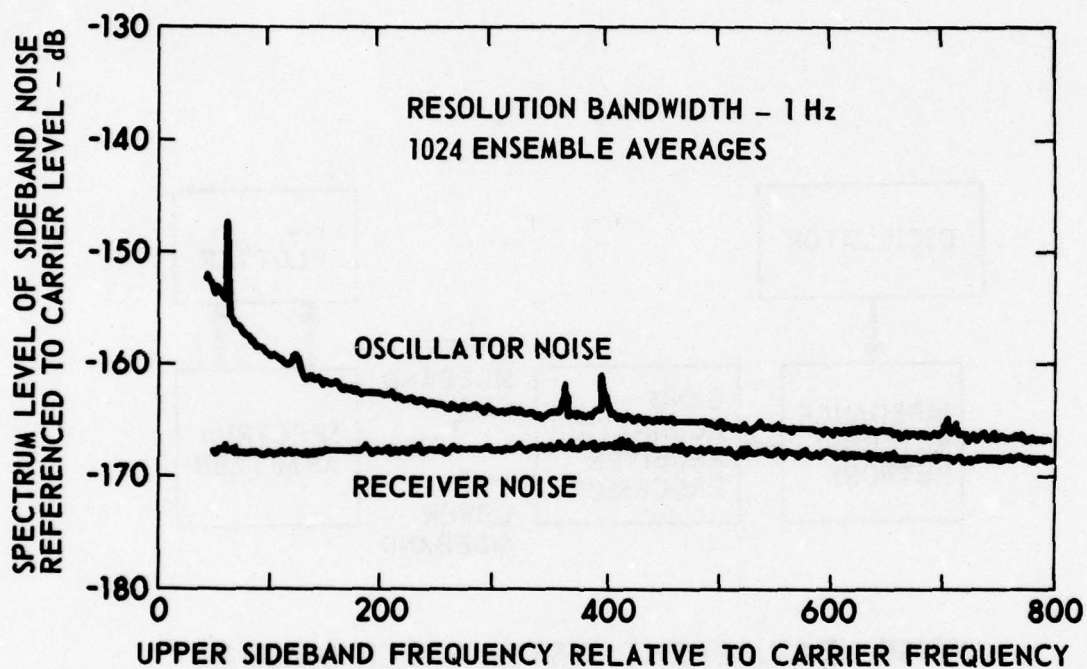
67
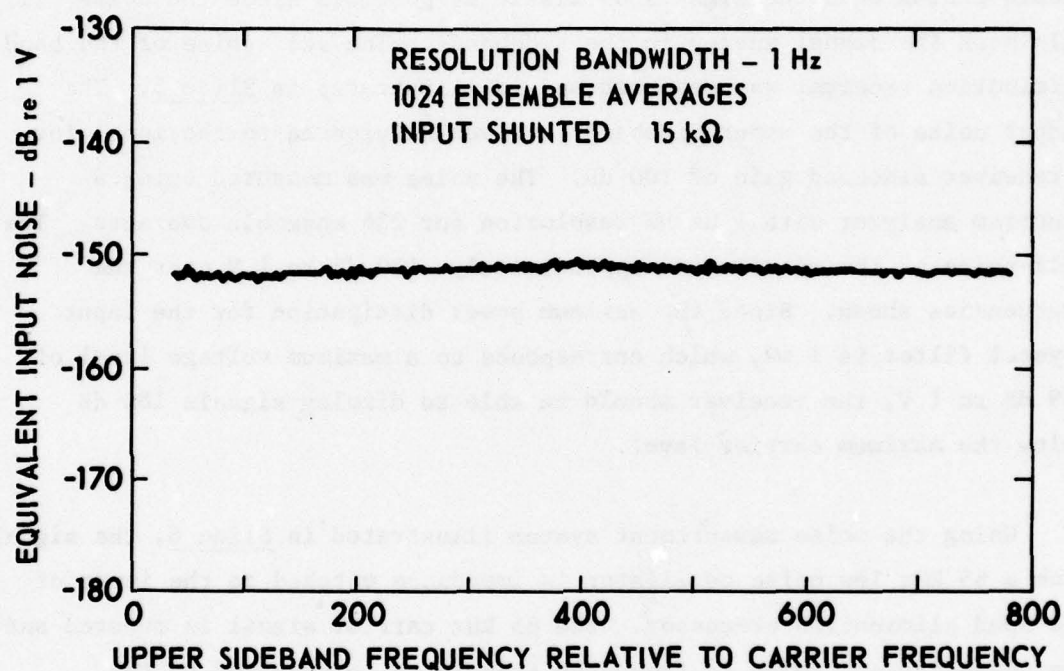
SIDEBAND NOISE OF BAND ELIMINATION RECEIVER

ARL - UT
AS-76-1156-S
DFR - DR
10 - 7 - 76

68

SLIDE 5
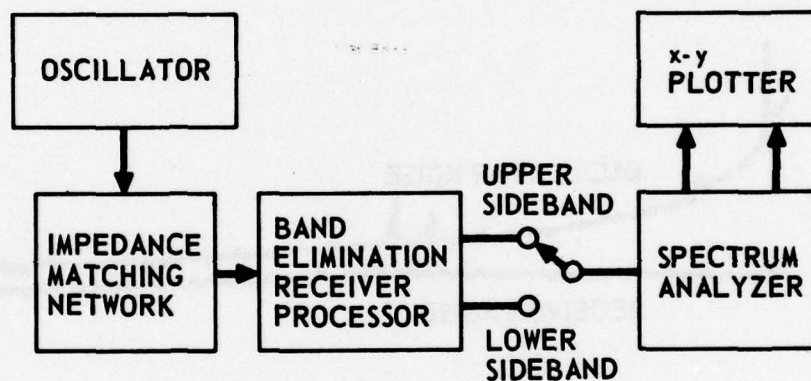
NOISE MEASUREMENT SYSTEM BLOCK DIAGRAM

SLIDE 6

SIDEBAND NOISE OF BAND ELIMINATION RECEIVER
FOR A 65 kHz OSCILLATOR

ARL - UT
AS-76-1157-S
DFR - DR
10 - 7 - 76

SLIDE 7

Summary and Conclusion

In conclusion, a band elimination processor has been developed which is capable of detecting both upper and lower sideband signals in an experimental parametric receiving array with carrier to sideband ratios approaching 180 dB. By using this basic receiver processor along with properly selected parameter values, it should be possible to utilize the parametric receiver characteristics in useful underwater acoustic systems.

REFERENCES

1. P. J. Westervelt, "Parametric Acoustic Array", J. Acoust. Soc. Am. 35, 535-537 (1963).

2. H. O. Berktay and C. A. Al-Temimi, "Virtual Arrays for Underwater Reception", J. Sound Vib. 9, 295-307 (1969).

3. W. L. Konrad, R. H. Mellen, and M. B. Moffett, "Parametric Sonar Receiving Experiments", NUSC TM No. PA4-304-71, Naval Underwater Systems Center, New London, Connecticut, 9 December 1971.

4. G. R. Barnard, J. G. Willette, J. J. Truchard, and J. A. Shooter, "Parametric Acoustic Receiving Array", J. Acoust. Soc. Am. 52, 1437-1441 (1972).

5. H. O. Berktay and T. G. Muir, "Arrays of Parametric Receiving Arrays", J. Acoust. Soc. Am. 53, 1377-1383 (1973).

6. H. O. Berktay and J. A. Shooter, "Parametric Receivers with Spherically Spreading Pump Waves", J. Acoust. Soc. Am. 54, 1056-1061 (1973).

7. P. H. Rogers, A. L. Van Buren, A. O. Williams, Jr., and J. M. Barber, "Parametric Detection of Low Frequency Acoustic Waves in the Nearfield of an Arbitrary Directional Pump Transducer, "J. Acoust. Soc. Am. 55, 528-534 (1974).

8. J. J. Truchard, "Parametric Acoustic Receiving Array. I. Theory", J. Acoust. Soc. Am. 58, 1141-1145 (1975).

9. J. J. Truchard, "Parametric Acoustic Receiving Array. II. Experiment", J. Acoust. Soc. Am. 58, 1146-1150 (1975).

10. T. G. Goldsberry, "Parameter Selection Criteria for Parametric Receivers", paper presented at the 88th Meeting of The Acoustical Society of America, St. Louis, Missouri, 4-8 November 1974 [Abstract in J. Acoust. Soc. Am. 56, S41 (1974)].

11. D. E. Norgaard, "The Phase-Shift Method of Single-Sideband Signal Reception", Proc. IRE, 1735-1743 (December 1956).

12. S. O. Bedrosion, "Normalized Design of 90 Degree Phase Difference Networks", IRE Trans. on Circuit Theory 60, 128-126 (June 1960).

13. R. K. Dickey, "Output of Op-amp Networks Have Fixed Phase Difference", Electronics 48(17), 82, 21 August 1975.

14. W. S. Olsen, T. G. Goldsberry, C. R. Reeves, D. F. Rohde, "A Crystal Controlled Pump Signal Source For An Experimental Parametric Acoustic Receiving Array", Paper No. 003, presented at the 92nd Meeting of The Acoustical Society of America, San Diego, California, 16-19 November 1976.

73

APPENDIX D

A CRYSTAL CONTROLLED PUMP SIGNAL SOURCE FOR AN EXPERIMENTAL

PARAMETRIC ACOUSTIC RECEIVING ARRAY

75

A CRYSTAL CONTROLLED PUMP SIGNAL SOURCE FOR AN EXPERIMENTAL
PARAMETRIC ACOUSTIC RECEIVING ARRAY

W. S. Olsen, T. G. Goldsberry, C. R. Reeves, D. F. Rohde

Applied Research Laboratories
The University of Texas at Austin
Austin, Texas   78712

ABSTRACT

In the Parametric Acoustic Receiving Array (PARRAY), a
locally generated, high frequency carrier (or pump) wave is
modulated in the water by a low frequency acoustic wave. The
information in the low frequency signal appears as low level
modulation sidebands of the pump wave; therefore, the side-
band noise of the pump signal source is an important PARRAY
system parameter. Since commercial oscillators with adequate
spectral purity were not available, a program was initiated
to develop a 65 kHz crystal controlled oscillator with suffi-
cient spectral purity for use as the pump signal source in
an experimental PARRAY. Application of state-of-the-art
techniques and components has enabled the design and construc-
tion of a crystal controlled oscillator with spectral purity
previously unattainable in this frequency region. Spectral
purity of this oscillator is approximately four orders of
magnitude better than commercially available oscillators in
the 65 kHz frequency region. Measurements performed on the
oscillator show that the spectrum level sideband noise
referenced to the carrier level is better than -170 dB for
frequencies greater than 100 Hz away from the carrier. The
oscillator design is described in detail and sideband noise
test data are presented and discussed.

77

In the parametric acoustic receiving array (PARRAY) a locally generated high frequency carrier (pump) wave is modulated in the water by a low frequency acoustic wave. Since the modulation process produces sideband signals on the high frequency carrier which are of a very low level, the sideband noise of the pump signal source is extremely important. The minimum detectable level of the low frequency wave is directly proportional to the noise level in the sidebands of the pump signal source.

Approximately two years ago a design study was begun to determine what type oscillator could be used for the pump signal source. The system parameters dictated that the pump signal source be crystal controlled with frequency shift of less than 2 Hz because it was to be used in a system with the receiver preprocessor described in another paper at this meeting.[1]

Crystal oscillators typically exhibit a spectral output like that shown in Fig. 1 where there is a strong line at the fundamental frequency of the oscillator. In the near-sidebands of the oscillator there is an enhanced noise region that has a slope changing as a function of frequency such that the enhanced noise diminishes until it falls below the constant noise floor of the oscillator.

Studies have shown that there are several distinct noise processes that determine the noise spectrum in the near-sidebands of the oscillator. The noise processes in crystal oscillators are actually phase modulation (PM) and frequency modulation (FM) as listed in Table I.[2] Typically there are five noise regions in the near-sidebands of the carrier. These regions have slopes that vary with the offset frequency from the carrier as $1/f^4$, $1/f^3$, ..., $1/f^0$. The higher ordered terms dominate at frequencies near the carrier frequency and the lower ordered terms dominate at frequencies farthest from the carrier.

The $1/f^4$ noise slope is the random walk FM and is due to perturbations of the crystal such as mechanical shock, vibration, and temperature changes that cause random changes in the carrier frequency. The $1/f^3$ noise, called
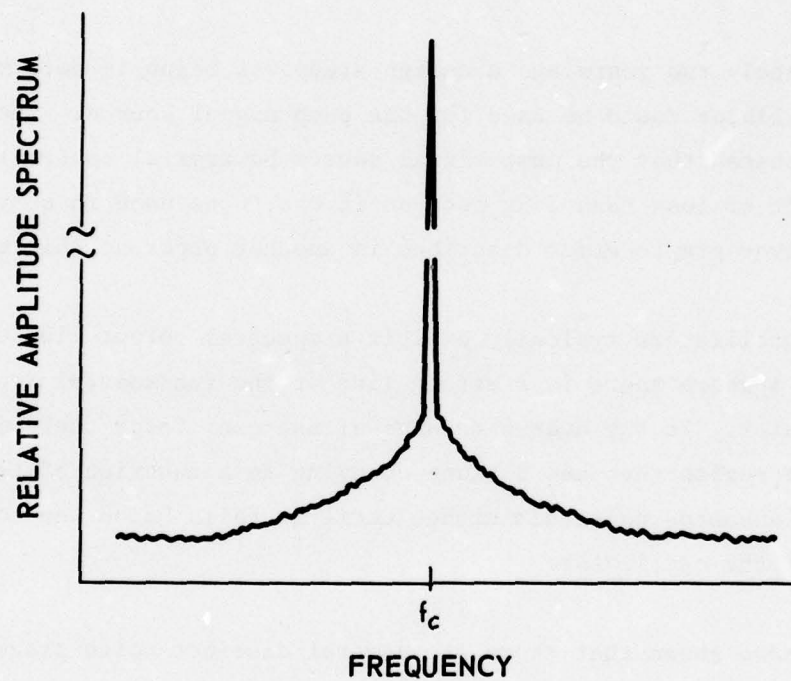
79

RELATIVE AMPLITUDE SPECTRUM

f_c

FREQUENCY

FIGURE 1
ILLUSTRATIVE OUTPUT SPECTRUM OF CRYSTAL OSCILLATOR

TABLE I
NOISE PROCESSES IN OSCILLATORS

TYPE	SLOPE	SOURCE
RANDOM WALK FM	$1/f^4$	MECHANICAL SHOCK, VIBRATION, AND TEMPERATURE CAUSING RANDOM CHANGES IN FREQUENCY
FLICKER FM	$1/f^3$	PHYSICAL CAUSE NOT UNDERSTOOD BUT POSSIBLY ATTRIBUTABLE TO ENVIRONMENTAL EFFECTS, CHOICE OF PARTS USED IN ELECTRONICS, OR RESONANCE MECHANISM OF OSCILLATOR
WHITE FM	$1/f^2$	DUE TO CHARACTERISTICS OF THE HIGH Q CRYSTAL RESONATOR
FLICKER PM	$1/f$	MAY RELATE TO MECHANICAL RESONATOR BUT IS MOST OFTEN CAUSED BY NOISY ELECTRONICS
WHITE PM	$1/f^0$	ELECTRONIC NOISE

flicker FM, is a noise that has an unexplained source. It is believed due to the resonance mechanism of the oscillator, the choice of parts for the electronics, environmental properties, or even a combined effect. Flicker FM is common in high quality oscillators but it is often masked by the lower ordered noise. The equipment used to measure the pump signal source does not have the capability of measuring these two noise types. However, they are included in this discussion for the sake of completeness. The third type of noise process, white FM $(1/f^2)$, will very often be seen in crystal oscillators as it is caused by the passive resonator, i.e., the crystal. Flicker PM which varies as $1/f$ is one of the most troublesome noise sources and is caused by the mechanical resonator or a poor choice of electronic components. Flicker is a nonconverging process and is multiplicative. The final noise process is the white PM $(1/f^0)$ noise process. This process is broadband noise and is attributable to the noise of the amplifier circuitry. White noise is the type of noise most often encountered by the designer and it can be kept very low by good amplifier design.

At the beginning of the PARRAY program a search of commercially available oscillators and synthesizers was made in an attempt to find an oscillator that conformed to the design requirements of the PARRAY. Many oscillators and synthesizers were measured and the approximate sideband noise levels of some of the types of frequency sources are shown in Table II. The noise of the standard laboratory oscillator showed a sideband noise level, $\mathcal{L}(f)$, measured in a 1 Hz bandwidth, on the order of -80 dB referenced to the carrier.[3] Two different brands of synthesizers were measured with one having a sideband noise on the order of -94 dB re the carrier and the other -103 dB re the carrier. Of the commercial units, fixed frequency crystal controlled oscillators had the best noise characteristics; in the 60 to 70 kHz region, the sideband noise to carrier level was typically measured at approximately -130 dB. This value was also obtained with some early breadboard oscillators that had been assembled in the laboratory. Some oscillators measured were more than ten years old. When the noise measurements of the old oscillators were compared with those

82

TABLE II
RELATIVE SIDEBAND NOISE TO SIGNAL
OF COMMERCIAL SIGNAL SOURCES

$\mathcal{L}$(f) – dB	SIGNAL SOURCE TYPE
-80	STANDARD OSCILLATOR
-90	
	FREQUENCY SYNTHESIZER
-100	FREQUENCY SYNTHESIZER
-110	
-120	
-130	COMMERCIAL CRYSTAL OSCILLATOR

NOTE
$\mathcal{L}$(f) IS DEFINED AS THE NOISE IN SINGLE
SIDEBAND REFERENCED TO THE CARRIER
AND MEASURED IN A 1 Hz BANDWIDTH

of the newer designs, it was obvious that oscillator technology had not improved during that ten year period.

Soon after the measurement program began, a major effort was begun to advance existing oscillator design or to design a source having sideband noise characteristics that met the design criteria of the PARRAY. Two types of signal source designs were investigated. The first was a fixed frequency digital synthesizer. Some researchers had discovered that, when a digital divider is used to divide an oscillator frequency to a lower frequency, an improvement in phase noise will result. The measurements showed that, where N is the divisor, an N^2 improvement could be expected in the sideband noise.[4]

The synthesizer shown in Fig. 2 used a high frequency oscillator which provided a 4.16 MHz clocking frequency for the digital divider logic. The output was maintained at a constant level by an AGC circuit. The buffer amplifier converted the 4.16 MHz signal to a level suitable for driving the "divide-by-64" logic circuit. Emitter coupled logic (ECL) is used in the divider because the high switching speed yields the least uncertainty in time of axis crossings during switching. The output from the divider was filtered to provide a sine wave output. It was estimated that the 4.16 MHz oscillator should have about a -130 dB noise floor and 20 log 64 would provide 36 dB of improvement over that. The sideband noise to carrier level of the digital synthesizer is shown in Fig. 3. The noise level at 100 Hz from the carrier was -145 dB relative to the carrier and declined to -151 dB at 800 Hz from the carrier. The slope does not follow the predicted slopes of oscillators but varies with a slope that is midway between $1/f$ and $1/f^0$. Although it did not behave predictably, the carrier-to-sideband noise ratio was significantly improved over earlier measurements; however, it was still short of the design goal. The noise floor was being set by the switching uncertainty of the logic and this approach was abandoned.
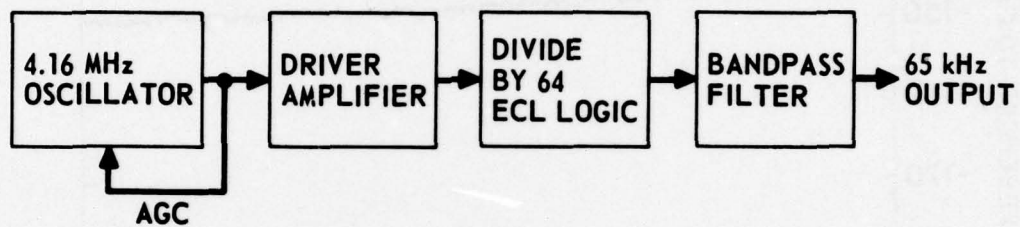
FIGURE 2
65 kHz FREQUENCY SYNTHESIZER
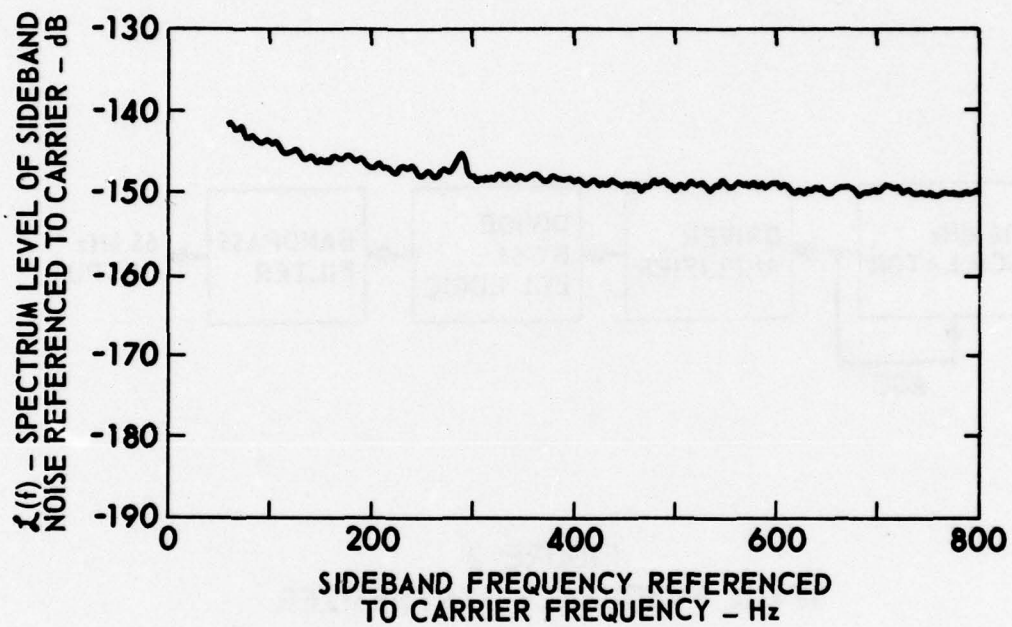
FIGURE 3
SIDEBAND NOISE OF 65 kHz PUMP SIGNAL SYNTHESIZER

At this time, it was learned that Austron, Inc., Austin, Texas, had made substantial improvement in the sideband noise of an oscillator operating at 5 MHz.[5] Through Austron, Inc., and the National Bureau of Standards, who confirmed the measurements of the sideband noise of the Austron oscillator, a number of facts were learned that proved important to the design of the pump signal source.[6] These important facts will be pointed out as the schematic of the pump signal source shown in Fig. 4 is discussed. Basically, the pump signal source is composed of three parts: an emitter coupled crystal oscillator, an AGC circuit, and a buffer amplifier. The oscillator is a modified Pierce design of the emitter coupled type. The 65 kHz signal current is limited only by the resistance of the series circuit, but the sideband noise current is attenuated because of the Q of the series circuit. The capacitor is used to amplify the signal voltage through the resonant circuit and, because of its low noise characteristics, it will not add noise to the sidebands of the oscillator signal.

The quartz crystal is 5° X cut with a Q greater than 100,000. The effective series resistance is approximately 100 Ω. Typically, manufacturers recommend a maximum driving power of 0.5 mW into the crystal. Flicker noise is added by many commonly used circuit components. To achieve the best noise performance from the circuit, all of the components must be chosen carefully. Resistors must be of the metal film type since this type is likely to produce less excess noise. The capacitors should either be glass or ceramic. The isolation amplifier is a "boot-strapped" source follower which has an input impedance greater than 10 MΩ. It provides power gain for the signal and a low output impedance.

The automatic gain control circuit maintains a constant drive level of less than 0.5 mW to the crystal. Fluctuations in the drive level can induce noise in the crystal.
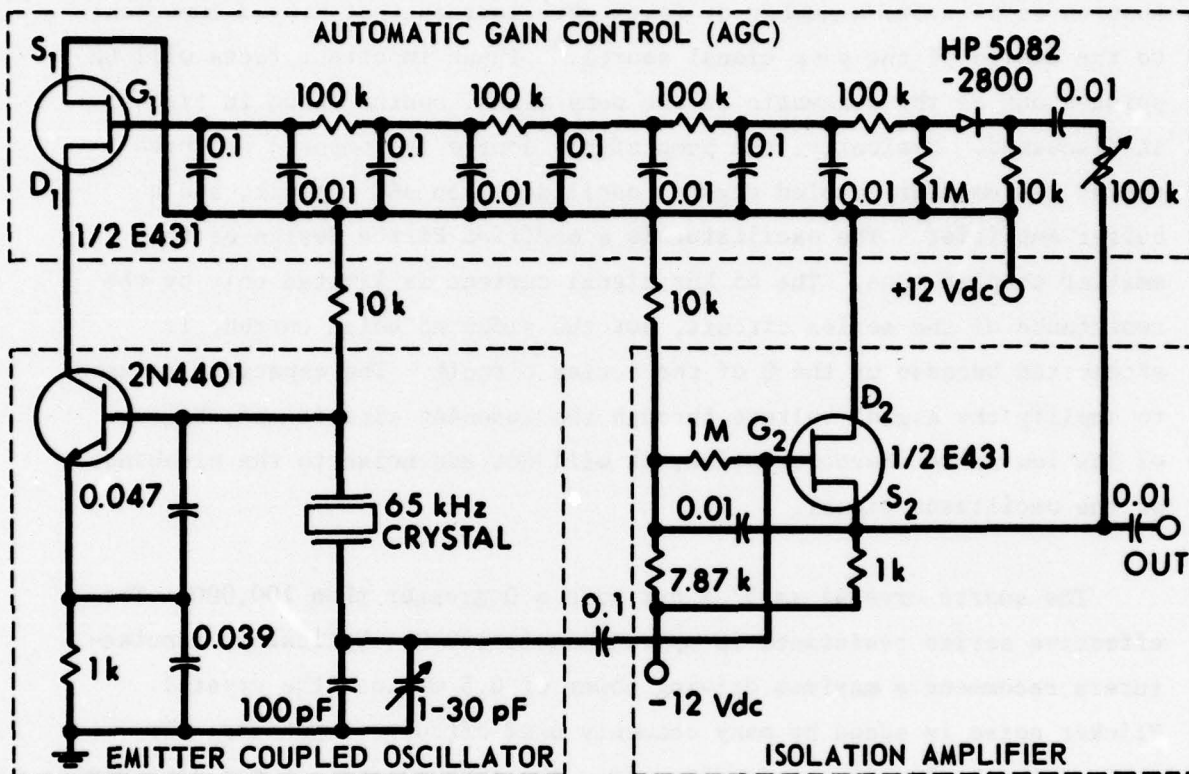
87

FIGURE 4
CRYSTAL CONTROLLED
PUMP SIGNAL SOURCE
$f_0 = 65.000$ kHz

The circuit, as it is described, has a sideband noise to carrier ratio that is shown in Fig. 5. The top curve is a summation of the sideband noise of the oscillator and the noise of the receiver used to measure the sideband noise. The curve labeled "receiver noise" represents the noise of the receiver with the input shunted by an equivalent source resistor. It can be seen that much of the noise was due to the receiver.

The top noise plot shows three spectral lines that should be mentioned; these appear at 63, 360, and 395 Hz. It is believed that these lines are the result of a spurious resonance in the crystal. With different crystals the lines may be moved or, by a careful choice of crystal, possibly removed. The same receiver preprocessor was used to obtain all the measurements for this paper.

The smooth curve is the inferred single sideband noise level referenced to the carrier, $\mathcal{L}(f)$. Since the noise level of the receiver is near the noise level of the oscillator, it is a major contributor to the oscillator noise data. The inferred noise curve is the result of subtracting the average receiver noise from the average receiver plus oscillator noise.

Figure 6 is a log-log plot of the inferred oscillator noise redrawn to show the characteristics of the sideband noise to carrier ratio. The curve clearly shows that from 40 to 180 Hz the oscillator noise follows a $1/f^2$ slope. From 180 Hz to 700 Hz the data follow a $1/f$ slope characteristic of flicker PM noise. Above 700 Hz the noise level is independent of frequency at -173 dB.

In summary, it has been shown that a major improvement in the short term phase noise of oscillators has been achieved in the frequency range near 65 kHz. As is shown in Table III, the sideband noise to carrier level has been improved by four orders of magnitude over designs that had continued for a number of years. Knowing the processes that generate the sideband noise will probably allow oscillators in this frequency region to be improved still further in the near future.
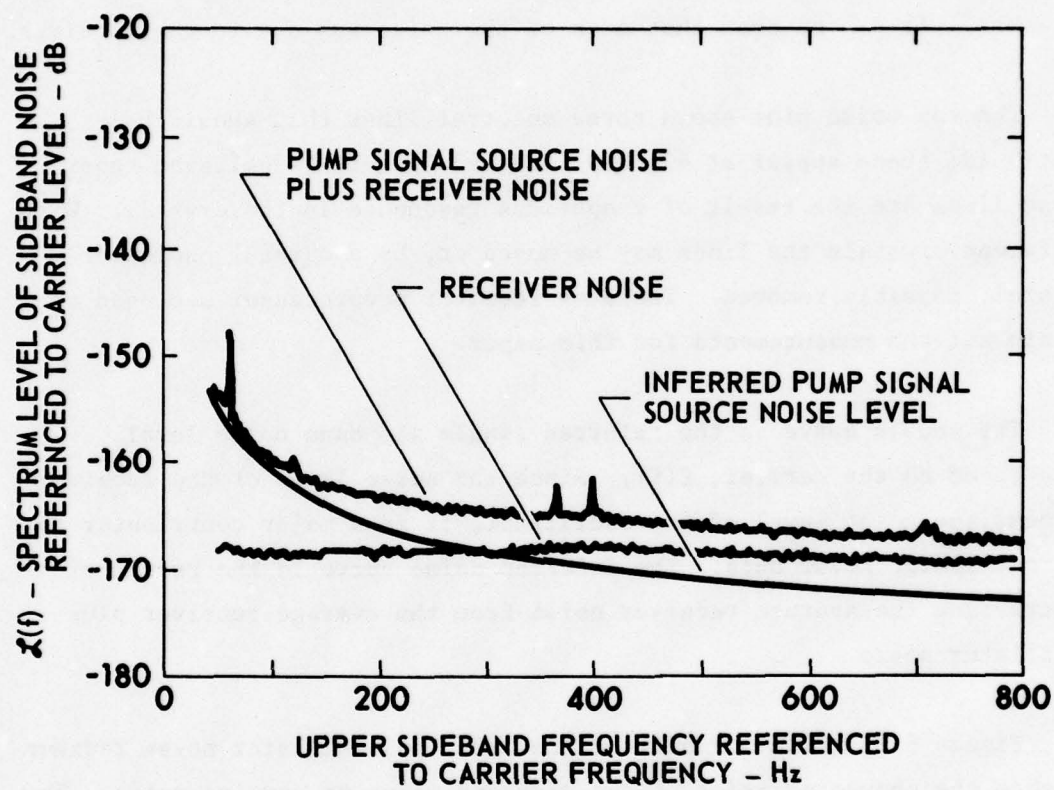
FIGURE 5

UPPER SIDEBAND NOISE OF 65 kHz PUMP SIGNAL SOURCE

NOISE DATA TAKEN WITH 1024 AVERAGES
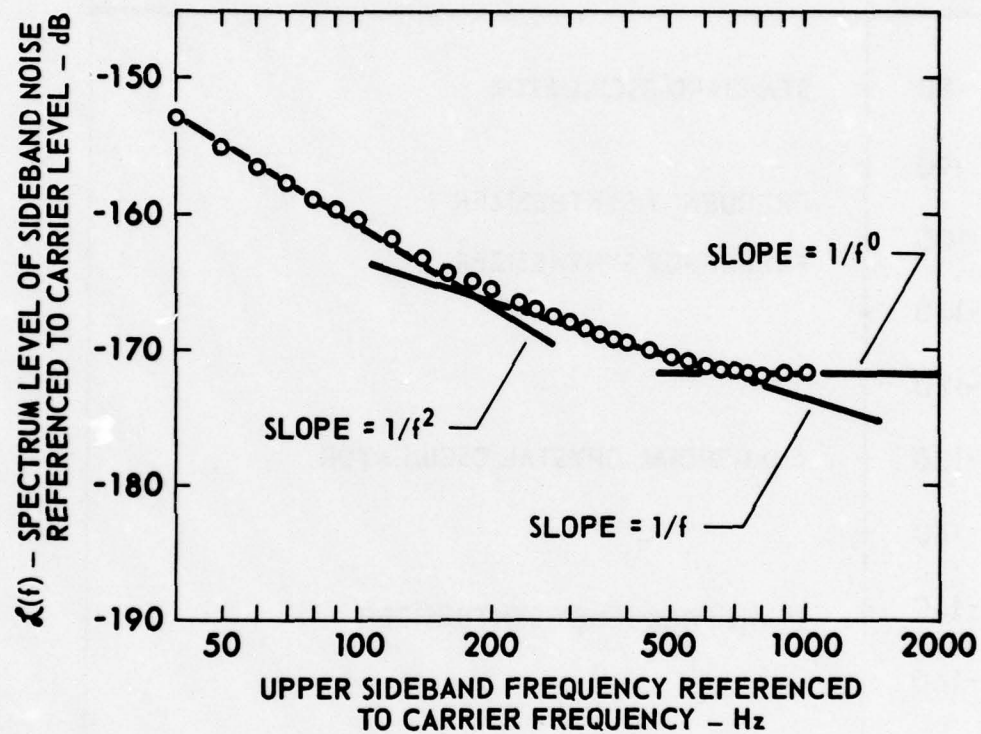
FIGURE 6

SIDEBAND NOISE OF CRYSTAL CONTROLLED
PUMP SIGNAL SOURCE

TABLE III
RELATIVE SIDEBAND NOISE TO SIGNAL
OF PUMP SIGNAL SOURCES

$\mathscr{L}$(f) – dB	SIGNAL SOURCE TYPE
-80	STANDARD OSCILLATOR
-90	FREQUENCY SYNTHESIZER
-100	FREQUENCY SYNTHESIZER
-110	
-120	
-130	COMMERCIAL CRYSTAL OSCILLATOR
-140	
-150	65 kHz FREQUENCY SYNTHESIZER
-160	
-170	CRYSTAL CONTROLLED PUMP SIGNAL SOURCE

REFERENCES

1. D. F. Rohde, T. G. Goldsberry, W. S. Olsen, and C. R. Reeves, "A Band Elimination Processor for an Experimental Parametric Acoustic Receiving Array", Paper No. 002, presented at The 92nd Meeting of The Acoustical Society of America, San Diego, California, 16-19 November 1976 [J. Acoust. Soc. Am. $\underline{60}$, Suppl. 1, 598].

2. D. W. Allan, "The Measurement of Frequency and Frequency Stability of Precision Oscillators", NBS Technical Note 669, National Bureau of Standards, Washington, DC.

3. D. Halford, J. H. Shoaf, and A. S. Risley, "Spectral Density Analysis: Frequency Domain Specification and Measurement of Signal Stability", Proceedings of 27th Annual Frequency Control Symposium, 12-14 June 1973, pp. 421-431.

4. M. M. Blachman and S. Mayerhofer, "An Astonishing Reduction in the Bandwidth of Noise", Proc. IEEE $\underline{63}$, 1077-1078 (July 1975).

5. Preliminary data on Austron Model 1120S low noise quartz oscillator manufactured by Austron, Inc., 1915 Kramer Lane, Austin, Texas 78758, December 1975.

6. F. L. Walls and A. E. Wainwright, "Measurement of the Short-Term Stability of Quartz Crystal Resonators and the Implication for Crystal Oscillator Design and Applications", IEEE Trans. Instrumentation and Measurement $\underline{IM-24}$, 15-20 (March 1975).

95

APPENDIX   E

THE DESIGN OF HIGH EFFICIENCY TRANSDUCER ELEMENTS AND ARRAYS

THE DESIGN OF HIGH EFFICIENCY TRANSDUCER ELEMENTS AND ARRAYS

M. W. Widener

Applied Research Laboratories
The University of Texas at Austin
Austin, Texas 78712

ABSTRACT

Parametric sound reception has created a need for pump
transducers capable of continuous operation with intense
sound fields. Reduction of internal losses and improved
heat transfer become important design goals. A transducer
structure has been developed in which the internal mechani-
cal energy dissipation is reduced dramatically and the
thermal coupling of the ceramic to the water is improved.
The basic design consists of a quarter wavelength mass
directly immersed in the fluid medium with the ceramic
element surrounded by an air cavity and driven in quarter
wavelength resonance. The assembly is suspended at the
vibrational node by a metal flange formed integrally with
the radiating mass. The resonance Q of the unloaded
assembly in air can be as high as 300 to 400. Water
loading diminishes the circuit Q to the order of 5 to 15
which corresponds to an effective electrical-to-acoustic
energy conversion efficiency in the range of 85 to 98%.
Practical elements exhibiting the same general quality of
operation over the frequency range from 7 kHz to 400 kHz
have been constructed.

Transducers used for the pump in parametric receivers must produce a very high sound level in a narrow beam with continuous transmission. High efficiency is needed to either reduce the electrical power input or to increase the sound power output. For continuous excitation, the transducer power limit is normally set by temperature rise rather than a mechanical stress failure. To put this into context consider a change in efficiency from 80% to 90%. The sound pressure level will change about 0.5 dB for a constant input electrical power; however, we can increase the drive level and the sound pressure by 3.5 dB and still keep the same internal heating losses. Our work has concentrated on finding the causes of internal power losses and reducing or eliminating them.

The basic estimate of mechanical loss that we use is the measurement of decay rate of natural resonance of the transducer structure. This can be expressed as the Q factor. This number is an indication of the energy loss per cycle of a resonant system. The decay rate may be observed directly when a steady excitation is removed as in a tone burst. Q is the product of n times π where n is the cycle count for a decay of $1/e$, or about 63% decrement.

Initial measurements were made on the ceramic alone to obtain a base line point. Much of our work has been done at 65 kHz and we prefer to use a ceramic cylinder in length mode resonance. The diameter is selected to give a minimum radial mode resonance above the operating range. Such a resonator has an unloaded Q in air in the range of 75 to 120 when driven with a constant current tone burst.

A test assembly was made with a rubber O-ring mounting and a thin window cast from RTV rubber. The design was an attempt to couple acoustic energy from the piston face only and to reduce other mechanical losses on the sides and rear of the element. The results were relatively good. The mounted Q was 36 which showed that the mounting losses were about equal to the internal losses of the ceramic. When this assembly was placed in the water, the Q further reduced to about 14. These numbers yielded the

101

following estimates of power division: 20% to the ceramic, 20% to the mounting, and 60% radiated into the water. These numbers do not show the percent power lost in the cable or the window so the actual acoustic power radiated is a smaller percent of the total electrical input. However, this kind of measurement will serve to indicate the effects of changes in the design.

The rubber mounted element was subjected to a continuous power level of 10 W electrical input and after about 10 minutes the acoustic output diminished due to a permanent shift in the polarization caused by heating. Heat does not flow easily from this assembly and the rubber appears to be absorbing too much power so we tried a different approach.

The fundamental mode of vibration was length resonance with an axial node at the center of the element. Thus, the obvious way to suspend the element was at this plane. Replacing one-half of the ceramic with a metal cylinder permits machining an integral flange for a mounting and eliminates the rubber O-rings on the ceramic. The ceramic was bonded directly to the metal quarter wave resonator with "5 Minute" epoxy. It was found that the two-part resonator now had an air Q much higher than the ceramic alone. Many types of front face seals were tried and all appeared to absorb the high Q obtained with the two-part structure. Eventually we attached the flange to an air filled housing and exposed the metal piston directly to the water. The result was a very large shift in the Q number between air and water which indicates a mechanical efficiency in excess of 95%.

The structural design was now opened to a great variety of materials and shapes for the radiating piston. One obvious design objective is to provide a better impedance match between ceramic and water. A simple expansion of the cylinder diameter in a flared cone gives a larger radiating area and more favorable impedance matching. The selection of the impedance of the piston material has a large effect on the Q measurements and the indicated efficiency. One of the most significant effects is the variations in bandwidth obtained from adjusting the design parameters.

102

Exposing the metal pistons to the water does restrict the selection of material so we have tried to optimize the design using brass. A series of conical pistons having angles from 0 to 100° was built. The Q measurements indicate satisfactory results up to about 60°; at this angle the edge becomes too flexible and the coupling begins to diminish. The pistons were machined after assembly to tune the resonance for a quarter wavelength mode thus assuring that the flange mounting was at the desired node. A dynamic measurement was made in the lathe during machining to speed the process of tuning. A single such element had an admittance circle diagram ratio of 30:1 which indicates a mechanical coupling efficiency of 96.7%. The addition of cables and tuning circuits decreases this figure some.

Experiments have been done at 10 kHz using aluminum pistons with 80° cone angle and a face diameter of 5 in. mounted in a sealed tube to exclude water except on the face. When tuned with an inductor, the response had a bandwidth from 8 to 12 kHz within 3 dB and the sound pressure was within 1 dB of 100% efficiency.

The single 65 kHz element was driven with 6000 V or 70 W electrical input and there was no apparent overheating. This represents a significant increase in the power limit for continuous excitation. The metal piston coupled directly to the water is an effective heat sink. We expect that an array of such elements will have a total power capability approaching the sum of the individual elements.

Several different arrays have been constructed from sets of the brass piston assemblies. The elements were machined on a turret lathe for a few cents each. The housing was a flat plate of brass with holes drilled in the desired array pattern. The back plate sealing the housing contacted the metal around each piston so that deep submergence is possible. The nodal flange is secured to the housing with conductive epoxy and a permanent epoxy seal is cast into a machined groove around each assembly. Elements are polarized oppositely in pairs so that the electrical drive is balanced and the housing is at common potential.

This design has been used to construct arrays of 4, 19, 84, and 432 elements arranged in a closely packed pattern approximating a circular aperture. Photographs of these arrays are presented in the slides and two beam patterns are shown. It is not always obvious that the side lobes in such patterns can contain a significant percentage of the power. For instance, in the 84-element beam pattern there is a sidelobe 35 dB down at 60° that contains 8% of the total radiated power. If we use the individual element performance to predict the power capability of the large array we get 43 kW and a sound level of 250 dB. The limits now become the cavitation level in the water and the electrical capacity of the wiring. Having high efficiency in the transducer has made it possible to have continuous radiation of an intense acoustic beam with modest electrical power input.

FIGURE 1
Q MEASUREMENT

$$Q = \pi n$$

POLARIZATION

$\frac{\lambda}{2}$
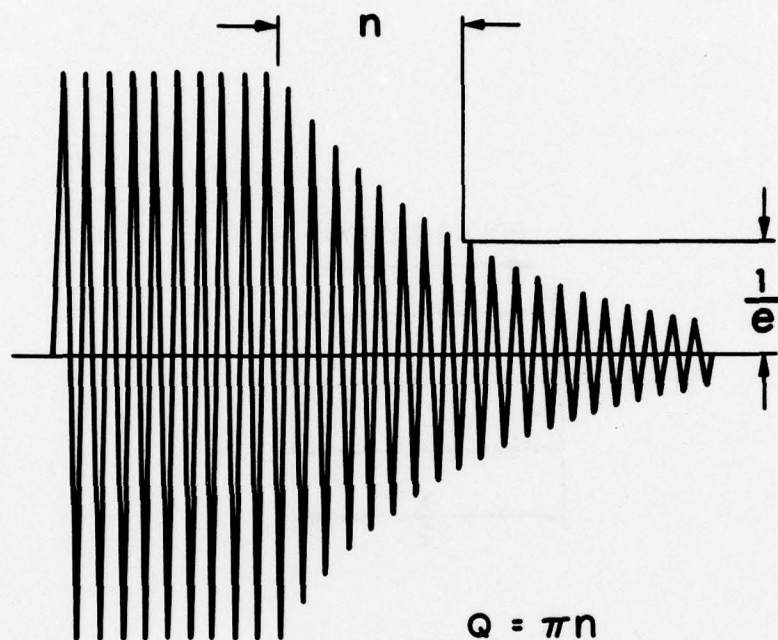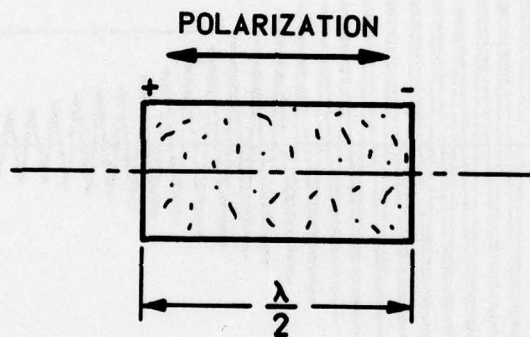
FIGURE 2
SOLID CERAMIC CYLINDER

$Q_A \approx 120$

106
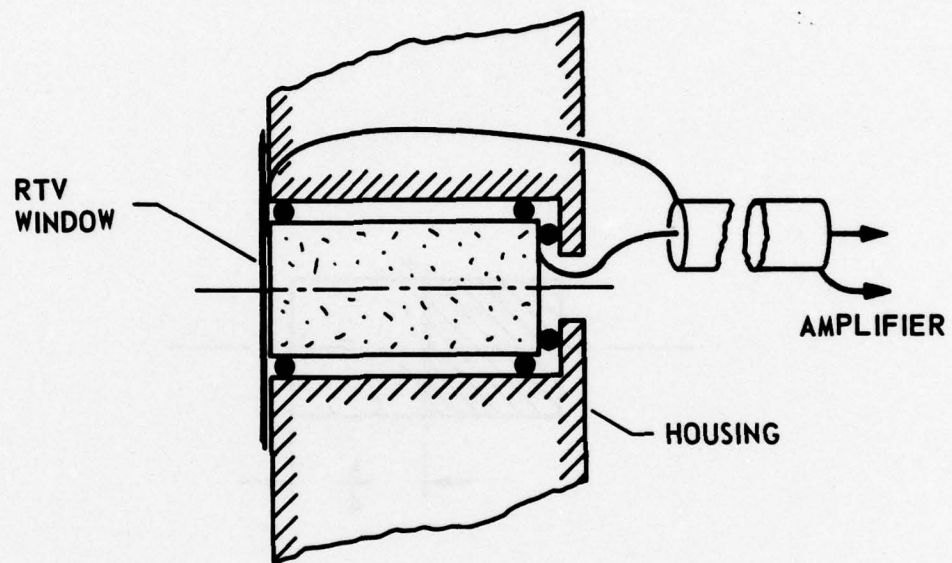
FIGURE 3
O-RING SUSPENSION
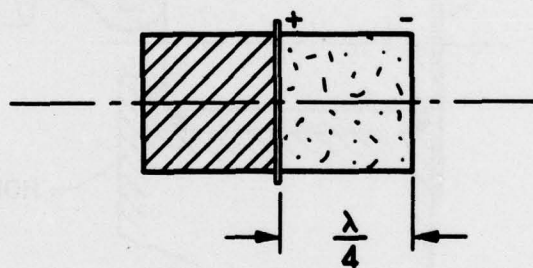
$Q_A = 250$

FIGURE 4
CERAMIC-BRASS RESONATOR
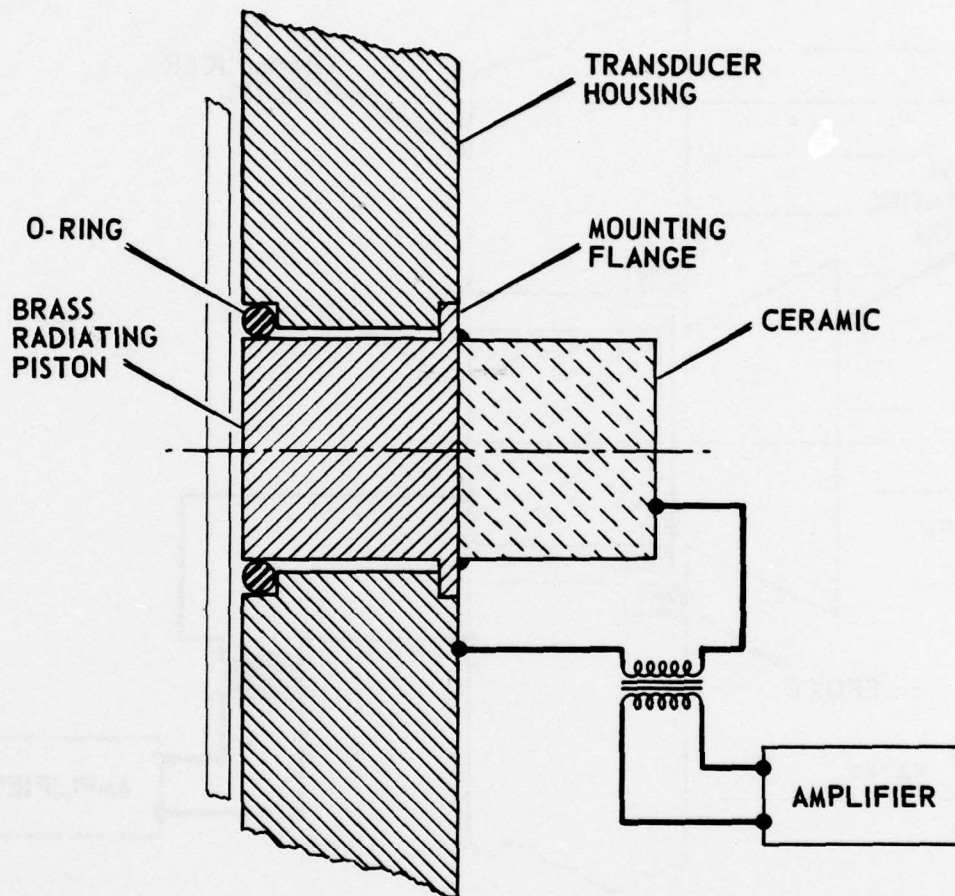
FIGURE 5

**TRANSDUCER STRUCTURE WITH RIGIDLY
MOUNTED ELEMENT AND O-RING SEAL**

FIGURE 6
EXPOSED PISTON TRANSDUCER STRUCTURE WITH
RIGIDLY MOUNTED ELEMENT AND EPOXY SEAL

110

FIGURE 7
RESONANCE QUALITY FOR
VARIATIONS IN CONE ANGLE

111

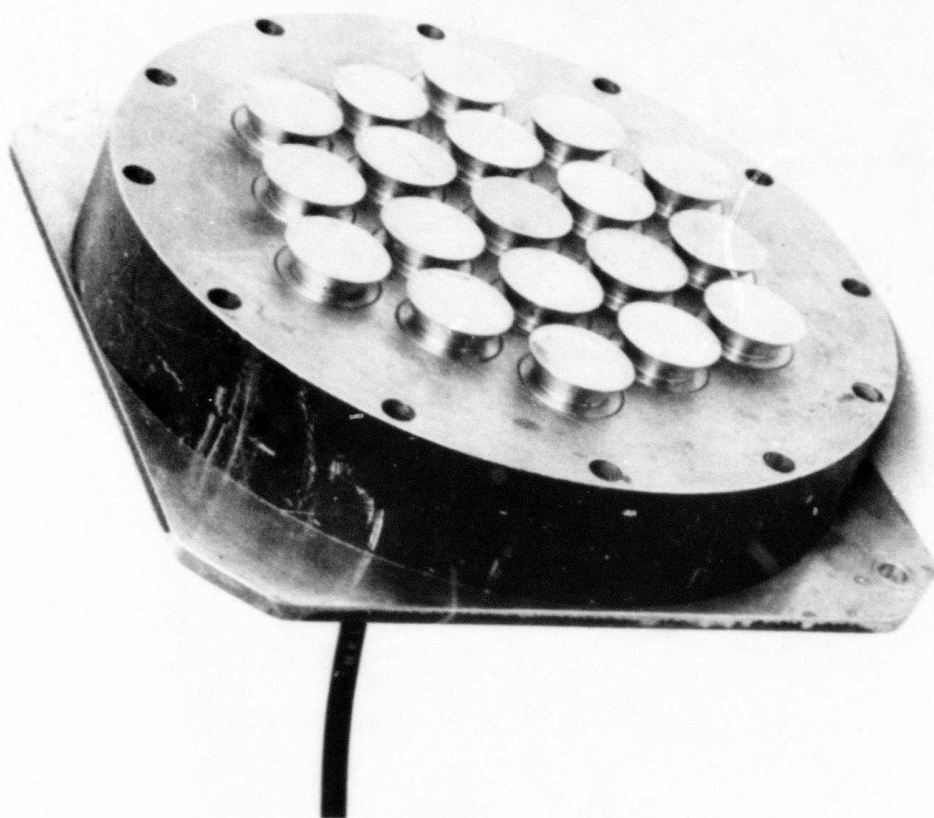**FIGURE 8
ADMITTANCE DIAGRAM**

FIGURE 9
19-ELEMENT ARRAY

0231-3

113

FIGURE 10
84- ELEMENT ARRAY

114
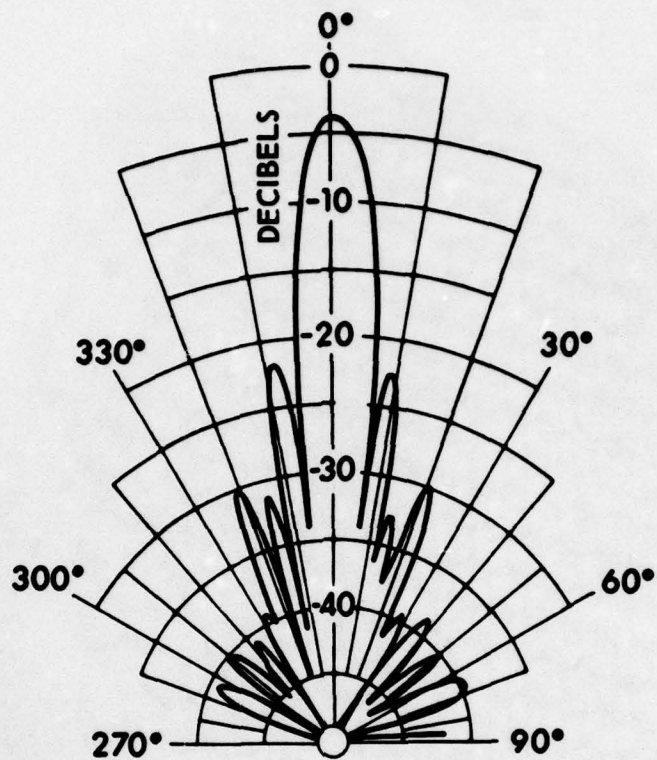
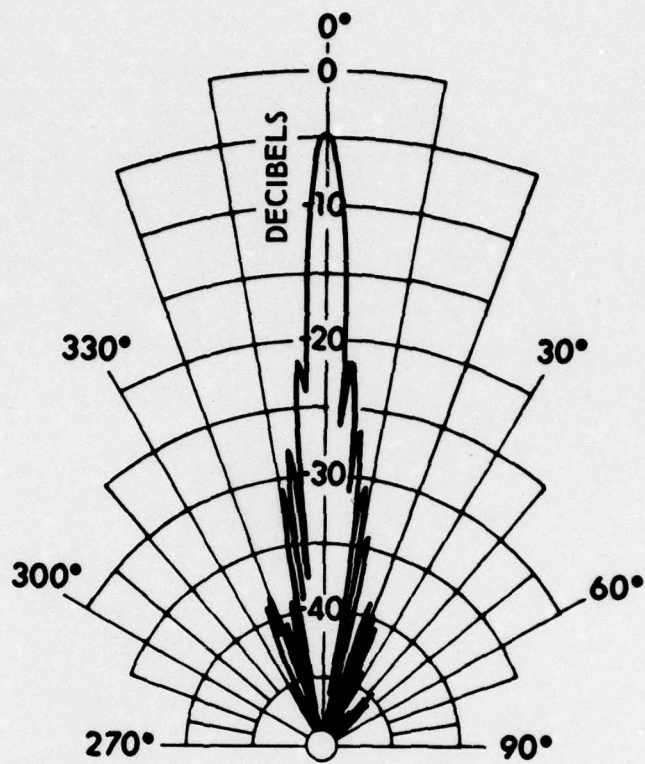FIGURE 11
432-ELEMENT ARRAY

115

0231-5

FIGURE 12

POLAR RESPONSE 84-ELEMENT ARRAY

FIGURE 13

POLAR RESPONSE 432-ELEMENT ARRAY

117

APPENDIX   F

THE DESIGN OF HIGH EFFICIENCY TRANSDUCER ELEMENTS AND ARRAYS

THE DESIGN OF HIGH EFFICIENCY TRANSDUCER ELEMENTS AND ARRAYS

M. Ward Widener

Applied Research Laboratories
The University of Texas at Austin
Austin, Texas 78712

Introduction

The detection of low frequency sound waves by parametric techniques
has created a need for pump transducers capable of continuous generation
of intense sound fields. The transducer must have good heat transfer to
the surrounding media and minimum internal electrical and mechanical
losses. A transducer element has been developed where the ceramic has
excellent thermal contact with the water and the mechanical resonance
has a high quality factor when not water loaded. Arrays built from the
design to be described have a large power handling capability, and the
measured directivity index is very close to the maximum calculated for
the aperture.

Design Approach

The evaluation of various means of transducer element mountings and
coupling to the water has been done in relation to the quality of reso-
nance observed between the unloaded air response and the tone burst
response when radiating sound in the water. The decay of a resonating
system when a steady state drive is terminated allows a measurement of
the energy loss per cycle indicated by the number of cycles, n, for the
excitation to decay to 1/e of the steady state value, as shown in Figure 1.
The Q of the circuit is given by the product n × π. The result of loading
a transducer element by water shows a significant change in the Q when the

121

$Q = \pi n$
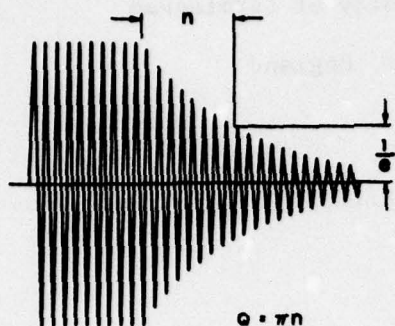
FIGURE 1
Q MEASUREMENT

element is delivering a large proportion of its input power to the water load. The relative efficiency is indicated by the change in the Q value.

An experimental program to determine a design with optimized loading efficiency has resulted in a practical and low cost construction technique. The first data base for the ceramic material was obtained by measuring the Q of a suitable cylinder form operated in axial mode resonance. A solid piece of PZT 8 or similar material was proportioned so that the radial mode frequency was higher than the axial length mode, the intention being to operate the transducer as a piston element at the lower frequency. A typical ceramic cylinder resonates with a Q of 75 to 120 in air. One such cylinder was mounted with a rubber suspension as shown in Figure 2. The face of the piston was covered with a thin layer of RTV rubber and the cylinder was held in place by O-rings. The results were relatively good and the air loaded Q was reduced to 35. This allows an estimate of an equal division of power loss between the ceramic material and the suspension rubber. When the element was placed in water, the Q further reduced to about 14, permitting an estimate of power division: 20% in ceramic, 20% in rubber, and 60% in
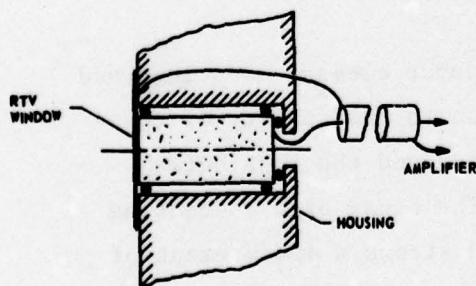
FIGURE 2
O-RING SUSPENSION

the sound radiation. When the resonance is simple and the Q measurements are single valued, this set of data points can be used to estimate where the power from the driving amplifier is being expended. This particular mounting was subjected to a 10 W drive for about 10 min and the material failed due to overheating. The design investigation now concentrated on removing the heat being generated in the ceramic.

122

Element Development

It was obvious that the suspension of the element was causing
mechanical losses and heat and that the heat was being retained in the
ceramic. Since the basic vibration of such a cylinder is axial and the
cylinder is a half-wavelength long, there would be a primary node at the
quarter wave point when the cylinder is operating at the fundamental
frequency. To minimize mounting losses, the ceramic should be supported
at this nodal point.

$Q_A = 250$
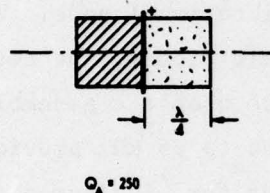
**FIGURE 3
CERAMIC-BRASS RESONATOR**

A simple way to do this is to replace half
of the ceramic with a metal piston having
an integral flange at the node. The flange
would serve to suspend the transducer
element in the housing. The resulting
construction shown in Figure 3 now had an
air resonance Q much higher than the
ceramic alone; this is due to the higher
quality of resonance in the quarter wave
piston. Several other advantages were now
apparent. The piston is solidly supported so that the transducer can be
exposed to high hydrostatic pressure. The ceramic can be enclosed in a
sealed, air filled housing with nothing touching the surface to absorb
power by mechanical friction. Acoustic radiation cannot occur through
the rear air loaded face of the ceramic so the front-to-back radiation
ratio should be very high. The design problem now concentrated on how to
couple the vibration from the metallic quarter wave piston to the water.

The piston was first mounted so that it was flush with the front of
the transducer housing plate and various types of seals were applied to
exclude the water. All such seals created significant mechanical losses.
It was eventually found that removing the seal and allowing the entire
quarter wave piston to be exposed to the water did not significantly
diminish the operating quality. By allowing a totally exposed piston to
be the radiating element, the piston design parameters can include

123

variations in shape as well as material. This freedom can be used to achieve an improved impedance match between the ceramic and the water; the shape can be used in array design where a large percentage of the aperture is active. The choice of the metal used for the piston greatly alters the operating Q and the resulting transducer bandwidth.

Sets of pistons of both brass and aluminum with conical flaring between the diameter of the ceramic driver and the radiating face have been made; flare angles were in the range 0 to 100°. In each test sample the metal material was machined such that the resonant operating frequency was a constant, thus assuring that the ceramic was operating in the quarter wave resonance and the support flange was at the vibrational node. When the ceramic piston is substituted for the two ceramic pieces, the ceramic-metal piston combination will be in proper resonance when the assembly is tuned to the same frequency. Typical elements tuned to 65 kHz provided a bandwidth of 4 to 5 kHz for brass pistons and 18 kHz for aluminum pistons. Relative Qs measured by tone burst signals for the brass elements operated in air and in water are given in Figure 4. At the higher flare angles the edge becomes too flexible and decouples from the piston so at the upper limit of 60° a rapid change in Q is observed. The admittance diagram for a typical element is shown in Figure 5 for air and water loaded conditions.
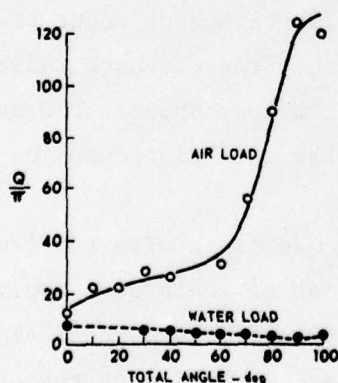
FIGURE 4
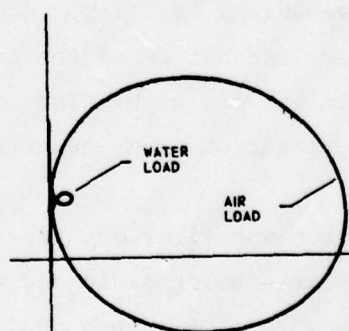RESONANT QUALITY FOR VARIATIONS IN CONE ANGLE

FIGURE 5
ADMITTANCE DIAGRAM

124

An element design using brass with 60° conical flare was subjected to a drive of 6000 Vp-p or about 70 W of electrical input. There was no apparent overheating after a period of continuous excitation at this high level. The metal piston coupled directly to the water forms an effective heat sink. The power capability of an array should approach the sum of the individual elements.

Several different arrays have been constructed using the brass piston assemblies with 60° conical angle. Since one electrode of the ceramic must be connected to the water, it is necessary and actually beneficial to operate the array with half of the elements mounted with reversed polarity. This permits a balanced drive with the transducer housing electrically at water potential. Each half is connected in parallel and a center tapped transformer is used to couple to single ended circuits where required.

Arrays have been constructed with 4, 19, 84, and 432 elements arranged with equal spacing in a triangular cell. The outer perimeter is adjusted by choosing elements approximating a circular aperture. The pistons were machined on a turret lathe at a low cost per unit. The assembly was done with fast setting epoxy in a clamping fixture with rotational smearing to make the epoxy bond as thin as possible. Final tuning of each element was done in a lathe while dynamic measurement of resonance frequency was done with a sweep generator and oscilloscope. Elements were secured by conductive epoxy to a housing plate having a machined hole, with the necessary shoulder to support the water pressure. The backing plate was in contact with the housing plate around each mounting hole so that great depth capability was obtained. Tests show that such a construction can withstand about 2000 psi before the support flange is crushed. Electrical bus bars insulated with Teflon tubing are mounted in machined slots connecting each row of mounting holes. Small wires connect to each element from the bus bars. After assembly the entire face seal is made by flowing epoxy into annular grooves around each element and its integrally machined flange mounting. The face could be better

protected by adding a window and filling the space with liquid, but such is not necessary for proper operation.

A photograph of an array having 84 elements is shown in Figure 6 and the measured beam pattern is shown in Figure 7. Note that the pattern is well controlled and there is very little radiation to the rear. The side-lobe at about 60° looks small but it actually contains about 10% of the total radiated power. The transmitting sensitivity is about 201 dB (re 1 μPa at 1 m) for an input power of 1 W electrical. Assuming an electrical to acoustical efficiency of near 100%, a directivity index of near 30 is indicated. The physical aperture size indicates the same directivity, and the measured beam major lobe size is in agreement. It would appear that the array performance is within 1 dB of perfect electrical-to-acoustical conversion. At this level of efficiency it is quite difficult to make measurements of sufficient accuracy to specify a value for the power conversion.
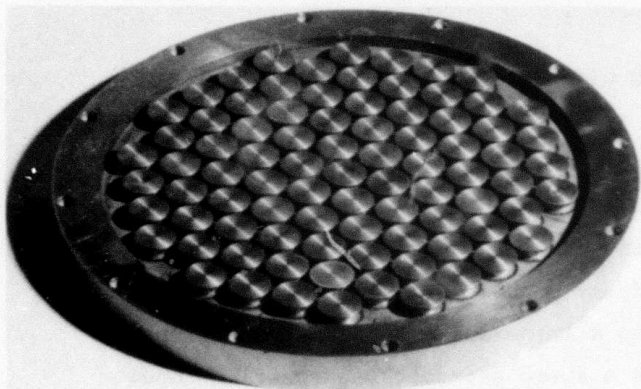
FIGURE 6
84-ELEMENT ARRAY
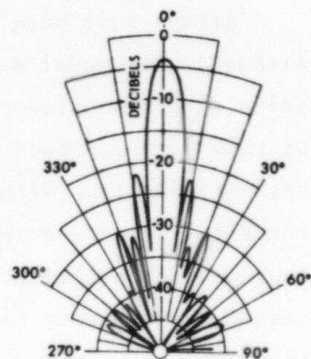
FIGURE 7
POLAR RESPONSE 84-ELEMENT ARRAY

All indications are that the design gives excellent results and the construction is simple and low cost. There are no special techniques or skills required and the parts can be built in a rather modest machine shop. For any given application, the material should be chosen for the environment and adjusted for the desired bandwidth by mechanical and

electrical tuning. The development of a simple high efficiency transducer
element has made possible the continuous radiation of an intense acoustic
beam with a modest electrical power input.

APPENDIX G

EXPERIMENTAL MEASUREMENT OF THE MODULATION
PROCESS INVOLVED IN NONLINEAR INTERACTION IN WATER

Paper X3, Presented at The 92nd Meeting of The Acoustical Society of America

16-19 November 1976, San Diego, California

EXPERIMENTAL MEASUREMENT OF THE MODULATION
PROCESS INVOLVED IN NONLINEAR INTERACTION IN WATER

C. R. Reeves, T. G. Goldsberry, W. S. Olsen, D. F. Rohde

Applied Research Laboratories
The University of Texas at Austin
Austin, Texas   78712

ABSTRACT

Nonlinear interaction between high and low frequency
sound fields in water has long been modeled as phase
modulation of the higher frequency by the lower frequency.
For the small modulation indices usually encountered in
a parametric acoustic receiving array, this is very nearly
a linear modulation process for which linear demodulation
techniques are appropriate. The optimum design of the
demodulator depends upon the parametric array sideband
phase relationships concerning which the literature is
not clear. For the phase modulation model the sidebands
should be oppositely phased. Simultaneous but independent
measurements of the sidebands resulting from the inter-
action of a 65 kHz signal with low frequency signals from
100 Hz to 1 kHz now permit a direct comparison of the
sidebands for verification of the theory. Results are
discussed for various frequencies, sound levels, and
interaction geometries.

Applied Research Laboratories, The University of Texas at Austin (ARL:UT), has constructed an experimental low frequency parametric acoustic receiving array (PARRAY). This paper presents some of the results of the current experimental program involving the PARRAY and discusses these results with respect to PARRAY system design and implementation.

The PARRAY operates as a low frequency acoustic sensor by taking advantage of the very slight nonlinearity involved in acoustic propagation through water. As shown in Slide 1, the PARRAY is an active system consisting of a high frequency signal source, called the pump, and a receiver. The pump signal is projected acoustically from the pump through the water to the hydrophone. During transmission through the water, the pump signal interacts with low frequency acoustic signals present in the water to form intermodulation products which may then be recovered by the receiver electronics. The magnitude of a particular intermodulation product appearing at the hydrophone depends strongly on the geometric relationship of the direction of arrival of the ambient low frequency signal, the pump, and the hydrophone. For the common case where the pump and hydrophone have symmetric beam patterns aimed directly at each other, the intermodulation product depends on the angle between the low frequency signal direction of arrival and the pump-hydrophone vector. This mechanism causes the PARRAY to exhibit low frequency directionality characteristic of a continuous end-fire array.[1]

Slide 2 shows typical spectra of the signals in the PARRAY system. The low frequency incoming signal interacts with the high frequency pump signal to produce modulation sidebands on the pump signal at the hydrophone. Since it is these modulation sidebands which reflect the low frequency directional characteristics of the PARRAY, is is evident that the receiver electronics must demodulate the hydrophone signal to recover the desired low frequency signal.
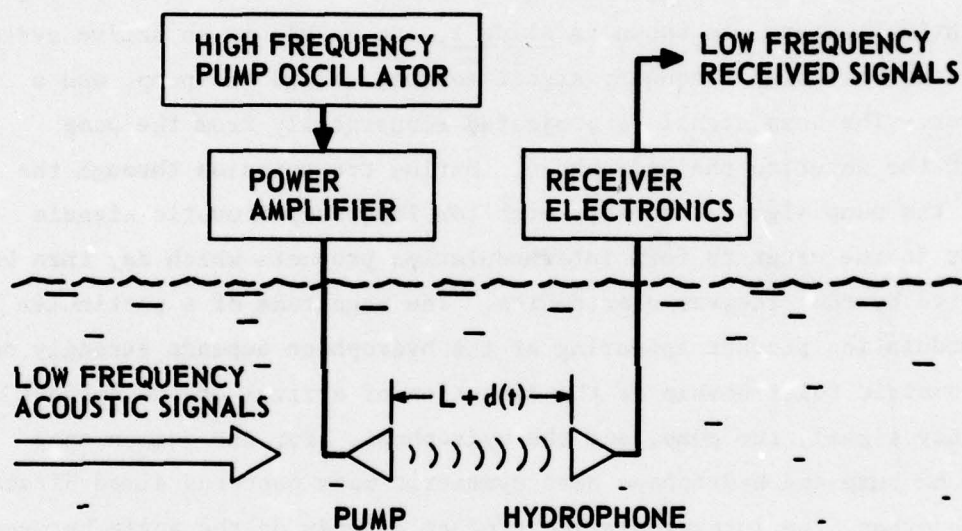
133

HIGH FREQUENCY
PUMP OSCILLATOR

LOW FREQUENCY
RECEIVED SIGNALS

POWER
AMPLIFIER

RECEIVER
ELECTRONICS

LOW FREQUENCY
ACOUSTIC SIGNALS

|← L + d(t) →|

)))))))

PUMP

HYDROPHONE

PARAMETRIC ACOUSTIC RECEIVING ARRAY (PARRAY)

134

SLIDE 1

PUMP SIGNAL
SPECTRUM

RECEIVED SIGNAL
SPECTRUM

$0 \qquad\qquad \omega_1 \quad \overrightarrow{\omega}$

$0 \quad \omega_2 \qquad \omega_1 \quad \overrightarrow{\omega}$

$(\omega_1 - \omega_2)$ $\qquad\qquad (\omega_1 + \omega_2)$

LOW FREQUENCY
SIGNAL SPECTRUM

PUMP))))))) HYDROPHONE

$0 \quad \omega_2 \qquad\qquad \overrightarrow{\omega}$
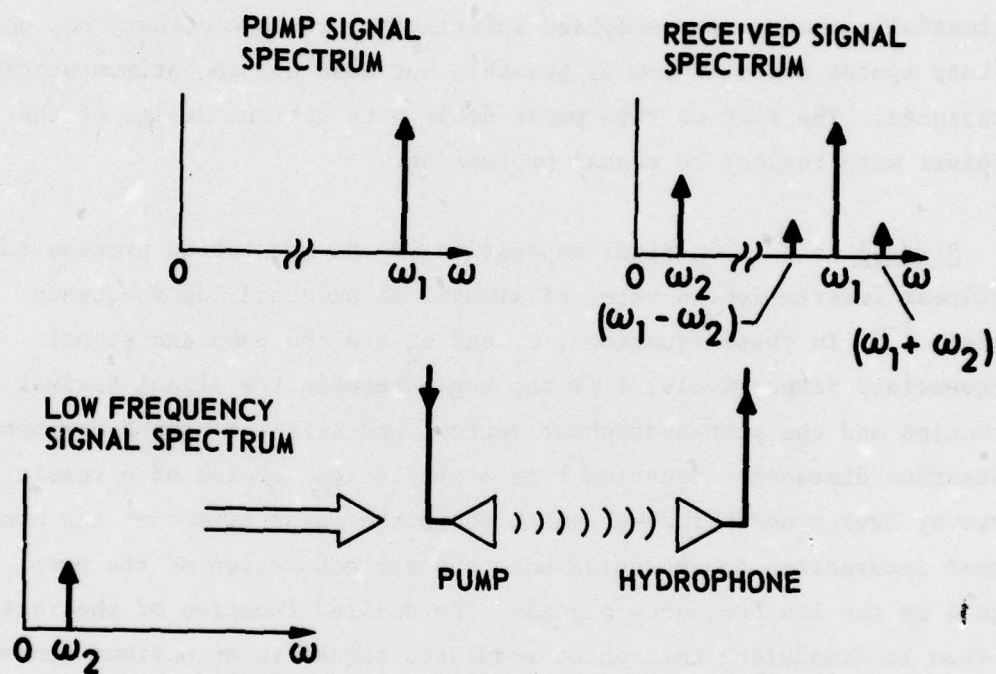
TYPICAL SPECTRA IN PARRAY

ARL - UT
AS-76-1130-S
CRR - DR
10 - 4 - 76

SLIDE 2

In spite of the apparent simplicity of the PARRAY, there are a number of difficult problems which must be overcome in the implementation of a practical system. Since acoustic propagation through water is only weakly nonlinear, the intermodulation products (modulation sidebands) at the hydrophone are very small in relation to the pump signal (carrier). In the experimental system for the reception of low frequency waves, the sidebands may be from 100 to 160 dB below the carrier. In order to successfully recover the sideband information, it is necessary not only to keep system noise as low as possible but also to use optimum processing techniques. The rest of this paper deals with optimum design of the receiver with respect to signal processing.

Slide 3 is a theoretical exposition of the modulation process for nonlinear interaction in water of sinusoidal pump and low frequency signals.[2-4] In these equations, ω_1 and ω_2 are the pump and signal frequencies, respectively, θ is the angle between the signal arrival direction and the pump-hydrophone vector, and L is the pump-hydrophone separation distance. Equation 1 is a simplified version of a result given by Zverev and Kalachev[3] which shows the major effect of the non-linear interaction to be equivalent to phase modulation of the pump signal by the low frequency signal. The desired function of the receiver is then to demodulate this phase modulated signal in an optimum manner to recover the low frequency signal.

Some insight as to how this may be accomplished is gained by expanding the right-hand side of Equation 1 into an infinite series. For small values of the phase modulation index, the series has only three significant terms representing the carrier and first modulation sidebands as shown in Equation 2. The higher order terms of the series, which represent modulation at harmonics of the signal frequency, are almost certain to be too small to represent a usable amount of energy in a prac-tical PARRAY system. The modulation process is then very nearly linear, for which linear demodulation techniques are appropriate. $Q(\theta)$ is the phase modulation index of the process and leads directly to the directiv-ity of the PARRAY.

136

$$r(t,\theta) = p_1 \cos(\omega_1 t + Q(\theta) \sin \omega_2 t) \tag{1}$$

$$\approx p_1 \cos \omega_1 t + \frac{p_1 Q(\theta)}{2} \cos(\omega_1 + \omega_2)t - \frac{p_1 Q(\theta)}{2} \cos(\omega_1 - \omega_2)t \tag{2}$$

$$Q(\theta) = \frac{\left(\frac{B}{2A} + \cos\theta\right) p_2 \omega_1 L}{\rho_0 c_0^3} \cdot \frac{\sin\left[\frac{k_2 L}{2}(1 - \cos\theta)\right]}{\frac{k_2 L}{2}(1 - \cos\theta)} \tag{3}$$

$\omega_1 = 65$ kHz

$\omega_2 = 100$ TO 1000 Hz

SIGNAL AT HYDROPHONE

137

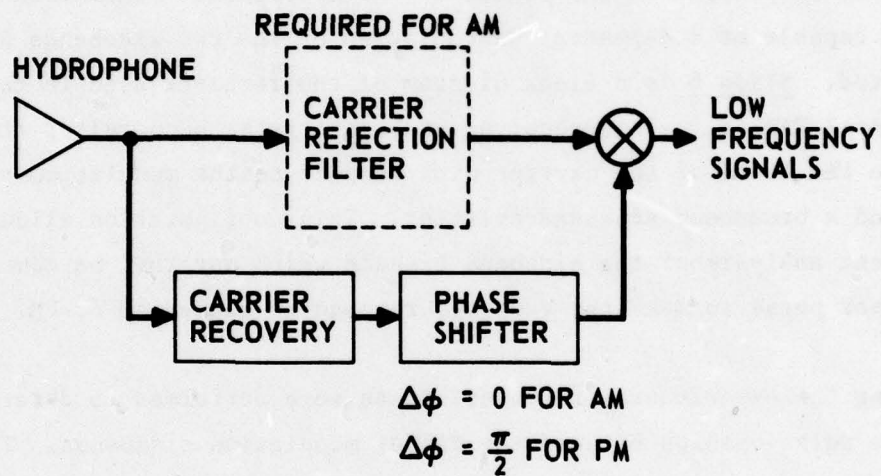SLIDE 3

We note at this point that some more detailed treatments of nonlinear interaction in water have indicated that the signal at the hydrophone contains both amplitude (AM) and phase (PM) modulation components.[5-6] The difference between phase and amplitude modulation is very slight in terms of Equation 2 in that the sign of the last term is changed; however, there are some important implications for the design of a practical receiver.

Slide 4 is a block diagram of a receiver which theoretically may be used for either PM signals of low modulation index or AM signals, depending only on the setting of the carrier phase shifter. The demodulation is performed by mixing the recovered carrier with the received signal in a balanced modulator. When the recovered carrier is phased properly, the mixing process produces coherent addition of the sideband signals during demodulation for optimum linear processing of the sideband energy. The present state of the art in balanced modulator design is such that a PM signal with modulation index as small as 10^{-8} may be successfully demodulated by this technique without need of the carrier rejection filter shown in the dashed block. This is possible for PM signals because the received carrier and recovered carrier are mixed in quadrature in the balanced modulator. The carrier contribution to the balanced modulator output is then only a double frequency term which may easily be removed by filtering. For AM signals with small modulation index, the carrier rejection filter is required to effectively increase the modulation index before demodulation.

The use of a realistic carrier rejection filter leads to phase shifts in the modulation sidebands which must be compensated for either directly or by additional phase shifting of the carrier used for demodulation. While this compensation may be easily accomplished for a single modulation frequency, it is a substantial problem in a broadband system. Therefore, the complexity of the receiver depends strongly on the type of modulation.

For phase modulation only, the carrier recovery and signal demodulation may be combined to yield a very simple receiver configuration

138

PARRAY RECEIVER

SLIDE 4

shown in <u>Slide 5</u>. This receiver is similar to an ordinary phase lock loop
FM demodulator; however, in the PARRAY application the loop bandwidth
should be just large enough to track phase changes in the carrier due to
drift of the pump signal. The loop then does not track the modulation
attributable to nonlinear interaction so these components appear with
maximum amplitude at the receiver output.

During the development of the experimental PARRAY it was not known
what type of modulation or, more generally, what sort of phase relation-
ships would be present in the signal at the hydrophone. Therefore a
receiver capable of independent demodulation of the two sidebands was
constructed. <u>Slide 6</u> is a block diagram of the receiver used in the
experimental PARRAY.[7] This receiver employs crystal band reject filters
to reduce the level of the carrier with respect to the modulation side-
bands, and a broadband sideband splitter. This configuration allows the
independent analysis of the sideband signals which may then be combined
with proper phase to make the receiver respond to either AM or PM.

Using the experimental receiver, tests were performed to determine
the phase relationships between the PARRAY modulation sidebands. These
tests were run at Applied Research Laboratories Lake Travis Test Station
(LTTS) near Austin, Texas. The PARRAY configuration employed a 66 m
pump-hydrophone separation, a 65 kHz pump frequency, and low frequency
acoustic signals in the range of 100 to 1000 Hz transmitted from a mobile
source at a range of 600 m. Tests were run for a number of angles between
the low frequency source direction and the pump-hydrophone vector; however
all tests had the source in the main lobe of the PARRAY response. Upper
and lower sideband data output by the experimental receiver was digitally
recorded and processed on a small computer.

In order to compare the PARRAY sideband signal phases, it was first
necessary to calibrate the experimental system to determine the phase
shifts internal to the system. This was accomplished by injecting signals
with known modulation characteristics into the hydrophone and measuring
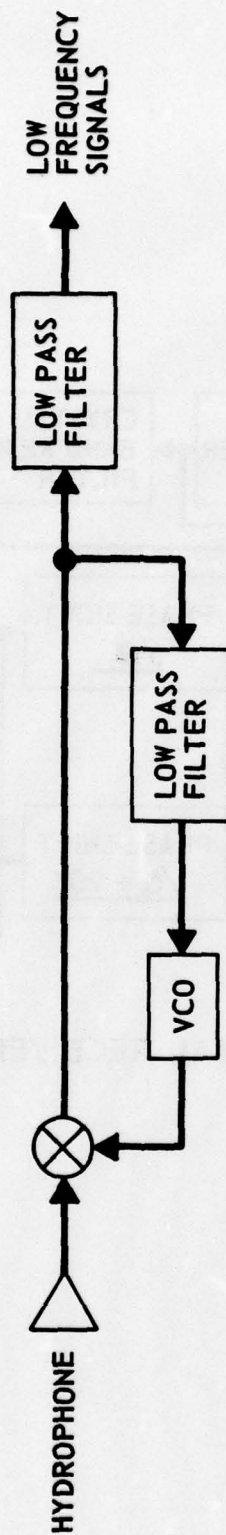
PHASE LOCK LOOP PARRAY RECEIVER

141
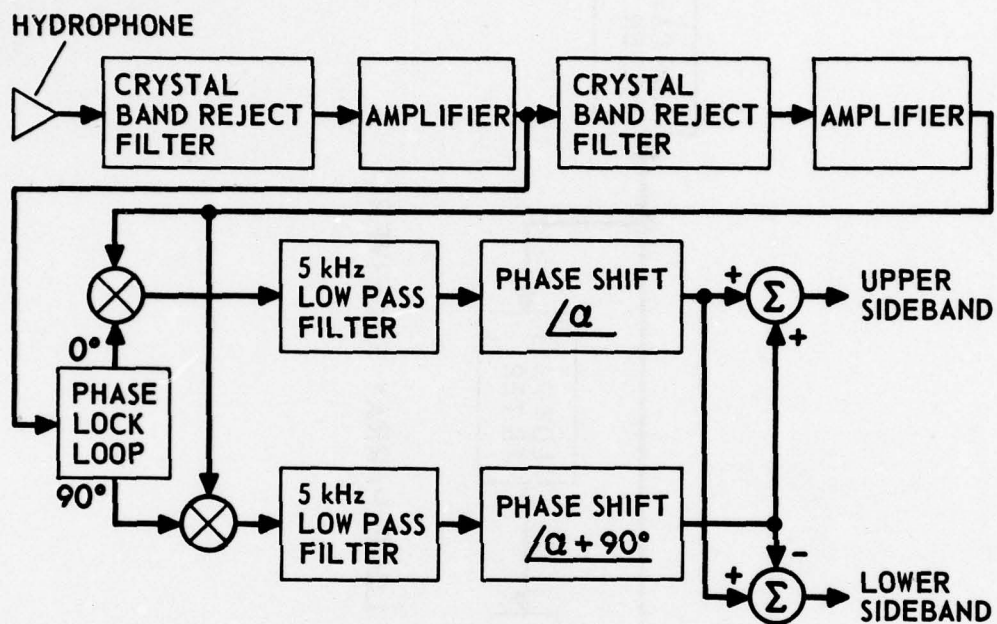
SLIDE 5

EXPERIMENTAL RECEIVER

the sideband output phase relationships. Then signals from the low frequency source were received by the PARRAY and compared with the calibration data.

Slide 7 shows the principal results of the investigation. The PARRAY experimental data is in good agreement with the phase modulation calibration; this indicates that the nonlinear interaction in water is primarily a phase modulation process for these conditions. The data for all tested source direction angles, ranges, and signal levels were in close agreement with the data shown. This implies no measurable dependency of the sideband signal phase relationships on these variables.

The results of this investigation then may be summarized as follows.
1) The phase modulation model for nonlinear interaction in water is confirmed.
2) An optimum practical receiver for a PARRAY may be easily constructed using the balanced modulator concept discussed here.

143
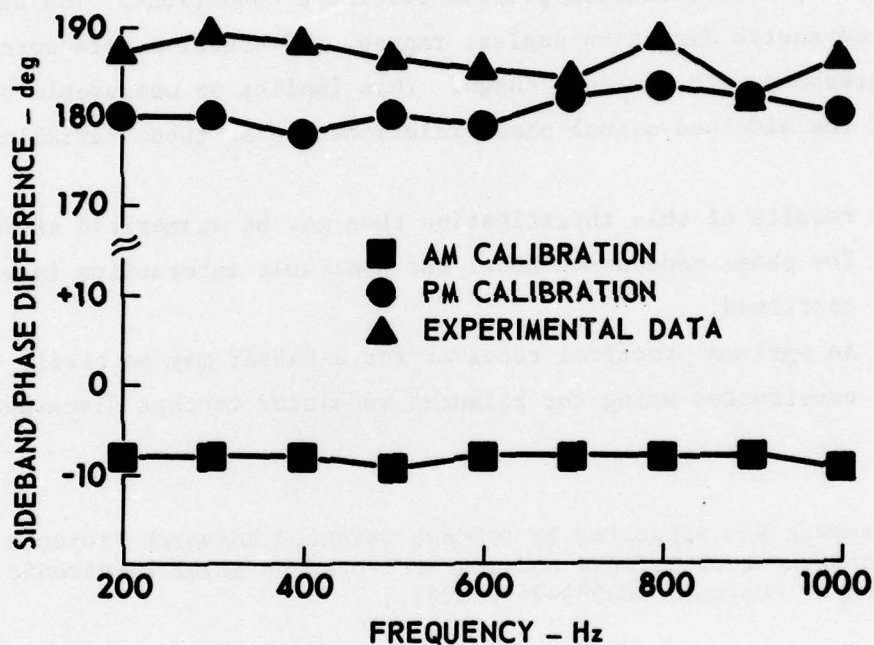
**COMPARISON OF AM AND PM CALIBRATIONS
WITH PARRAY EXPERIMENTAL DATA**

144

SLIDE 7

REFERENCES

1. H. O. Berktay and J. A. Shooter, "Parametric Receivers with Spherically Spreading Pump Waves", J. Acoust. Soc. Am. 54, 1056-1061 (1973).

2. H. Date and Y. Tozuka, "Parametric Directional Microphone", The 6th International Congress on Acoustics", Tokyo, Japan, 21-28 August 1968.

3. V. A. Zverev and A. I. Kalachev, "Modulation of Sound by Sound in the Intersection of Sound Waves", Soviet Phys.-Acoust. 16, 204-208 (October-December 1970).

4. J. J. Truchard, "Signal Processing for Parametric Acoustic Receiving Array Experiments", Paper No. N12, The 91st Meeting of The Acoustical Society of America, Washington, DC 4-9 April 1976.

5. H. O. Berktay and C. A. Al-Temimi, "Virtual Arrays for Underwater Reception", J. Sound Vib. 9, 295-307 (1969).

6. J. J. Truchard, "Parametric Acoustic Receiving Array, I. Theory", J. Acoust. Soc. Am. 58, 1141-1145 (1975).

7. D. F. Rohde, T. G. Goldsberry, W. S. Olsen, and C. R. Reeves, "A Band Elimination Processor for an Experimental Parametric Acoustic Receiving Array", Paper No. 002, The 92nd Meeting of The Acoustical Society of America, San Diego, California, 16-19 November 1976 [J. Acoust. Soc. Am. 60, Suppl. 1, 598 (1976)].

APPENDIX   H

VIBRATION SENSITIVITY OF THE PARAMETRIC ACOUSTIC RECEIVING ARRAY

147

VIBRATION SENSITIVITY OF THE PARAMETRIC ACOUSTIC RECEIVING ARRAY

by

C. Richard Reeves
Voldi E. Maki, Jr.
Tommy G. Goldsberry
David F. Rohde

Applied Research Laboratories
The University of Texas at Austin
Austin, Texas   78712

ABSTRACT

A parametric (nonlinear) receiving array exhibits sensitivity to motion of its transducers in a manner significantly different from that of conventional arrays. An understanding of this sensitivity is necessary for the proper evaluation of the benefits of parametric arrays in many applications of interest. In this paper a theory relating motion of the array transducers to the array output signal is developed, and predictions from the theory are compared with experimental observations on both 5 m and 340 m parametric arrays used for low frequency reception. Several methods of counteracting the detrimental effects of transducer motion are discussed.

VIBRATION SENSITIVITY OF THE PARAMETRIC ACOUSTIC RECEIVING ARRAY

C. Richard Reeves
Voldi E. Maki

Tommy G. Goldsberry
David F. Rohde

Applied Research Laboratories, The University of Texas at Austin
P. O. Box 8029, Austin, TX 78712

ABSTRACT

A parametric (nonlinear) receiving array exhibits sensitivity to motion of its transducers in a manner significantly different from that of conventional arrays. An understanding of this sensitivity is necessary for the proper evaluation of the benefits of parametric arrays in many applications of interest. In this paper a theory relating motion of the array transducers to the array output signal is developed, and predictions from the theory are compared with experimental observations on both 5 m and 340 m parametric arrays used for low frequency reception. Several methods of counteracting the detrimental effects of transducer motion are discussed.

FIGURE 1. PARRAY FUNCTIONAL DIAGRAM

I. INTRODUCTION

The Parametric Acoustic Receiving Array (PARRAY) is a technique for obtaining directional reception of low frequency acoustic waves with only two relatively small high frequency transducers [1,2]. Recent development efforts have led to practical design procedures for PARRAY's which are significantly different from design procedures for conventional hydrophone arrays [3]. This paper addresses the response of the PARRAY to mechanical vibration of its transducers. It is shown that the response is predictable and not necessarily detrimental if the response is taken into account in the system design.

II. THE PARRAY

A PARRAY functions as an acoustic sensor by taking advantage of the small nonlinearity involved in acoustic propagation through water. Because of the nonlinearity, multiple acoustic signals in water produce intermodulation products which are detected in the PARRAY. Figure 1 shows the basic elements of a PARRAY. A narrowband ultrasonic signal generated by the PARRAY pump constitutes one of the signals in the water. As this pump signal propagates toward the hydrophone, it mixes with ambient signals to produce products which, along with the pump signal, are received by the hydrophone. Conventional but state-of-the-art techniques recover the ambient acoustic signal by detecting the intermodulation products in the pump carrier sidebands.

The primary reason for receiving ambient acoustic signals by this method is that desirable directional response characteristics may be obtained. The amplitude of an intermodulation pro-

duct received by the hydrophone is dependent upon the angle between the direction of propagation of the ambient signal and the pump-hydrophone axis. This angular dependence is very similar to that of an end-fired array with length equal to the pump-hydrophone separation. Hence, the PARRAY is more than an acoustic sensor; it is a directional array.
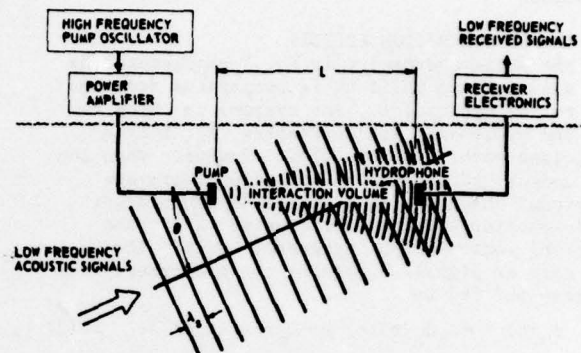
The pump signal and intermodulation products appearing at the hydrophone can be expressed in closed form as a phase modulation of the pump carrier by the ambient acoustic signals [4]. Let the pump signal be a sinusoid $C \cos \omega_0 t$. Then the hydrophone signal can be expressed as

$$s(t) = C' \cos[\omega_0 t + \phi(t) + \psi] \quad , \qquad (1)$$

where C'/C represents losses between the pump and hydrophone, ψ is a phase constant determined by the pump-hydrophone separation, and the phase modulation due to nonlinear interaction is given by

$$\phi(t) = \frac{\left(\frac{B}{2A} + \cos \theta\right) \omega_0 L}{\rho_0 c_0^3} \frac{\sin\left[\frac{\omega_1 L}{2c_0}(1 - \cos \theta)\right]}{\frac{\omega_1 L}{2c_0}(1 - \cos \theta)} p(t) , \quad (2)$$

where

$p(t)$ = ambient pressure signal at frequency ω_1
B/A = parameter of nonlinearity of water (≈ 5)
θ = angle between direction of ambient signal propagation and pump-hydrophone axis
ρ_0 = density of water
c_0 = sound speed in water
L = pump-hydrophone separation distance

FIGURE 2. PARRAY RECEIVER BLOCK DIAGRAM

For most values of ω_1, the term with the form $(\sin x)/x$ in Eq. 2 dominates the angular dependence of the phase modulation index and gives the PARRAY its end-fired array directional characteristics.
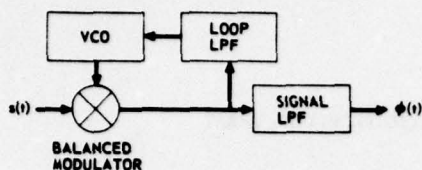
III. TRANSDUCER MOTION EFFECTS

The phase constant ψ in Eq. 1 represents the pump signal phase shift as it propagates from the pump to the hydrophone. For systems in which the pump and hydrophone are stationary, Eq. 1 is a sufficient model with $\psi = \omega_0 L/c_0$. However, when the pump and/or hydrophone are in motion there are additional phase shifts in the hydrophone signal due to Doppler effects. We consider first the effect of motion of the hydrophone only. The pump carrier signal as seen by the hydrophone will be phase shifted by

$$\phi_h(t) = -\omega_o d_h(t)/c_o = -\omega_o \iint a_h(t) dt^2/c_o \quad , \quad (3)$$

where $d_h(t)$ is the displacement of the hydrophone along the pump-hydrophone axis in the direction away from the pump and $a_h(t)$ is the corresponding acceleration. Transducer motion in directions other than along the pump-hydrophone axis causes no Doppler effect and therefore is not considered here or in the following development.

Motion of the pump transducer produces a similar effect on the signal at the hydrophone except that the propagation delay from pump to hydrophone must be taken into account. Here the phase shift is

$$\phi_p(t) = \omega_o d_p(t-L/c_o)/c_o = \omega_o \iint a_p(t-L/c_o) dz^2/c_o . (4)$$

The phase shifts due to pump and hydrophone motion are summed as

$$\phi_m(t) = \phi_h(t) + \phi_p(t) = \frac{\omega_o}{c_o}\left[d_p\left(t - \frac{L}{c_o}\right) - d_h(t)\right]. (5)$$

Then the pump signal and nonlinear interaction products received by the hydrophone are

$$s(t) = C' \cos[\omega_o t + \phi(t) + \phi_m(t) + \psi] \quad , \qquad (6)$$

and it is apparent that the phase modulation introduced by transducer motion, $\phi_m(t)$, is added to the desired signal, $\phi(t)$, and so cannot be easily disregarded. This expression may also be used to show the quantitative equivalence between acoustic sound pressure level (SPL) and vibration level in the PARRAY. That is, the sensitivity of the PARRAY to vibration can be expressed as an equivalent acoustic sensitivity by setting

$$\phi_m(t) = \phi(t) \qquad (7)$$

and solving for the relationship between SPL and

vibration level. The general result is

$$p(t) = \frac{\left[d_p\left(t - \frac{L}{c_o}\right) - d_h(t)\right]\rho_o c_o^2\left[\frac{\omega_1 L}{2c_o}(1 - \cos\theta)\right]}{\left(\frac{B}{2A} + \cos\theta\right)L \, \sin\left[\frac{\omega_1 L}{2c_o}(1 - \cos\theta)\right]} \qquad (8)$$

which for on-axis arrival angle ($\theta=0$) reduces to

$$p(t) = \frac{[d_p(t-L/c_o) - d_h(t)]\rho_o c_o^2}{(B/2A+1)L} \qquad (9)$$

This shows that the PARRAY vibration sensitivity is independent of pump frequency and inversely proportional to array length.

A few computations indicate that the PARRAY is sensitive to vibration at practical levels. For example, for a 5 m long PARRAY in water, a sound pressure level of 100 dB re 1 μPa rms corresponds to a displacement of one transducer by 7.58×10^{-10} m rms. This displacement is equivalent to an acceleration level of 30 dB re 1 μg at 100 Hz or 70 dB re 1 μg at 1000 Hz.

IV. PARRAY SIGNAL PROCESSING

Since the modulation index of the phase modulation due to acoustic nonlinear interaction in water is ordinarily very small, 10^{-4} to 10^{-8} for SPL's typically encountered in underwater acoustics, the phase modulation process in the absence of vibration is for all practical purposes linear. Equation 1 may be rewritten

$$s(t) = C' \cos(\omega_o t + \psi) \cos\phi(t)$$
$$- C'\sin(\omega_o t + \psi) \sin\phi(t) \quad , \quad (10)$$

which, for small $\phi(t)$, reduces to

$$s(t) = C' \cos(\omega_o t + \psi) - C'\phi(t) \sin(\omega_o t + \psi) . \quad (11)$$

In this form it is apparent that the hydrophone signal consists of the pump carrier and a quadrature amplitude modulation component which carries the desired information $\phi(t)$.

The block diagram of a linear receiver for this signal is shown in Fig. 2. It consists principally of a phase locked loop which recovers the quadrature carrier. The bandwidth of this loop is made very small so that only the carrier and not the modulation sidebands are tracked by the loop. The sideband signals are demodulated by the loop mixer and $\phi(t)$ remains after removal of double frequency components by the low pass filter.

In a similar manner, Eq. 6, which includes the effects of transducer motion, may be expressed as

$$s(t) = C' \cos[\omega_o t + \phi_m(t) + \psi]$$
$$- C'\phi(t) \sin[\omega_o t + \phi_m(t) + \psi] \quad , \quad (12)$$

which equation is of the same form as Eq. 11 but includes transducer motion induced phase modulation in all the carrier terms. Equation 12 is the general model for the hydrophone signal in the presence of transducer motion. If $\phi_m(t)$ is small, then Eq. 12 may be linearized as
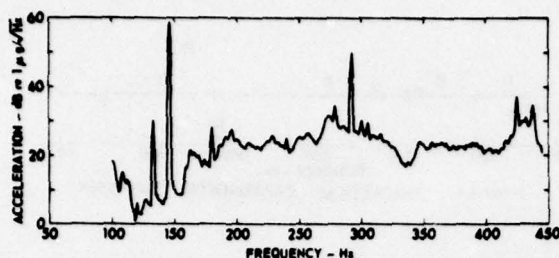
152

FIGURE 3. ACCELERATION SPECTRUM

FIGURE 4. SOUND PRESSURE LEVEL SPECTRUM

$$s(t) \approx C' \cos(\omega_o t + \psi)$$
$$- C'[\phi(t) + \phi_m(t)] \sin(\omega_o t + \psi) \quad . \quad (13)$$

This model is appropriate when transducer motion is very small.

When transducer motion is small the receiver configuration of Fig. 2 may be used with satisfactory results if the presence of $\phi_m(t)$ in the output can be tolerated. The receiver output is $\phi(t) + \phi_m(t)$ for this case.

It is informative to express the signal models of Eqs. 11, 12, and 13 in the frequency domain because all experimental data is presented in this form. For Eq. 11, the linear acoustic signal only model, the power spectrum of $s(t)$ consists of the carrier at frequency ω_o with symmetric upper and lower sidebands of the same form as the power spectrum of $\phi(t)$. The sideband power spectrum of $s(t)$ is proportional to the power spectrum of $\phi(t)$:

$$\left|S(\omega + \omega_o)\right|^2 \alpha \left|\phi(\omega)\right|^2 \quad . \quad (14)$$

Similarly, for the linear small vibration model of Eq. 13,

$$\left|S(\omega + \omega_o)\right|^2 \alpha \left|\phi(\omega) + \phi_m(\omega)\right|^2 \quad . \quad (15)$$

However, when the vibration is of sufficient magnitude to warrant the use of the nonlinear model of Eq. 12 the power spectrum of $s(t)$ is

$$\left|S(\omega)\right|^2 \alpha \left|H(\omega) + j\phi(\omega) * H(\omega)\right|^2 \quad , \quad (16)$$

where $H(\omega)$ is the spectrum of $\cos[\omega_o t + \phi_m(t) + \psi]$ and * indicates convolution. The point to be noted here is that the spectral products in $S(\omega)$ are not linearly related to $\phi(\omega)$ and $\phi_m(\omega)$. This occurs both because $H(\omega)$ is not linearly related to $\phi_m(\omega)$ and because of the convolution with $\phi(\omega)$. In the linear models neither of these events occurred.

The equivalence between on-axis acoustic and vibration induced signals, Eq. 9, in the frequency domain is

$$\left|P(\omega)\right|^2 = \frac{\rho_o^2 c_o^4}{(B/2A+1)^2 \, L^2} \left|D(\omega)\right|^2$$

$$= \frac{\rho_o^2 c_o^4}{(B/2A+1)^2 \, L^2 \omega^4} \left|A(\omega)\right|^2 \quad (17)$$

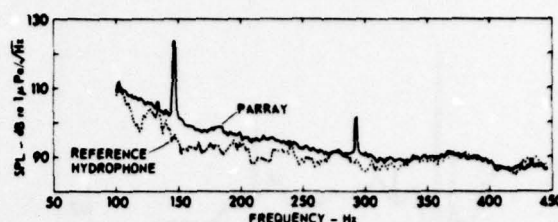where $D(\omega)$ is the spectrum of $d_p(t-L/c_o) - d_h(t)$,

the composite transducer displacement, and $A(\omega)$ is the composite transducer acceleration.

V. EXPERIMENTAL VERIFICATION

Measurements to verify the theory were made at Applied Research Laboratories' Lake Travis Test Station using both 5 m and 340 m PARRAY's in fresh water. An accelerometer and shaker were mounted on the hydrophone of the 5 m PARRAY so that the motion of the hydrophone along the pump-hydrophone axis could be controlled and measured while the PARRAY electronic signal output was being measured simultaneously. For these tests, vibration levels were low enough that the linear model of Eqs. 13 and 15 held and an experimental receiver which detected only the upper sideband of the hydrophone signal was used rather than the receiver shown in Fig. 2. The PARRAY output was converted to its equivalent acoustic input signal for comparison with the accelerometer signal. This measured equivalence between acoustic and accelerometer signals was then compared with the theory using Eq. 17.

For the 5 m PARRAY, Eq. 17 may be expressed as

$$P_{dB}(\omega) = 150 - 40 \log_{10} f + G_{dB}(\omega) \quad , \quad (18)$$

where $P_{dB}(\omega)$ is SPL in dB re 1 μPa and $G_{dB}(\omega)$ is acceleration in dB re 1 μg. Figure 3 is a plot of the hydrophone acceleration spectrum measured with the accelerometer while the hydrophone was being shaken at a fundamental frequency of 146 Hz and its 292 Hz harmonic. Figure 4 shows the simultaneously measured PARRAY equivalent on-axis SPL and the actual SPL measured with an independent omni-directional reference hydrophone. The 146 and 292 Hz components seen in the PARRAY data are clearly due to the vibration since they do not appear in the reference hydrophone measurement. PARRAY background noise is apparently a combination of broadband acoustic noise and PARRAY receiver noise, which in this case is rather high because system parameters are not matched to the short length of this PARRAY. The equivalent SPL obtained by applying Eq. 18 to the acceleration data of Fig. 3 is shown in Fig. 5. Figures 4 and 5 exhibit agreement within expected experimental accuracy at both 146 and 292 Hz.

The same experiment was repeated several times at different vibration levels and frequencies. Differences between the theory and experimental results are shown in Fig. 6 for a number of vibration frequencies. These differences are believed to be due to inaccuracies in measuring the transducer acceleration.
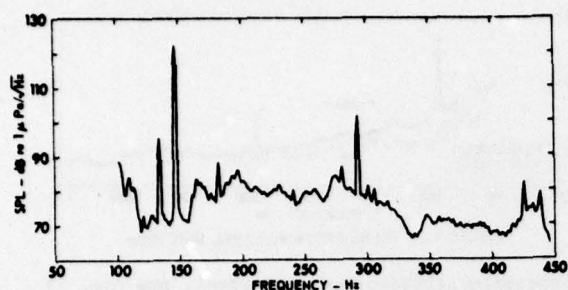
153

FIGURE 5. EQUIVALENT SOUND PRESSURE LEVEL SPECTRUM

FIGURE 6. THEORETICAL - EXPERIMENTAL COMPARISON

FIGURE 7. PARRAY SIDEBAND CONVOLUTION
COMPONENTS FOR HIGH LEVEL VIBRATION

For high amplitude vibration, the nonlinear model of Eqs. 12 and 16 must be used to relate the hydrophone sideband signal to the acoustic pressure and vibration. A single experiment to verify the form of this model was conducted using a 340 m PARRAY and the single sideband receiver used previously. In this experiment a diver rhythmically shook the PARRAY hydrophone while a 150 Hz acoustic signal was received by the PARRAY. For these conditions, Eq. 16 predicts spectral components deriving directly from vibration induced phase modulation of the carrier, and also deriving from the convolution of the modulated carrier spectrum with the 150 Hz acoustic signal spectrum. The receiver was not capable of receiving the carrier and its sidebands created by the vibration, but the spectral components resulting from the convolution were observed as shown in Fig. 7. Since the acoustic signal was very stable at 150 Hz, the carrier and its vibration-induced sidebands are reproduced exactly, but are centered at 150 Hz in this sideband spectrum. From these data one may deduce that the hydrophone was shaken at a frequency of 0.75 Hz with a displacement of 4.9 X 10^{-3} m rms which corresponds to an acceleration of 0.011 g rms. The phase modulation index of this process is 1.9. These derived parameters are in general agreement with observations made during the experiment.

VI. MINIMIZING THE EFFECTS OF VIBRATION

From a theoretical point of view, the effects of transducer vibration on PARRAY operation can be completely eliminated. This is so because the actual vibration of the transducers may be measured using, for instance, accelerometers, and the PARRAY signal output due to vibration can then be determined by using the models presented here. The vibration induced signal components can be subtracted from the PARRAY output, leaving only the acoustic signals. In practice, this technique will require extraordinary accuracy if it is to be effective.

If the vibration and acoustic signals occupy exclusive frequency bands, more easily implemented techniques may suffice. In the case of low level vibration where Eqs. 13 and 15 hold, the acoustic signals may be separated from vibration signals at the output of the receiver by filtering.

For high level vibration where the nonlinear model of Eqs. 12 and 16 hold, a straightforward
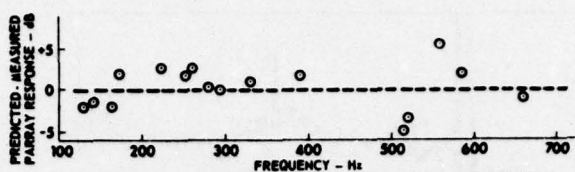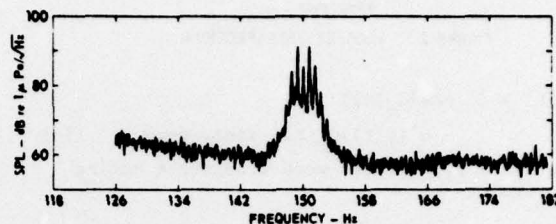
approach is to change the phase locked loop in the receiver, Fig. 2, so that the loop tracks the vibration induced phase modulation. The loop filter must pass the vibration frequencies. This linearizes the PARRAY response so that acoustic and vibration signals may be separated by filtering at the receiver output, as in the case of low level vibration.

VII. CONCLUSIONS

Models relating the response of a PARRAY to vibration of its transducers have been developed and predictions using the models have been shown to agree with experimental data. Electronic techniques for counteracting the effects of vibration are available and should be considered in PARRAY system design. [This research was supported by the Advanced Research Projects Agency of the Department of Defense and was monitored by the Naval Electronic Systems Command under Contract N00039-76-C-0231.]

REFERENCES

1. P. J. Westervelt, "Parametric Acoustic Array," J. Acoust. Soc. Am. 35, No. 4, pp 535-537, 1963.

2. H. O. Berktay and C. A. Al-Temimi, "Virtual Arrays for Underwater Reception," J. Sound Vib. 9, No. 2, pp 295-307, 1969.

3. T. G. Goldsberry, "Parameter Selection Criteria for Parametric Receivers," presented at 88th meeting of the Acoustical Society of America, St. Louis, MO, 4-8 Nov 1974.

4. V. A. Zverev and A. I. Kalachev, "Modulation of Sound by Sound in the Intersection of Sound Waves," Sov. Phys. Acoust. 16, No. 2, pp 204-208, 1970.

APPENDIX I

EXPERIMENTS WITH A LARGE APERTURE PARAMETRIC

ACOUSTIC RECEIVING ARRAY

155

EXPERIMENTS WITH A LARGE APERTURE PARAMETRIC ACOUSTIC RECEIVING ARRAY

by

C. Richard Reeves
Tommy G. Goldsberry
David F. Rohde

Applied Research Laboratories
The University of Texas at Austin
Austin, Texas   78712

ABSTRACT

The Parametric Acoustic Receiving Array (PARRAY) is a receiving array which achieves the directional reception characteristics of a continuous end-fire line array by the use of only two transducers (pump and hydrophone). The PARRAY synthesizes a virtual receiving array with acoustic aperture equal to the pump-hydrophone separation. Since the PARRAY is a system involving a number of active components which are required to process signals with wide dynamic ranges, the implementation of a practical and useful PARRAY involves meeting stringent system self-noise requirements. A PARRAY with 340 m pump-hydrophone separation operating over the 35 to 800 Hz range has been tested in a fresh water lake, with results showing that the self-noise level of the PARRAY is below the ambient noise level in this environment. A description of the PARRAY implementation is presented with the test results.

EXPERIMENTS WITH A LARGE APERTURE PARAMETRIC ACOUSTIC RECEIVING ARRAY

C. Richard Reeves, Tommy G. Goldsberry, and David F. Rohde

Applied Research Laboratories, The University of Texas at Austin
P. O. Box 8029, Austin, TX 78712

ABSTRACT

The Parametric Acoustic Receiving Array
(PARRAY) is a receiving array which achieves the
directional reception characteristics of a continu-
ous end-fire line array by the use of only two
transducers (pump and hydrophone). The PARRAY
synthesizes a virtual receiving array with acoustic
aperture equal to the pump-hydrophone separation.
Since the PARRAY is a system involving a number of
active components which are required to process
signals with wide dynamic ranges, the implementa-
tion of a practical and useful PARRAY involves
meeting stringent system self-noise requirements.
A PARRAY with 340 m pump-hydrophone separation
operating over the 35 to 800 Hz range has been
tested in a fresh water lake, with results showing
that the self-noise level of the PARRAY is below
the ambient noise level in this environment. A
description of the PARRAY implementation is pre-
sented with the test results.

I. INTRODUCTION

The Parametric Acoustic Receiving Array
(PARRAY) is a technique for implementing an
acoustic receiving array by means of only two
small transducers with some electronics [1,2].
The PARRAY offers the potential for significant
savings in the cost and complexity of large arrays
when compared with conventional techniques. This
paper discusses tests made with a 340 m long
PARRAY which give an indication of the performance
capabilities of a large PARRAY.

II. THE PARRAY

The PARRAY functions as an acoustic sensor by
taking advantage of the slight nonlinearity in-
volved in acoustic propagation through water.
Because of the nonlinearity, two (or more) primary
acoustic signals produce intermodulation products
which are large enough to be observed under the
proper circumstances. Figure 1 shows the basic
elements of a PARRAY. In this system, one of the
primary signals is supplied by a local source
called the pump; ambient signals act as other
primary signals. All these primary signals pro-
duce intermodulation products which are then re-
ceived by a hydrophone. Because the pump signal
is of much greater amplitude and frequency than
the ambient signals, the strongest intermodulation
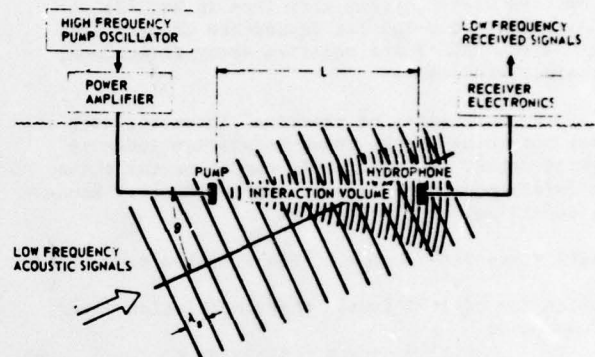products are those between the pump and ambient

Fig. 1. PARRAY Functional Diagram

signals rather than between different ambient
signals. The ambient signals are recovered by
demodulating the products which appear as modula-
tion sidebands on the pump carrier.

The principal reason for receiving ambient
acoustic signals by this method is that desirable
directional response characteristics are obtained.
The amplitude of the product between the pump and
a particular ambient signal depends upon the angle
between the propagation directions of the two
signals. The angular dependence is very similar
to that of a continuous end-fire line array with
length equal to the pump-hydrophone separation.
Therefore, the PARRAY acts as a continuous array
but uses only two small transducers.

The pump signal and intermodulation products
appearing at the hydrophone can be expressed in
closed form as a phase modulation of the pump
carrier by the ambient acoustic signals [3]. If
the pump signal is a pure sinusoid at frequency
ω_o, the signal received by the hydrophone is

$$s(t) = \cos[\omega_o t + \phi(t)] \qquad (1)$$

with phase modulation term

$$\phi(t) = \frac{\left(\frac{B}{2A} + \cos\theta\right)\omega_o L}{\rho_o c_o^3} \ \frac{\sin\left[\frac{\omega_1 L}{2c_o}(1-\cos\theta)\right]}{\frac{\omega_1 L}{2c_o}(1-\cos\theta)} \ p(t), \quad (2)$$

where

$p(t)$ = ambient pressure signal (n/m^2)
ω_1 = angular frequency of $p(t)$
B/A = parameter of nonlinearity of water (≈ 5)
θ = angle between direction of ambient signal propagation and pump-hydrophone axis
ρ_o = density of water (kg/m^3)
c_o = sound speed (m/sec)
L = pump-hydrophone separation distance (m).

The desired array output is $\phi(t)$. When the array is at least a few wavelengths long $\left(\omega_1 L/(2c_o)>1\right)$, the term with the (sin x)/x form in Eq. (2) dominates the θ-angular dependence of $\phi(t)$ and gives the PARRAY its end-fire array directional characteristics.

In most cases of practical interest, even the maximum value of the phase modulation index is quite small, and under this condition the phase modulation process is very nearly linear. Equation (1) may be rewritten as

$$s(t) = [\cos\phi(t)]\cos\omega_o t - [\sin\phi(t)]\sin\omega_o t, \quad (3)$$

which for $\phi(t)\ll 1$ (small phase modulation index) reduces to

$$s(t) \simeq \cos\omega_o t - \phi(t)\sin\omega_o t . \quad (4)$$

In this form it is apparent that the hydrophone signal consists of the pump carrier plus a double sideband suppressed carrier quadrature amplitude modulation component in which the modulating signal is the desired array output, $\phi(t)$. The array output can be obtained from the hydrophone signal by a single or double sideband linear receiver.

III. PARRAY PERFORMANCE CRITERION

As with any directional receiving array, a primary measure of performance of the PARRAY is its array gain, which is the increase in signal-to-noise ratio for a signal arriving from the on-axis direction ($\theta=0$) at the PARRAY output compared to the output of an ideal omnidirectional sensor. Since the PARRAY and omnidirectional sensor are calibrated so that they have equal response to an on-axis signal, the gain of the PARRAY results in a decrease in its noise output. The lower the noise output of the PARRAY is, the higher is its array gain. The gain of the PARRAY depends not only upon the relationship between its directional characteristics and the noise environment but, potentially, upon the self-noise of the system. Because the modulation products at the hydrophone are very small, very low levels of self-noise are required of the system components if self-noise is not to increase the PARRAY output noise and thereby lower the array gain.

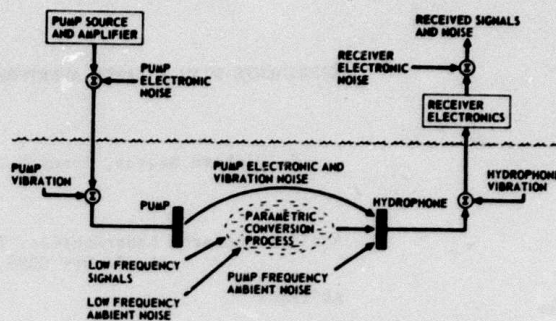Figure 2 shows the principal sources of noise in the PARRAY. They are:

Fig. 2. Signal and Noise Sources in a PARRAY

(1) pump electronic noise
(2) receiver electronic noise
(3) pump frequency ambient noise
(4) pump and hydrophone vibration
(5) low frequency ambient noise

The effects of the first four listed sources are determined by the construction and operating parameters of the PARRAY [4,5]. The effect of the fifth source, low frequency ambient noise, is determined by the directional characterisitcs of the PARRAY in a manner identical to that for any type array. PARRAY self-noise, then, is noise arising from all sources other than low frequency ambient noise.

As a practical matter, it is necessary only to reduce the self-noise levels so that they contribute somewhat less to the array output than the low frequency ambient noise contributes in order to reduce self-noise effects to a negligible point. When this is accomplished, the PARRAY is said to be ambient noise limited, and the array gain of the PARRAY is at its maximum and cannot be exceeded by any array having the same directional characteristics. Experimental data discussed in the next section shows both ambient and self-noise limited operation of a PARRAY.

IV. EXPERIMENTS

A 340 m PARRAY designed for low frequency operation has been tested in Lake Travis, a fresh water lake near Austin, Texas. The pump and hydrophone of this PARRAY are mounted on underwater towers so that they are 22 m above the bottom in an area 45 m deep. The PARRAY pump operates at frequency 65 kHz with source level 220 db re 1 μPa at 1 m (approximately 50 W electrical). The pump signal source is a crystal controlled 65 kHz oscillator with 170 dB spectral purity at 400 Hz; that is, the spectrum level of the oscillator sideband noise 400 Hz away from the carrier is 170 dB below the carrier level [6]. At 100 Hz the spectral purity is 160 dB. This signal is amplified to drive the pump transducer with negligible loss in spectral purity. Transducers used as pump and hydrophone have 29 dB directivity index

at 65 kHz and are constructed to a unique high efficiency design [7]. A single sideband receiver linearly detects the intermodulation products in the upper or lower sideband of the hydrophone signal [8]. The output of the PARRAY is digitally recorded and analyzed to determine system performance under various experimental conditions.

It is found that at frequencies below 200 Hz the dominant source of self-noise is the pump electronics. Between 200 and 400 Hz both pump electronic and pump frequency ambient noises are of comparable levels. At higher frequencies the pump frequency ambient noise is the greatest contributor to self-noise. Whether or not self-noise limits the PARRAY gain depends upon the low frequency ambient noise level. At high ambient noise levels, the PARRAY is ambient noise limited and the full array gain is realized; at low ambient noise levels, self-noise may limit the array gain.

To compare the ambient noise to self-noise, both are converted to equivalent on-axis, plane wave acoustic levels. In the test system, the equivalent on-axis, plane wave ambient noise is measured as the electrical noise at the PARRAY output converted to its acoustic equivalent by the electric/acoustic calibration of the PARRAY. This measurement technique is successful only when the ambient noise is higher than PARRAY self-noise; that is, when the array is ambient noise limited. If the array is self-noise limited, the same measurement yields the self-noise level. For all practical purposes, the measurement of both ambient and self-noise and the determination of whether the PARRAY is ambient or self-noise limited is done in the same experiment.

If the PARRAY is limited by isotropic ambient noise, one expects the PARRAY output to show the ambient noise reduced in level by the PARRAY directivity index (DI) compared to the output of an omnidirectional sensor. That is, the array gain is equal to the DI for this case. For the PARRAY

$$DI = 10 \log \frac{4Lf}{c} \ dB \qquad (5)$$

where L is array length, f is noise frequency, and c is sound speed. In the test environment it is known that the ambient noise is not isotropic at all frequencies; however, the comparison of the actual array gain to the theoretical DI is still informative.

Figure 3 is a plot of the noise spectrum measured both with the PARRAY and with an omnidirectional hydrophone. This is a case in which the ambient noise levels are high, particularly at the lower frequencies, and the PARRAY is ambient noise limited over the entire 35 to 800 Hz frequency range. The array gain is easily compared with the DI by subtracting the DI from the omnidirectional hydrophone spectrum and then comparing the result (included in Figure 3) with the PARRAY spectrum. If the omnidirectional hydrophone spectrum minus the DI is higher than the PARRAY output, the PARRAY gain is greater than the DI,
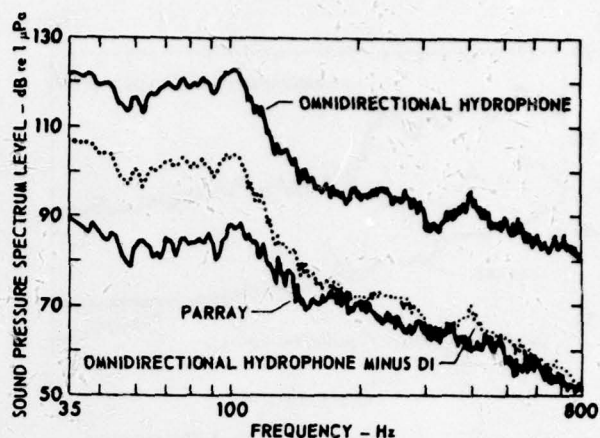

Fig. 3. PARRAY and Omnidirectional Hydrophone Outputs Showing Ambient Noise Limited Operation of PARRAY

and conversely. Comparison of the curves indicates that at most frequencies below 150 Hz the array gain actually exceeds the DI by a significant level; this is due to the fact that in this case the noise is not isotropic. The dominant low frequency noise sources are hydroelectric generators and spillways in a dam located behind the array. Much of this directly radiated noise is rejected by the front-to-back ratio of the PARRAY beam pattern, given by

$$FB = 20 \log \frac{14.6 \ Lf}{c} \ dB \qquad (6)$$

rather than the DI. At higher frequencies, however, other noise sources and reverberation in the lake make the noise more nearly isotropic, and the array gain approximately equals the DI, as indicated by agreement of the adjusted omnidirectional hydrophone and PARRAY spectra above 150 Hz. For this environment, the PARRAY achieves the full array gain expected from its directional characteristics. No array with the same directional characteristics will perform better.

Next, consider the results of a similar experiment conducted in a much lower level ambient noise environment. Figure 4 shows the omnidirectional hydrophone and PARRAY output spectra for some of the quietest conditions in Lake Travis. Most of the generating equipment is off and all the spillways in the dam are closed. At low frequencies, from 35 to 120 Hz, the PARRAY shows array gain exceeding its DI because much of the noise in this band still is radiated from the dam toward the back of the array. At midfrequencies, from 120 to 300 Hz, the noise is more isotropic and array gain approximates the DI. At frequencies greater than 300 Hz, self-noise limits the array gain to values somewhat less than the DI; however, the array gain is still quite large and is more than 20 dB everywhere in this band. For this environment the PARRAY is ambient noise
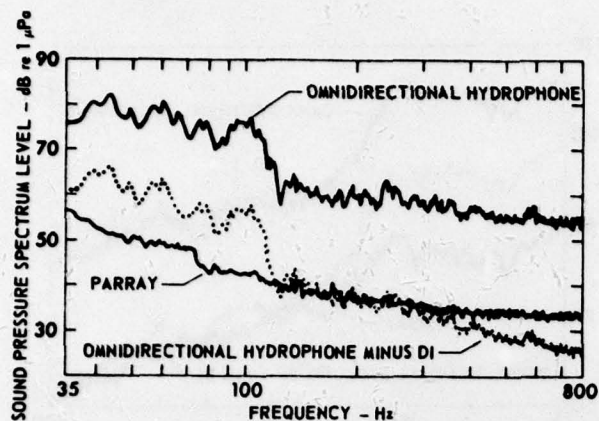
Fig. 4. PARRAY and Omnidirectional Hydrophone
Outputs Showing PARRAY Ambient Noise Limited
Below 300 Hz and Self-Noise Limited Above 300 Hz

limited and achieves maximum array gain at
frequencies below 300 Hz.

V. CONCLUSIONS

Operation of a 340 M PARRAY has been
demonstrated in a fresh water lake. This array
is ambient noise limited, rather than self-noise
limited, under most conditions in this environ-
ment, and therefore achieves the maximum array
gain attainable by any array with the same
directional characteristics. For very quiet
ambient noise conditions, the PARRAY is self-noise
limited for received signal frequencies greater
than 300 Hz. Even for these conditions the
PARRAY is ambient noise limited below 300 Hz.
[This research was supported by the Defense
Advanced Research Projects Agency and was mon-
itored by the Naval Electronic Systems Command
under Contract N00039-76-C-0231.]

REFERENCES

[1] P. J. Westervelt, "Parametric Acoustic Array,"
    J. Acoust. Soc. Am. 35, no. 4, pp. 535-537,
    1963.
[2] II. O. Berktay and C. A. Al-Temimi, "Virtual
    Arrays for Underwater Reception," J. Sound
    Vib. 9, no. 2, pp. 295-307, 1969.
[3] V. A. Zverev and A. I. Kalachev, "Modulation
    of Sound by Sound in the Intersection of
    Sound Waves," Sov. Phys. Acoust. 16, no. 2,
    pp. 204-208, 1970.
[4] T. G. Goldsberry, "Parameter Selection
    Criteria for Parametric Receivers," 88th
    Meeting of the Acoustical Society of America,
    St. Louis, MO, 4-8 November 1974.
[5] C. R. Reeves, T. G. Goldsberry, D. F. Rohde,
    and V. E. Maki, "Vibration Sensitivity of
    the Parametric Acoustic Receiving Array,"
    1978 IEEE International Conference on
    Acoustics, Speech, and Signal Processing,
    Tulsa, OK, 10-12 April 1978.
[6] W. S. Olsen, T. G. Goldsberry, C. R. Reeves,
    and D. F. Rohde, "A Crystal Controlled Pump
    Signal Source for an Experimental Parametric
    Acoustic Receiving Array," 92nd Meeting of the
    Acoustical Society of America, San Diego,
    CA, 16-19 November 1976.
[7] M. W. Widener, "The Design of High Efficiency
    Transducer Elements and Arrays," 92nd
    Meeting of the Acoustical Society of America,
    San Diego, CA, 16-19 November 1976.
[8] D. F. Rohde, T. G. Goldsberry, W. S. Olsen,
    and C. R. Reeves, "Band Elimination Pro-
    cessor for an Experimental Parametric
    Acoustic Receiving Array," submitted for
    publication J. Acoust. Soc. Am., June 1978.

2 August 1979

DISTRIBUTION LIST FOR
ARL-TR-79-4
UNDER CONTRACT N00039-76-C-0231
UNCLASSIFIED

<u>Copy No.</u>

Commander
Naval Electronic Systems Command
Department of the Navy
Washington, DC 20360
1   Attn: CAPT H. Cox, PME 124
2   CAPT D. B. Murton, PME 124
3   CAPT R. B. Gilchrist, Code 03
4   CDR D. J. Griffiths, Code 320
5   Dr. G. Hetland, PME 124-62
6   Dr. J. A. Sinsky, Code 320A
7   Ms. Joan C. Bertrand, Code 3202

Defense Advanced Research Projects Agency
1400 Wilson Boulevard
Arlington, VA 22209
8   Attn: CDR V. P. Simmons (TTO)
9   Dr. T. Kooij

Commander
Naval Sea Systems Command
Department of the Navy
Washington, DC 20362
10   Attn: CAPT A. H. Gilmore, Code 63X
11   Mr. C. D. Smith, Code 06R/63R
12   Mr. D. E. Porter, Code 63R
13   Mr. D. L. Baird, Code 63X3
14   Mr. C. E. Fox, Code 63Z2B
15   CDR D. F. Bolka, Code 63G1
16   Mr. D. M. Early, Code 63D
17   CAPT W. A. White, Code 63X3
18   Mr. John Neely, Code 63X3

Chief of Naval Material
Department of the Navy
Washington, DC 20360
19   Attn: RADM D. M. Jackson, Code ASW-00
20   Mr. Lou Griffith, Code 031

163

Copy No.

21   Office of Assistant Secretary
            of the Navy (R,E&S)
        The Pentagon
        Washington, DC 20350
        Attn: Dr. Richard F. Hoglund
                Special Deputy for Advanced Technology

        Director
        Naval Research Laboratory
        Department of the Navy
        Washington, DC 20375
22   Attn: Code 8150
23   Dr. M. Potosky, Code 8109
24   Dr. J. Jarzynski, Code 8131

        Naval Research Laboratory
        Underwater Sound Reference Division
        P. O. Box 8337
        Orlando, FL 32806
25   Attn: Dr. Lee Van Buren
26   Dr. Peter H. Rogers

        Commanding Officer
        Naval Ocean Systems Center
        Department of the Navy
        San Diego, CA 92152
27   Attn: Dr. H. Schenck, Code 71
28   Mr. M. Akers, Code 714
29   Dr. H. P. Bucher

        Office of the Chief of Naval Operations
        The Pentagon
        Washington, DC 20350
30   Attn: CAPT J. W. Van Metre, Code 224
31   CDR R. H. Scales, Code 224 F

        Officer-in-Charge
        New London Laboratory
        Naval Underwater Systems Center
        Department of the Navy
        New London, CT 06320
32   Attn: M. B. Moffett, Code TD 124
33   W. L. Konrad

Copy No.

Chief of Naval Research
Department of the Navy
Arlington, VA 22217
34   Attn: R. F. Obrochta, Code 212
35   Dr. L. E. Hargrove, Code 421

Commander
Naval Ocean Research and Development Activity
NSTL Station, MS 39529
36   Attn: Dr. A. L. Anderson
37   Dr. S. W. Marshall

38   Commanding Officer
USCG Research and Development Center
Avery Point
Groton, CT 06340
Attn: CAPT M. Y. Suzich

39 - 50   Commanding Officer and Director
Defense Documentation Center
Defense Services Administration
Cameron Station, Building 5
5010 Duke Street
Alexandria, VA 22314

51   Battelle Columbus Laboratories
505 King Avenue
Columbus, OH 43201
Attn: TACTEC

52   Dr. F. H. Fenlon
Applied Research Laboratory
The Pennsylvania State University
State College, PA 16801

53   Mr. A. Nelkin
Westinghouse Electric Corporation
P. O. Box 1488, MS9R40
Annapolis, MD 21404

54   Mr. J. F. Bartram
Raytheon Company
P. O. Box 360
Portsmouth, RI 02871

55   Mr. E. P. Aurand
19 Hanapepe Place
Honolulu, HI 96825

<u>Copy No.</u>

56 Dr. P. M. Schultheiss
  Department of Engineering and
   Applied Science
  Yale University
  New Haven, CT 06520

57 Mr. V. J. Lujetic
  RAMCOR, Inc.
  800 Follin Lane
  Vienna, VA 22180

58 Mr. Jack Fagan
  Systems Planning Corporation
  1500 Wilson Blvd., Suite 1500
  Arlington, VA 22209

59 Dr. F. J. Jackson
  Bolt, Beranek, and Newman, Inc.
  1701 North Fort Myer Drive
  Arlington, VA 22209

60 Dr. J. E. Barger
  Bolt, Beranek, and Newman, Inc.
  50 Moulton Street
  Cambridge, MA 02138

61 Dr. William S. Hodgkiss
  Marine Physical Laboratory of
  The Scripps Institution of Oceanography
  San Diego, CA 92152

62 Mr. J. Dow
  TRACOR, Inc.
  6500 Tracor Lane
  Austin, TX 78721

  Radian Corporation
  8500 Shoal Creek Blvd.
  Austin, TX 78758
63 Attn: Mr. Jerry L. Bardin
64   Dr. C. Richard Reeves

65 Office of Naval Research
  Resident Representative
  Room 582, Federal Building
  Austin, TX 78701

Copy No.

66	Physical Acoustics Division, ARL:UT
67	Garland R. Barnard, ARL:UT
68	Tommy G. Goldsberry, ARL:UT
69	Robert A. Lamb, ARL:UT
70	Thomas G. Muir, ARL:UT
71	Wiley S. Olsen, ARL:UT
72	David F. Rohde, ARL:UT
73	M. Ward Widener, ARL:UT
74	Reuben H. Wallace, ARL:UT
75	Library, ARL:UT
76 - 105	ARL:UT Reserve